

Title of thesis

**Modelling and simulation of autothermal reformer for
synthesis gas production**

I, MOUSAB SALAH ELDEEN MIRGHANI MOHAMMED

hereby allow my thesis to be placed at the Information Resource Center (IRC) of Universiti Teknologi PETRONAS (UTP) with the following conditions:

1. The thesis becomes the property of UTP.
2. The IRC of UTP may make copies of the thesis for academic purposes only.
3. This thesis is classified as

Confidential

Non-confidential

If this thesis is confidential, please state the reason:

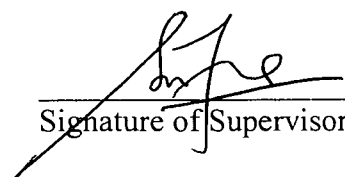
The contents of the thesis will remain confidential for _____ years.

Remarks on disclosure:

Endorsed by



Signature of Author



Signature of Supervisor

Permanent: *Faculty of engineering and technology*
Address *Gezira University*
Wad Madani, Sudan

Name of Supervisor
AP. Dr. Suzana Yusup

Date: 23/07/07

Date: 23/07/07

UNIVERSITI TEKNOLOGI PETRONAS

Approval by Supervisor

The undersigned certify that they have read, and recommend to The Postgraduate Studies

Programme for acceptance, a thesis entitled

Modelling and simulation of autothermal reformer for synthesis gas production

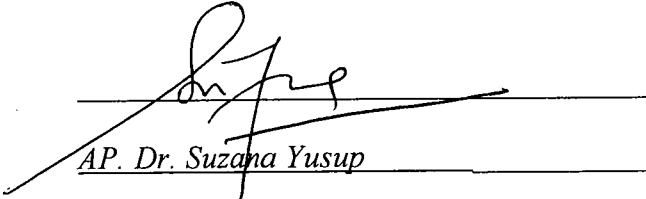
submitted by

Mousab Salah Eldeen Mirghani

for the fulfilment of the requirements for the degree of

Masters of Science in Chemical Engineering

23/07/07
Date

Signature : 
Main Supervisor : AP. Dr. Suzana Yusup
Date : 23/07/07
Co-Supervisor : _____

UNIVERSITI TEKNOLOGI PETRONAS

Modelling and simulation of autothermal reformer for synthesis gas production

By

Mousab Salah Eldeen Mirghani

A THESIS

SUBMITTED TO THE POSTGRADUATE STUDIES PROGRAMME

AS A REQUIREMENT FOR THE

DEGREE OF MASTERS OF SCIENCE IN CHEMICAL

ENGINEERING

Chemical Engineering

BANDAR SERI ISKANDAR,

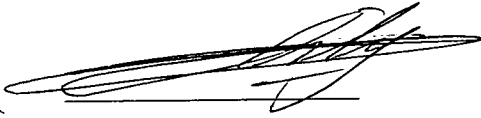
PERAK

June, 2007

DECLARATION

I hereby declare that the thesis is based on my original work except for quotations and citations which have been duly acknowledged. I also declare that it has not been previously or concurrently submitted for any other degree at UTP or other institutions.

Signature:



Name : Mousab Salah Eldeen Mirghani

Date : 28/07/07

ACKNOWLEDGEMENT

First and foremost, I would like to thank God the almighty, for without his consent, it would be impossible to achieve what had been done in this work. And I would like to thank my parents and all of my family members for their love and support from a distance to go on.

Special acknowledgement goes for the soul of my previous supervisor, Prof. Dr. V. R. Radhakrishnan, the one who used to push me hard to overcome the complications of this project with all of his knowledge, experience and critical thinking. And I would also like to thank my supervisor, AP. Dr. Suzana Yusup for her innumerable and invaluable contribution in this work as well as her ongoing support to complete the project in the right way and time.

Thanks and gratitude must be given to the members of Chemical Engineering Department whom contributed their ideas, expertise and advices. Special thanks for Dr. Ramasamy for the time that he had given to me to find out the right path as well as Mrs. Haslinda Zabiri, the coordinator of Grant Assistantship in the department.

Thanks are extended for the members of Post Graduate Studies Office for their invaluable help, and I would like to especially thank Mrs. Haslina, Mr. Fadil Ariff, Mrs. Norma, and Mrs. Kamalia.

Last but not least, thanks are given to my colleagues and friends, whom support and comfort me through the good and bad times; they have given me a lot of fun and unforgettable moments.

ABSTRACT

One dimensional heterogeneous adiabatic fixed-bed reactor with supported nickel catalyst is used to model the autothermal reformer for synthesis gas production. The flow rate of natural gas along the catalyst bed is considered to vary in the axial direction. The modeling and simulation of autothermal reformers is complex and requires detailed understanding of natural gas reactions kinetics. To investigate these kinetics, different kinetics models such as De Groote and Froment model are employed and predictions of the kinetics parameters such as activation energies, rate constants, and adsorption constants are made. An industrial plant for production of synthesis gas from natural gas, for methanol production is taken as a case study. A material and energy balance is carried out for prediction of the input flow rates, feed composition to the autothermal reactor, and the partial pressures to the reactants. The pressure drop is calculated using Ergun equation. For the developed model, the rate of coke formation is neglected since suitable CH_4/O_2 ratio of 1.7 in the feed and natural gas stream temperature of higher than 8500C are assumed. The effect of catalyst volume, gas superficial velocity, and combustion temperature on temperature profile of autothermal reformer, conversion and rate of reactions are studied. It is found that, the bed temperature can be reduced by 200 C , and each 1.5 m^3 reduced of catalyst volume increased the bed temperature by 160 C . While increment of gas superficial velocity of 1 m/s decreased the bed temperature by 150 C . As for the effect of combustion temperature, it is found that, the outlet temperature of the reactor remains approximately constant in spite of the wide range of combustion temperature used ($11000\text{C} - 14000\text{C}$). Conversion of methane and oxygen to carbon monoxide and carbon dioxide are studied. It is noted that as the conversion of methane and oxygen increased, the amount of CO and CO_2 also increased. It is found that, lower mole fractions of CH_4 and O_2 and higher mole fractions of CO and CO_2 in the reactor output can be achieved when a higher combustion temperature is used.

TABLE OF CONTENT

STATUS OF THESIS.....	i
APPROVAL PAGE.....	ii
TITLE PAGE.....	iii
DECLARATION.....	iv
ACKNOWLEDGEMENT.....	v
ABSTRACT.....	vi
TABLE OF CONTENT.....	vii
LIST OF TABLES.....	x
LIST OF FIGURES.....	xi
NOMENCLATURE.....	xiii
CHAPTER 1.....	1
1. INTRODUCTION.....	1
1.1 Background.....	1
1.1.1 Natural Gas.....	1
1.1.2 Alternative processes for production of synthesis gas.....	3
1.2 Autothermal reactor operation.....	4
1.3 Combination between autothermal reforming and steam reforming.....	4
1.4 The main units in synthesis gas production plants.....	5
1.5 Problem statement.....	8
1.6 Objectives.....	8
1.7 Scope of study.....	9
CHAPTER 2.....	10
2. LITERATURE REVIEW.....	10
2.1 Alternative routes for synthesis gas production.....	10
2.2 Steam methane reforming:.....	10
2.3 Partial oxidation:.....	11
2.4 Autothermal reforming:.....	12

2.4.1	Autothermal reforming for hydrogen production	15
2.4.2	Temperature profiles in autothermal reforming process:.....	16
2.5	Kinetic models:	17
2.6	Reactor models:	19
2.7	Parametric study:	22
2.7.1	Effect of H ₂ content in the feed mixture:	22
2.7.2	Effect of CO ₂ in the feed mixture:	23
2.7.3	Effect of air on the steam methane reforming:	25
2.8	Types of catalysts for synthesis gas production:.....	26
2.8.1	Rhodium catalysts:.....	27
2.8.2	Metal oxides catalysts:.....	28
2.8.3	Palladium catalysts:	29
2.8.4	Platinum catalysts:	30
2.8.5	Effect of adding metals to catalysts:	32
2.8.6	Summary of literature review	32
CHAPTER 3		34
MODELING OF SYNTHESIS GAS LOOP		34
3.0	Introduction.....	34
3.1	Research methodology.....	35
3.1.1	Data collection:	35
3.1.2	Kinetics model investigation:	38
3.1.3	Determination of reactions rates	39
3.1.4	Reactor model and simulation:	40
3.1.5	Reactor model validation:	41
3.1.6	Effect of process variables study:	41
3.1.7	Calculations of conversion.....	41
3.2	Model Configuration.....	43
3.2.1	Process description.....	43
3.2.2	Reactor parameters.....	46
3.2.3	Methane reactions	47

3.2.4	Calculations of kinetics model parameters	49
3.2.5	Energy balance	50
3.2.6	Kinetic equations	52
3.2.7	Calculation of the pressure drop	55
3.2.8	Solution procedure	59
3.2.9	Calculations of conversion.....	61
CHAPTER 4	63
4.	RESULTS AND DISCUSSION	63
4.0	Introduction.....	63
4.1	Variation of autothermal reformer temperature profile	63
4.1.1	Comparison between the predicted temperature profile and actual plant data	66
4.2	Rate of reactions	67
4.2.1	Rate of reactions as functions of distance:.....	71
4.3	Effect of catalyst volume:	74
4.4	Effect of gas superficial velocity:	76
4.5	Effect of burner temperature (combustion temperature):	78
4.6	Rate of reactions using different combustion temperatures:.....	80
4.7	Conversion study	83
4.7.1	Molar flow rates and molar fractions.....	87
4.7.2	Molar fractions at different temperatures	93
4.7.3	Calculations of the overall selectivity	96
4.7.4	Comparison between autothermal reforming and partial oxidation	96
CHAPTER 5	98
5.	CONCLUDING REMARKS.....	98
5.1	Conclusions.....	98
5.2	Future work.....	100
APPENDIX	101
Appendix A	101
Appendix B	102
Appendix C	105
REFERENCES	114

LIST OF TABLES

Table 3.1: Composition of natural gas and steam reformer outlet:.....	44
Table 3.2: Flow rates and Molar fractions of reactor input:	44
Table 3.3: Flow rates and molar fractions of reactor output:.....	45
Table 3.4: Reactor parameters:	46
Table 3.5: Arrhenius parameter values for combustion, reforming, and water-gas shift reaction from Smet and et al (2001) [23].....	50
Table 3.6: Van't Hoff parameters values for the adsorption reactions from Smet and et al (2001) [23].	50
Table 4.1: Comparison between the temperatures at different positions with PML data.	66
Table 4.2: Molar fractions of compounds after each meter of catalyst bed height (T = 1250 ⁰ C):	87
Table 4.3: Molar fractions of compounds after each meter of catalyst bed height (T = 1100 ⁰ C):	88
Table 4.4: Molar fractions of compounds after each meter of catalyst bed height (T = 1200 ⁰ C):	89
Table 4.5: Molar fractions of compounds after each meter of catalyst bed height (T = 1300 ⁰ C):	90
Table 4.6: Molar fractions of compounds after each meter of catalyst bed height (T = 1400 ⁰ C):	91
Table 4.7: selectivity at different combustion temperatures.....	96
Table 4.8: Conversion of compounds via autothermal reforming and partial oxidation. .	96

LIST OF FIGURES

Figure 1.1: Demonstration unit for production of methanol from synthesis gas via autothermal reforming [5].....	7
Figure 4.1a: Temperature profile along the catalyst bed height of the autothermal reformer.....	64
Figure 4.2: Rate of reaction 1 as a function of temperature.....	67
Figure 4.3: Rate of reaction 2 as a function of temperature.....	68
Figure 4.4: Rate of reaction 3 as a function of temperature.....	68
Figure 4.5: Rate of reaction 4 as a function of temperature.....	69
Figure 4.6: Rate of reaction 1 as a function of distance inside the reactor, z m.	71
Figure 4.7: Rate of reaction 2 as a function of distance inside the reactor, z m.	72
Figure 4.8: Rate of reaction 3 as a function of distance inside the reactor, z m.	72
Figure 4.9: Rate of reaction 4 as a function of distance inside the reactor, z m.	73
Figure 4.10: Temperature profile using different catalyst volumes.....	74
Figure 4.11: Temperature profile with different superficial velocities (u_s).....	76
Figure 4.12: Temperature profile using different burner temperatures.	78
Figure 4.13: Rate of reaction (1) using different inlet temperatures.....	80
Figure 4.14: Rate of reaction (2) using different inlet temperatures.....	81
Figure 4.15: Rate of reaction (3) using different inlet temperatures.....	81
Figure 4.16: Rate of reaction (4) using different inlet temperatures.....	82
Figure 4.17: Percentage of consumption and generation at combustion temperature of 1250 ⁰ C):	83
Figure 4.18: Percentage of consumption and generation at combustion temperature of 1100 ⁰ C:	84
Figure 4.19: Percentage of consumption and generation at combustion temperature of 1200 ⁰ C:	84
Figure 4.20: Percentage of consumption and generation at combustion temperature of 1300 ⁰ C:	85
Figure 4.21: Percentage of consumption and generation at combustion temperature of 1400 ⁰ C:	86

Figure 4.22: Output flow rates after each meter of catalyst bed height where the combustion temperature of 1250 ⁰ C was used:.....	87
Figure 4.23: Output flow rates after each meter of catalyst bed height where the combustion temperature of 1100 ⁰ C was used:.....	88
Figure 4.24: Output flow rates after each meter of catalyst bed height where the combustion temperature of 1200 ⁰ C was used:.....	89
Figure 4.25: Output flow rates after each meter of catalyst bed height where the combustion temperature of 1300 ⁰ C was used:.....	90
Figure 4.26: Output flow rates after each meter of catalyst bed height where the combustion temperature of 1400 ⁰ C was used:.....	91
Figure 4.27: Molar fractions of compounds as function of catalyst bed height, z.....	93
Figure 4.28: Molar fraction of methane at different combustion temperatures.....	94
Figure 4.29: Molar fraction of oxygen at different combustion temperatures.....	94
Figure 4.30: Molar fraction of carbon monoxide at different combustion temperatures..	95
Figure 4.31: Molar fraction of carbon dioxide at different combustion temperatures.....	95

NOMENCULATURE

A	Reactor cross-sectional area, (m ²).
A _i	Pre-exponential factor, reaction dependent
B _A	Flow rate of component A, (Nm ³ /h).
C _p	Specific heat of fluid (kJ/kg K).
d	Reactor diameter (m).
D _p	Particle diameter (m).
E	Activation energy (kJ/mol).
F	Gas flow rate (Nm ³ /h).
G	Superficial mass velocity (kg/h.m ²)
g _c	Conversion factor in Ergun equation, dimensionless.
h	Catalyst bed height (m).
k _i	Reaction rate constant of reaction i, reaction dependent
K _i	Equilibrium constant of reaction i.
K _j	Adsorption constant for component j.
P	Total pressure (bar).
P _A	Partial pressure of component A (bar).
Q	Mass flow rate (kg/h).
r ₁	Reaction rate of total combustion (kmol/kg _{cat} s).

r_2	Rate of the steam reforming reaction (kmol/kg _{cat} s).
r_3	Rate of CO ₂ production by steam reforming (kmol/kg _{cat} s).
r_4	Rate of WGS reaction (kmol/kg _{cat} s).
r_5	Rate of Boudouard reaction (kmol/kg _{cat} s).
r_6	Rate of methane cracking (kmol/kg _{cat} s).
r_7	Rate of carbon gasification by steam (kmol/kg _{cat} s).
r_8	Rate of carbon gasification by oxygen (kmol/kg _{cat} s).
R	Universal gas constant, (8.3145 J/mol K).
S	Steam flow rate (Nm ³ /h).
T	Temperature (K).
u	Gas superficial velocity (m/s).
V _c	Catalyst volume (m ³).
V _T	Total bed volume (m ³).
V _v	Volume of void in the catalyst bed (m ³).
x _i	Molar fraction of component i.
X _i	Conversion of component i (%).
y _i	Molar fraction of component i in the reactor outlet.
z	Axial position (m).

GREEK SYMPOLS

ΔH_i	Standard enthalpy of reaction i (kJ/mol).
ρ	Gas density (kg/m ³).
ρ_c	Catalyst density (kg/m ³).
Φ	Porosity, dimensionless.
ΔP	Pressure drop (bar).
η_i	Effectiveness factor of reaction i, dimensionless.
μ	Viscosity of the gas passing through the bed (kg/m.h).

CHAPTER I
INTRODUCTION

CHAPTER 1

1. INTRODUCTION

1.1 Background

1.1.1 Natural Gas

Natural gas is a mixture of hydrocarbons, mainly methane as a dominant constituent beside ethane, propane, butane, and C_5^+ . Beside hydrocarbons natural gas usually contains small or large amount of non-hydrocarbons gases such as carbon dioxide, nitrogen, and hydrogen sulfide. Natural gas can be found with crude oil ('associated gas') or in reservoirs in which no oil is present ('non-associated gas'). Table 1 and Table 2 show the composition of a wide variety of natural gases [1].

Natural gas can be classified as a 'Dry' or 'Wet' according to the amount of condensable hydrocarbons (at ambient conditions) it contains. Associated gas usually is wet, whereas the non-associated gas is dry. Natural gas that contains an amount of H_2S and CO_2 is called the sour gas, while the gas that does not contain H_2S and CO_2 is called the sweet gas.

Natural gas has a great importance, not only as a source of energy, but also as a raw material for petrochemical industry. An increasing number of schemes are being developed in order to utilize the natural gas. In recent years, natural gas has received special attention as a main source of energy and chemicals, and due to this conditions, natural gas has become the second most used source of energy after crude oil and before coal which used to be the second source 40 years ago.

Table 1.1 Composition of selected non-associated natural gases (volume %) (1992)[1].

Area	Algeria	France	Holland	New Zealand	North Sea	N. Mexico	Texas	Texas	Canada
Field	Hasi-R'1 Mel	Lacq	Gron.	Kapuni	West Sole	Rio Arriba	Terrell	Cliffside	Olds
CH ₄	83.5	69.3	81.3	46.2	94.4	96.9	45.7	65.8	52.4
C ₂ H ₆	7.0	3.1	2.9	5.2	3.1	1.3	0.2	3.8	0.4
C ₃ H ₈	2.0	1.1	0.4	2.0	0.5	0.2	-	1.7	0.1
C ₄ H ₁₀	0.8	0.6	0.1	0.6	0.2	0.1	-	0.8	0.2
C ₅ ⁺	0.4	0.7	0.1	0.1	0.2	-	-	0.5	0.4
N ₂	6.1	0.4	14.3	1.0	1.1	0.7	0.2	26.4	2.5
CO ₂	0.2	9.6	0.9	44.9	0.5	0.8	53.9	-	8.2
H ₂ S	-	15.2	Trace	-	-	-	-	-	35.8

Table 1.2 Composition of selected associated natural gases (volume %) (1992)[1].

Area	Abu Dhabi	Iran	North Sea	North Sea	N. Mexico
Field	Zakum	Agha Jari	Forties	Brent	San Juan
County					
CH ₄	76.0	66.0	44.5	82.0	77.3
C ₂ H ₆	11.4	14.0	13.3	9.4	11.2
C ₃ H ₈	5.4	10.5	20.8	4.7	5.8
C ₄ H ₁₀	2.2	5.0	11.1	1.6	2.3
C ₅ ⁺	1.3	2.0	8.4	0.7	1.2
N ₂	1.1	1.0	1.3	0.9	1.4
CO ₂	2.3	1.5	0.6	0.7	0.8
H ₂ S	0.3	-	-	-	-

Most of natural gas can be used for production of synthesis gas (a mixture of hydrogen and carbon monoxide) as an intermediate step for production of many chemicals such as methanol and ammonia or for energy such as fuel cells and hydrogen for hybrid engines [1, 2, 4].

1.1.2 Alternative processes for production of synthesis gas

There are three main processes for production of synthesis gas, and the use of specific process depends mainly on the use of downstream (specifications of produced synthesis gas) and other economical issues such as the availability of feedstock, because synthesis gas can be produced from coal as well as natural gas.

These processes are:

- 1- Steam reforming of natural gas and light hydrocarbons that involves reactions of hydrocarbons with steam in the presence of a catalyst.
- 2- Partial oxidation of hydrocarbons with steam and oxygen, which describes the non-catalytic reaction of hydrocarbons with oxygen and steam. Sometimes this process is called catalytic partial oxidation (CPO) if a catalyst is usable. A combination of Steam reforming and partial oxidation is often referred to as Autothermal reforming.
- 3- Partial oxidation of coal with steam and oxygen, but this is not very common for the production of synthesis gas for chemical use according to the availability of the raw material.

These three processes will be discussed further in the later chapters.

1.2 Autothermal reactor operation

If a reaction requires a relatively high temperature before it proceeds at a reasonable rate the products of the reaction will leave the reactor at a high temperature and, in the interests of economy, heat will normally be recovered from them. Since heat must be supplied to the reactants to raise them to the reaction temperature, a common arrangement is to use the hot products to heat the incoming feed.

If the reaction is sufficiently exothermic, enough heat will be produced in the reaction to overcome any losses in the system and to provide the necessary temperature difference in the heat exchanger. The term autothermal is used to describe such a system, which is completely self-supporting in its thermal energy requirements.

The essential feature of an autothermal reactor system is the feedback of reaction heat to raise the temperature and hence the reaction rate of the incoming reactant stream.

Autothermal reforming has become the most important method to produce synthesis gas from natural gas due to the features of the final product that can be achieved through autothermal reforming such as the final product composition and downstream pressure, in other words, autothermal reforming process is more flexible in order to control the composition of the produced synthesis gas by controlling the operating conditions such as the combustion temperature, also this process gives high downstream pressure which is required to reduce the cost of compression of synthesis gas for methanol synthesis reactors.

1.3 Combination between autothermal reforming and steam reforming

Commercially, autothermal reforming is not a single process for production of synthesis gas due to the high cost of operation (especially oxygen production), but it has been taken as a refining step after the main process which is steam reforming.

This combination between autothermal reforming and steam reforming is mainly used for production of synthesis gas for methanol production because the amount of carbon monoxide produced from steam reforming is too low for methanol production, so, it can be raised by adding autothermal reforming.

1.4 The main units in synthesis gas production plants

Practically, production of synthesis gas for methanol production involves many steps which can be shown as following:

1- Pretreatment of natural gas:

This step contains desulphurization unit to remove the sulfur content from natural gas.

2- Steam reforming of natural gas:

This step is often taken into two steam reformers to convert methane to hydrogen and carbon monoxide using steam at high pressure. Carbon dioxide can be produced in this step as well.

3- Air separation:

This level is to produce oxygen with purity of 99.5% for combustion in the autothermal reformer.

4- Autothermal reforming:

In this unit, additional reforming of remaining natural gas from steam reformers takes place into autothermal reformers using steam and oxygen to produce additional amount of carbon monoxide.

Carbon dioxide is also produced in this step. If the amount of carbon dioxide can not be neglected (from economical point of view), it can be recycled for additional reforming called *carbon dioxide reforming* to produce more hydrogen and carbon monoxide [1, 2, 3].

5- Heat recovery system:

Mainly, it comprises of heat exchanger built to utilize the hot gas from the autothermal reformer to supply the heat input for the steam reformer. It also called as gas – heated reformer. This would eliminate the expensive fired reformer.

Figure 1.1 shows the production of synthesis gas via autothermal reforming.

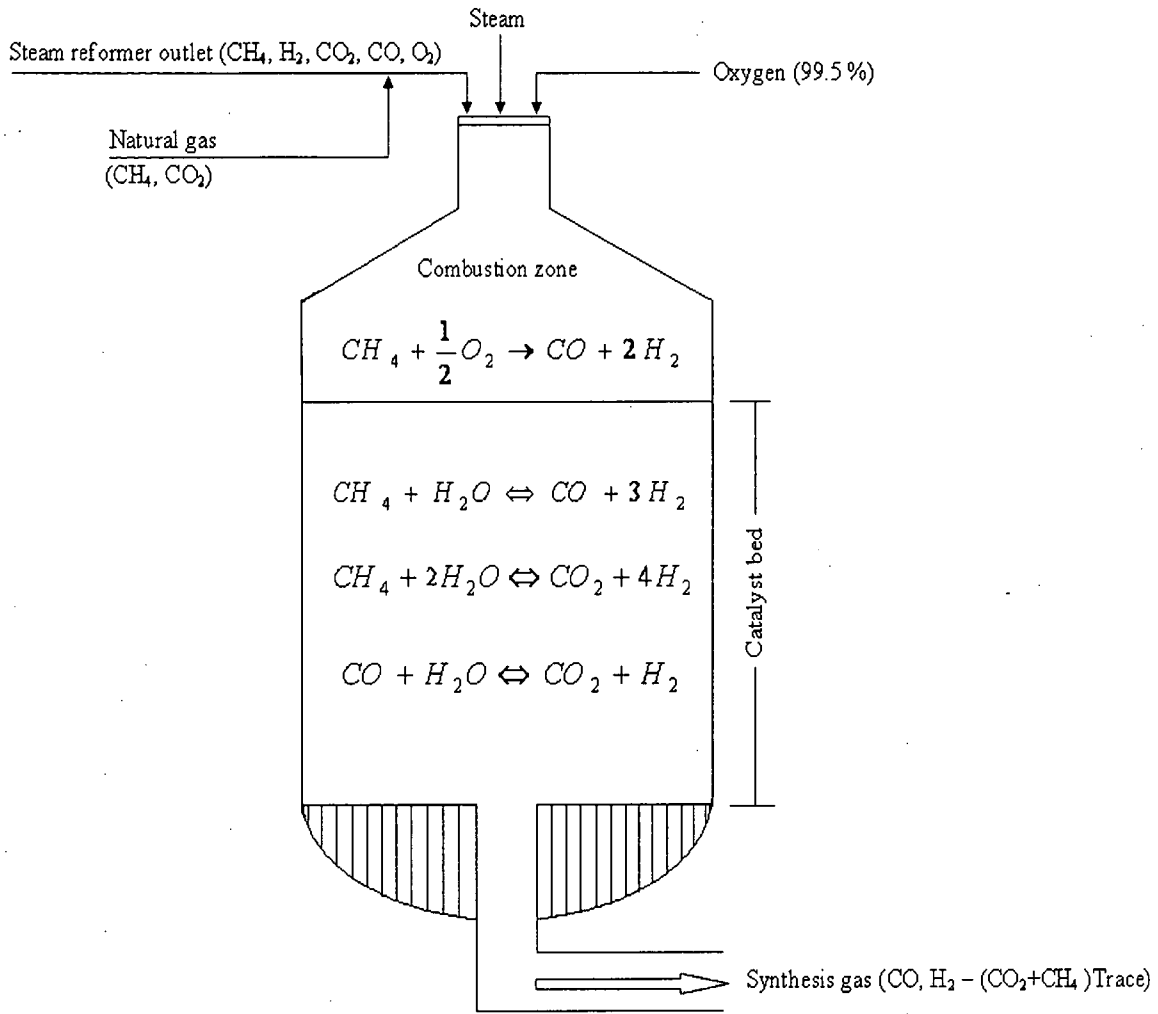


Figure 1.1. Synthesis gas production via autothermal reforming.

1.5 Problem statement

Autothermal reforming process is an established process, research in this area is divided into two main parts, the first part has taken natural gas reactions to study the kinetics of reactions which include activation energies, rate constants, and adsorption constants, and the second part has studied the effect of types of catalysts, compared between them, and the features of each catalyst such as Rhodium, Palladium, platinum, and metal oxides on process performance.

Nevertheless, practical problems still arise in plant operation such as determination of the amount of the catalyst volume that can be reduced due to some commercial constraints to control the specifications of the products and adjustment of temperature profile of autothermal reformer. By choosing effective temperature control of the unit, a long catalyst life and safer operating conditions due to high temperature and pressure can be achieved.

Thus, this study focused on simulation of autothermal reforming of PETRONAS Methanol Labuan Company (PML) as a case study by varying operating conditions such as catalyst volume, combustion temperature, and gas superficial velocity. By study these variables, better results of process performance can be achieved.

1.6 Objectives

- 1- To model the autothermal reformers by taking PETRONAS Methanol Labuan Company as a case study.
- 2- To study the effect of varying process variables such as the catalyst volume and combustion temperature on the temperature profile of the autothermal reformer as well as conversion of reactants and yield.
- 3- To validate the developed model with autothermal reforming plant data.

1.7 Scope of study

The scope of this work is to study the production of synthesis gas from natural gas via autothermal reforming, to build a model derived from the kinetics of natural gas reactions and the plants operating conditions and test the developed model by studying the effect of process variable on the temperature profile and conversion using the most commonly used catalyst on synthesis gas production plants which is supported Nickel catalyst.

The kinetics of natural gas reactions are referred from the previous work done in the area of synthesis gas production. The developed kinetics model was achieved by comparing many models according to the operating conditions and the type of catalyst used to derive the specific kinetics model.

Process data such as feed flow rates and operating pressure have been taken from PETRONAS Methanol Labuan (PML), where production of methanol from synthesis gas using autothermal reforming approached.

CHAPTER II
LITERATURE REVIEW

CHAPTER 2

2. LITERATURE REVIEW

2.1 Alternative routes for synthesis gas production

Production of synthesis gas "syngas" takes place in several steps. Firstly, a synthesis gas feed stock (such as natural gas or coal) is pretreated by desulphurization to prepare it for reforming, and then reforming takes place at high temperature (higher than 1075°C) in the presence of a catalyst [1]. Here *reforming* can be defined as a thermodynamically processing of synthesis gas feed stock in high temperature chemical reactors to produce a synthesis gas which can be used for production of many chemicals [2].

Depending on the type of reformers, synthesis gas feed stock reacts with steam or oxygen at high temperature (1000°C to 1200°C) and high pressure (15 to 30 bar) to produce a synthesis gas of hydrogen and carbon monoxide mainly with additional amount of carbon dioxide, methane, and steam. This produced synthesis gas is further processed according to the required final product which can be methanol, ammonia, and pure hydrogen [1, 2].

Industrially, there are three main routes to produce synthesis gas [1, 2] as discussed in the following sections.

2.2 Steam methane reforming

The steam methane reforming involves a reaction of hydrocarbons with steam in the presence of a catalyst, which is commonly supported nickel; this process is also known as *catalytic steam reforming* [2].

It is interesting that even though steam reforming reactions take place at high temperature (higher than 1000 K), a catalyst is still required to accelerate the reaction due to the high stability of methane [1]. Catalytic steam reforming of methane is a well known and commercially available process for synthesis gas production. In the United States, most of hydrogen today (over 90 %) is manufactured via steam reforming of natural gas [2].

The steam reforming reaction is represented by the following reaction:



$$\Delta H (\text{enthalpy of reaction}) = 206 \text{ kJ/mol}$$

This reaction is endothermic and requires heat input.

Mainly the reactor operated at pressure of 5 – 30 bar and temperature of 970K to 1120K. The external heat needed to derive the reaction is often provided by the combustion of a fraction of the incoming natural gas feed stock (up to 25 %) and some times – specially incase of hydrogen production – the heat required comes from burning waste gases such as purge gas from the hydrogen purification system.

2.3 Partial oxidation

This process is another commercially available method for deriving synthesis gas. It can be defined as the non-catalytic reaction of hydrocarbons with oxygen and usually steam (if catalyst is used, the process is referred to as *catalytic partial oxidation* CPO) [1].

Here methane (or some another hydrocarbon feed stocks such as oil) is oxidized to produce carbon monoxide and hydrogen (synthesis gas) according to the following reaction:



ΔH (enthalpy of reaction) = -36 kJ/mol

The reaction is exothermic and no indirect heat exchanger is needed. Catalysts are not required because of the high temperature. However, the synthesis gas yield per mole of methane input (and the system efficiency) can be significantly enhanced by use of catalysts [1].

The partial oxidation reaction is more compact than a steam reformer, where heat must be added indirectly via a heat exchanger. The efficiency of the partial oxidation unit is relatively high (70 – 80 %). However, partial oxidation systems are typically less energy efficient than steam reforming because of the high temperature involved (which exacerbates heat losses) and the problem of heat recovery [3].

In case of hydrogen production, in steam methane reforming plants, heat can be recovered from the flue gas to raise steam temperature for the reaction and the purge gas can be used as a reformer burner fuel to help provide heat for the endothermic steam reforming reaction. In partial oxidation reactor where the reaction is exothermic, the energy in the purge gas can't be fully recovered.

Because they are more compact and don't require indirect heat exchange (as in steam reforming), it has been suggested that partial oxidation systems could be lower cost than steam reformers. Although the partial oxidation reactor is likely to be less expensive than a steam reformer vessel, the downstream shift and purification stages are likely to be more expensive [2].

2.4 Autothermal reforming

Autothermal reforming is a combination between steam reforming and partial oxidation, in another way; it is a combination between exothermic and endothermic reactions. Autothermal reformers combine some of the best features of steam reforming and partial oxidation systems.

In autothermal reformers a synthesis gas feed (methane in natural gas) is reacted with both steam and oxygen to produce synthesis gas (oxygen here either to be pure oxygen or air according to the usage of produced synthesis gas)

The main autothermal reforming reactions are:



ΔH (enthalpy of reaction) = 206 kJ/mol



ΔH (enthalpy of reaction) = -803 kJ/mol



ΔH (enthalpy of reaction) = -36 kJ/mol

Autothermal reformers utilize all the heat generated by the partial oxidation reaction to accelerate the steam reforming reaction. Thus, autothermal reformers typically offer higher system efficiency than partial oxidation systems, where excess heat is not easily recovered [2].

Autothermal reformers are refractory lined vessels. Therefore, higher pressures can be applied than in steam reformers. Part of the feed is oxidized in the combustion zone (the top of the reactor). In the lower part the remaining feed is catalytically reformed with the produced carbon dioxide and steam. Figure 2.1 below shows the schematic features of an autothermal reformer [2, 4].

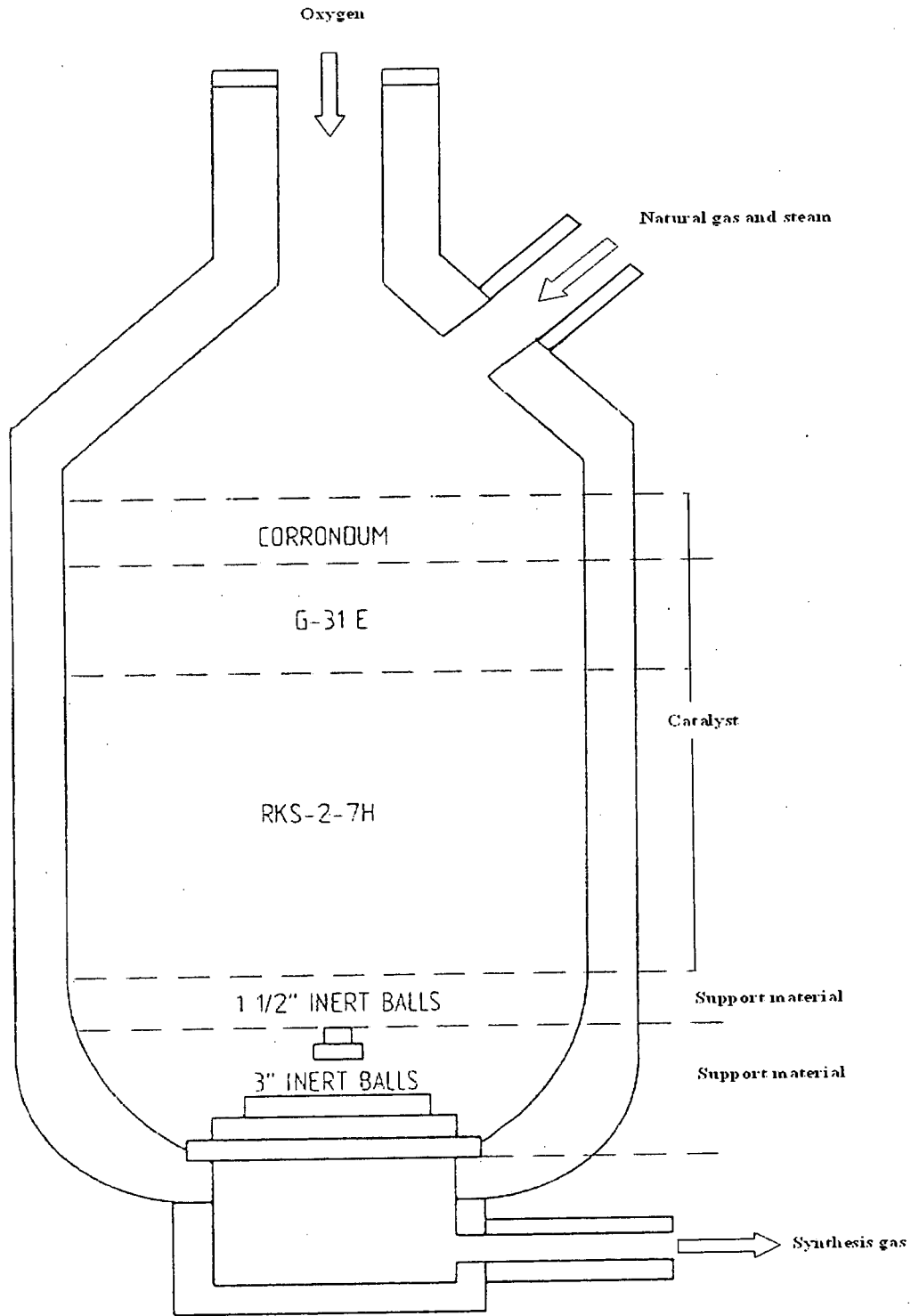


Figure 2.1: Autothermal reformer used in PML.

2.4.1 Autothermal reforming for hydrogen production

Various experimental and modeling studies have been conducted for autothermal reforming process for hydrogen production. D. L. Hoang and et al [6, 7] have performed experiments with different feedstock using sulfide nickel supported on a gamma alumina as a catalyst to investigate hydrogen production for fuel cells by autothermal reforming. Their results show that the performance of the reformer is dependent on the molar air to fuel ratio, the molar water to fuel ratio and the flow rate of the feedstock. They have found that, a methane conversion of about 95 – 99 % and hydrogen yield of 39 – 41 % on a dry basis can be achieved. And 1 mole of methane can produce 1.8 moles of hydrogen at an equilibrium reactor temperature of not exceeding 850⁰C.

Generally, the results show that the conversion behavior of the reactor strongly depends on the air to fuel ratio, water to fuel ratio and the inlet mixture flow rate. The optimum values of these parameters are 3 – 3.5, 2 – 2.5, and 250 L/h respectively [6]. The same trends on hydrogen production have been achieved by other researchers such as Cunping Huang and Ali T-Raissi [8], P. J. Dauenhauer and et al [9], and Murata et al. [10].

2.4.2 Temperature profiles in autothermal reforming process

James R. Lattner and Michael P. Harold [11] have constructed a bench-scale fixed-bed reactor for the autothermal reforming of methanol under near-adiabatic conditions to experimentally demonstrate the conversion of methanol to hydrogen over copper-based catalysts. The temperature measured at discrete axial positions and the maximum temperature achieved was 360°C. The results of temperature profiles under these conditions show that the maximum temperature is the combustion temperature after the inlet of the reactor, then, the temperature decreases along the axial position until the outlet of the reactor where the minimum temperature recorded [11]. Same kinds of temperature profiles were observed for alumina-supported noble metals catalysts [12, 13], rhodium catalysts [14], and metal oxides catalysts [15].

Generally, the maximum temperature of autothermal reformers occurs directly after the inlet of the reformer where the combustion of methane takes place, then; the temperature starts to decrease along the axial position due to the endothermicity of the reactions (steam reforming reactions) where the heat needed for these reactions will be supplied by the heat generated from methane combustion. The temperature reaches the minimum value at the outlet of the autothermal reformer [16, 17, 18, 19].

2.5 Kinetic models:

In the modeling of all the reactions for synthesis gas production, it is necessary to choose the proper values for the rate constants and all the parameters of the rate equations such as rate constants and activation energies.

Kinetic equations for some of the reactions were proposed by Hickman and Schmidt [20], built upon Pt and Rh catalysts. Also Trimm and Lam [21] have published a kinetic equation for the complete combustion of methane to CO₂ and H₂O over Pt/Al₂O₃ catalyst, under the assumption that the rate determining step is the surface reaction between adsorbed oxygen and oxygen from the gas phase [22]. This set of kinetic equations has been used by De Groote and G. Froment [22].

Smet and et al [23] have taken the kinetics of methane combustion from Trimm and Lam and since the kinetic model was derived using Pt catalyst, the corresponding adsorption parameters were adjusted for Ni catalyst. Ni catalyst was assumed to be in the reduced state, which implies that, the total combustion reaction and reforming reactions are in parallel.

In order to investigate the influence of the reforming kinetics on their simulation results, they have considered two intrinsic kinetic models:

- (i) Reforming model proposed by means of Xu and G. Froment (1989).
- (ii) Kinetic model derived by means of Numaguchi and Kikuchi (1988).

Xu and Froment reforming model was obtained using relatively low temperature ($773\text{K} < T < 848\text{K}$) and operating pressure between 3 and 15 bar. In this model, the Ni content is 15.2 wt %, and the metal surface area is 4.1 m²/g [39, 42].

For production of synthesis gas from natural gas, the exothermic total combustion may lead to high catalyst temperatures, and an increase in methanol production from synthesis gas, high operating pressure will be required (25 – 30 bar).

The second model which is derived by means of Numaguchi and Kikuchi was derived at high catalyst temperature (up to 1160 K), and high operating pressure (up to 25 bar). The Ni content in this model is 8.7 wt %, and the metal surface area is 3.6 m²/g.

According to the operating conditions (temperature and pressure), the second model seems to be more suitable in case of methanol production, but the nickel content and the metal surface area are higher in the first model so it should be taken into account as well.

The C-formation zones were based upon thermodynamic calculations. Wagner and Froment [24] predicted the zones in which C-formation is possible through methane cracking and through the Boudouard reaction by means of experimentally determined 'threshold constants'. To go beyond this and to predict the amounts of carbon that can be formed on the catalyst requires kinetic equations. These were also derived by Wagner and Froment [25] from experiments in a differentially operated electrobalance reactor [22, 37, 38].

2.6 Reactor models:

De Groote and Froment [22] has simulated adiabatic fixed-bed reactors with a catalytic combustion zone fed with methane / oxygen or methane air mixture based upon the kinetics of total combustion, steam reforming, and water – gas shift reaction on a Ni catalyst.

They have assumed that the steam reforming reactions and water – gas shift reaction are in parallel or more or less consecutive to the total combustion and depending upon this assumption, they have proposed a kinetics model and they have calculated the net rate of coke formation in their simulation and also investigated the influence of carbon dioxide in their study.

In their case, they proposed to keep the operating temperature as low as possible because of the bifunctional combustion / steam reforming catalyst. In this case, there is availability for carbon (coke) formation (carbon can be formed if the inlet temperature is lower than 450°C), so, the kinetics of carbon formation reactions must be included and this is why they have taken the carbon formation into their account.

For the simulation of the partial oxidation of methane to synthesis gas via Ni catalysts, a one dimensional heterogeneous model was used. Since the reactor is adiabatic, concentration and temperature gradients only occur in the axial position [22].

C. R. H. de Smet and et al [23] have designed adiabatic fixed – bed reactors for the catalytic partial oxidation (CPO) of methane to synthesis gas for the production of methanol and fuel – cells based on supported Ni catalysts.

In their simulation, they have used a steady – state, one dimensional heterogeneous reactor model and they have taken the intra – particle concentration gradients into account by solving the continuity equations in the catalyst pallet at each position along

the fixed – bed reactor. They considered the transport mechanism in the axial direction to be plug – flow type and it has been checked that axial dispersion of heat and mass could be neglected as well as the pressure drop according to their operating conditions.

In this model, the fixed – bed reactor (lab scale reactor) was operated at high pressure in case of methanol production to reduce the compression costs, and they have used a reactor length of 3 m to obtain equilibrium conditions. The reactor diameter was calculated from the required methanol capacity and the equilibrium methane conversion rate. Oxygen was used instead of air to avoid downstream nitrogen separation; water was included in the feed to suppress coke formation

As a result of these parameters, they have shown the temperature profile using both kinetics models of Xu and Froment and Namaguchi and Kikuchi. The temperature profile shows that the catalyst temperature starts from 1330 K (combustion temperature in this case), then increases in the first part of the catalyst bed until it reaches the maximum temperature after 0.5 m of the catalyst bed height and then decreases again regularly until it reaches the outlet temperature of 1275 K.

These results seems to be acceptable from a point of view of inlet and outlet temperature, but it contrasts some of plants data which it shows that there is no oscillation or peaks in the temperature profile (e. g. PETRONAS Methanol Labuan in Malaysia and Lurgi Mega Methanol in Germany) shows that the maximum temperature inside the reactor is the combustion temperature and then the temperature decreases until the outlet temperature at the end of the reactor bed.

Because of the assumption (in this research and all the models which have been done by the others [21,22,23]) which is assumed that the methane combustion is the first reaction inside the autothermal reformer, then followed by steam reforming and water – gas shift reaction (these two reactions can be in parallel or consequently), it can said that, it must not be any peaks or increase in the temperature gradient, because the temperature of combustion (in the first part of the bed height) is the highest temperature in this process,

and this temperature is the source of heat for the whole endothermic reactions, so, the temperature must decrease along the height of the reactor bed.

Another reactors model has been studied by Ostrowski, Giroir – Fendler, Mirodatos, and Mleckzo [26]. They have simulated the catalytic partial oxidation of methane to synthesis gas at industrial conditions (pressure between 5 to 30 bar and temperature between 1023 – 1073 K) using both fixed – bed and fluidized – bed reactors with the kinetics models proposed by De Groote and Froment for Ni catalysts.

The simulation results indicated that low synthesis gas yield are obtained in case of fixed – bed reactors, because of the large influence of intra – particle diffusion limitation. Equilibrium conditions were obtained in this case when the space – time was increased by a factor of 6. In the fluidized – bed reactor, significantly higher yields were achieved at identical space – time.

In the later case, small catalyst particles were applied compared to the fixed – bed reactors and the effect of pore diffusion on the reaction rates were negligible. It was shown that integrated product separation by means of membrane can improve the synthesis gas yield significantly [7, 8].

2.7 Parametric study:

Effect of H₂ and CO₂ content in the feed mixture

2.7.1 Effect of H₂ content in the feed mixture

Specific amount of hydrogen is required in the feed mixture to avoid the infinity of the rate of reactions, because these rate equations are functions of the partial pressure of hydrogen, so, it is necessary to avoid the partial pressure of hydrogen equal to zero by adding hydrogen to the feed mixture [22]. These reactions are discussed further in the next chapters.

Autothermal reformers do not need any additional amount of hydrogen, because the amount of hydrogen in the feed from the downstream of steam reformers of 50 % is sufficient.

Influence of hydrogen in the feed mixture has been investigated by adding H₂ to the feed mixture, where 10 % of H₂ added, the percentage carbon deficiency is lower by about 6%, but the conversion of methane is about 3 % lower [22].

For a mixture containing hydrogen, the maximum temperature in the catalyst bed is slightly lower. In the presence of H₂, there is no temperature decrease near the reactor inlet and the temperature peak is shifted upstream. It is clear that when hydrogen is added to the feed mixture there is no carbon formation due to the endothermic methane cracking near the reactor inlet. Because of this, there is no temperature decrease and the combustion reaction starts further upstream in the reactor [22].

The fraction of the catalyst bed covered with carbon is significantly smaller for a feed mixture containing hydrogen, but the net coking rate is higher than for a hydrogen-lean feed, so that this part of the catalyst bed is subject to severe deactivation.

It may be concluded that adding hydrogen to the feed mixture only prevents methane cracking in the first part of the reactor and it is not efficient for avoiding carbon deposition [22].

2.7.2 Effect of CO₂ in the feed mixture

Most of natural gas contains carbon dioxide. According to the amount of CO₂, natural gas can be pretreated for CO₂ removal. In spite of CO₂ removal process, small amount of CO₂ remains in natural gas, so, it is necessary to investigate the effect of CO₂ in the feed mixture [1].

Influence of carbon dioxide and hydrogen in the feed mixture for autothermal reformers using Ni catalysts have been investigated by De Groot and G. Froment [22].

Effect of carbon dioxide in the feed mixture was investigated at pressure of 25 bar and constant methane feed using a reactor length of 3 m and 6 m for another model called BV-model. It has been achieved that addition of carbon dioxide and steam to the feed is mainly reflected in the H₂ / CO product ratio. Adding carbon dioxide to the feed decreases the conversion of methane, but increases the conversion towards CO, thus leading to a synthesis gas with lower H₂ / CO product ratio. On the other hand, the H₂ / CO ratio in the effluent become higher when steam is added.

By adding carbon dioxide or steam to the feed mixture, a synthesis gas with a desired H₂ / CO ratio in the effluent can be produced. A given H₂ / CO ratio in the effluent can also be obtained by changing the CH₄ / O₂ feed ratio. The low carbon balance result either from a high rate of carbon deposition or from its insufficient gasification.

As mentioned before, natural gas may contain a high amount of CO₂ which can be separated, recovered, and purified based on either absorption or adsorption or membrane separation for further CO₂ reforming to produce synthesis gas.

A process concept called tri-reforming of methane has been proposed by means of Chunshan Song and Wei Pan [27], using CO₂ in the flue gases from fossil oil-based power plants without CO₂ separation.

The proposed tri-reforming process is a combination of CO₂ reforming, steam reforming, and partial oxidation of methane in a single reactor for production of synthesis gas.

This process has been taken place in a fixed-bed flow reactor at 850⁰ C and 1 atm pressure with supported nickel as catalyst. Different nickel catalysts were studied to investigate tri-reforming process [27].

The results of this study show that, over 95 % of methane conversion and about 80 % of CO₂ conversion can be achieved in tri-reforming process over nickel catalysts supported on an oxide substrate. CO₂ and methane conversion increase with the increasing of reaction of all nickel catalyst types.

At equilibrium, the minimum conversion of methane achieved was 86% at 700⁰ C, where the maximum conversion was 97.9% at 850⁰C. For CO₂, the minimum conversion achieved was 55.6% at 700⁰ C, where the maximum conversion was 87% at 850⁰C [27].

It has been shown that, coke formation in this process can be avoided at temperature higher than 800⁰ C. Amount of coke of 0.25 to 0.8 mol/mole methane can be obtained at 700⁰ C. and this amount increases at lower temperatures.

These results show that, a suitable conversion of methane and CO₂ can be achieved at atmospheric pressure, but most of synthesis gas is used for production of chemicals requires a relatively high pressure (15 to 40 bar), so, from economical point of view, it is

favorable to use a high synthesis gas stream pressure to reduce the costs of compression for the downstream and this feature can not be achieved via tri-reforming process which has been obtained at 1 atm, but this process can be useful for production of synthesis gas for fuel cells where no high pressure of downstream is required.

2.7.3 Effect of air on the steam methane reforming:

The effect of adding air to the feed in steam methane reforming was investigated by Joelmir A. C. Dias and Jose M. Assaf [28] over nickel catalyst. The catalyst exhibited a high specific surface area, but low metal surface area. It has been found that, the addition of air to the feed mixture in the steam reforming of methane offers some advantages. The first is a decrease in the amount of carbon deposited on the catalyst. Another advantage of adding air to the feed mixture is that the endothermicity of the process is reduced, so that hydrogen may be generated without consumption of external energy, making it viable to produce this gas for use as a fuel [28].

2.8 Types of catalysts for synthesis gas production:

Various types of metals can be used as catalysts to promote natural gas to synthesis gas including nickel, cobalt, iron, and the platinum group metals, the use of these metals as catalysts were reviewed by means of S. C. Claridge and M. L. H Green [29].

It has been shown in their study that, nickel catalysts emerged as the most practical catalysts because of their fast turnover rates, long-term stability, and cost.

The major technical problem for the nickel catalysts is whisker carbon deposition on the catalyst surface which can lead to the plugging of the reformer tubes. It has been found that, carbon deposition could be substantially reduced by the use of an excess water and temperature of about 1073 K. Under these conditions carbon deposition is thermodynamically unfavorable [29].

Also they have shown the effect of temperature on the equilibrium partial pressure at 1 atm. They have found that, the equilibrium partial pressure of methane, carbon dioxide, and water decrease with the increasing of temperature from a maximum of 0.15 bar to 0.05 bar minimum, whereas the equilibrium partial pressure of hydrogen and carbon monoxide increase with the increasing of temperature from 0.15 bar as minimum to 0.4 bar as maximum for hydrogen and from 0.05 bar as minimum to 0.2 bar as maximum for carbon monoxide.

A further investigation on carbon deposition using different catalysts has been done in this study. It was found that the relative rate of carbon deposition follows the order of Ni > Pd >> Rh, Ru, Pt, Ir. Very little carbon deposition was found over the noble metals catalysts especially those of palladium and iridium for which, even after 200 hours, negligible carbon deposition and catalyst deactivation was observed. This observation shows that carbon deposition can be avoided by using the suitable catalysts.

The choice of specific catalyst depends not only on the effect of carbon deposition, catalyst deactivation, or the conversion which can be achieved, it also depends on other constraints such as the availability of this catalyst, the cost, and life time.

2.8.1 Rhodium catalysts:

Goralski, O'Connor, and Schmidt [30] have modeled a high temperature short – contact time catalytic rhodium monolith reactor for the production of synthesis gas from methane as a plug – flow tubular reactor using detailed heterogeneous and homogeneous reactions. They have performed their simulation at different pressure; preheat temperatures, compositions, and catalyst pore sizes.

In their calculations, they have shown that there is a significant interplay between heterogeneous and homogeneous reaction, which is generally unselective for synthesis gas production, it favored by high pressure, large catalyst pores, and high preheat temperature. Also in this case, they have shown that the onset of gas – phase chemistry can be avoided by feeding air rather than oxygen into the reactor.

The results of this model shown that it is preferable to operate the reactor using this catalyst at lower temperature, because the selectivity of carbon monoxide and hydrogen decrease with the increasing of the operating pressure and temperature inside the reactor. The catalyst temperature increases with the increasing of preheat temperature, this leads to a higher methane conversion (the highest catalyst temperature gives the highest methane conversion), but for this type of catalysts, it is preferable to operate the reactor at high temperature (higher than 600⁰C) so, it is important to balance it to achieve an economical methane conversion using moderate temperatures. Also the results of this model show that the highest catalyst pore size gives the highest selectivity of carbon monoxide and hydrogen, but at the same time, it gives the lowest selectivity of carbon dioxide and water, which it means the composition of the produced synthesis gas can be

controlled by controlling the catalyst pore size. The catalyst pore size effect intrinsically the composition of produced synthesis gas [30].

Production of synthesis gas using this type of catalysts can be applied for production of hydrogen and fuel cells (from a point of view of operating conditions, specially temperature and pressure), but it is not suitable for production of methanol due to the low temperature and pressure of the effluent (methanol reactors operated at temperature higher than 1000 K and pressure of 40 bar approximately), and in this case, the effluent temperature and pressure are 620⁰C and 15 bar respectively, which can lead to higher costs by adding heat and compression for the downstream [30].

2.8.2 Metal oxides catalysts:

Depending on Ga₂O₃, SnO₂, or V₂O₅ supported on γ – Al₂O₃ catalysts, Wierzchowski and Zatorski (2003) [31] have studied the kinetics of carbon monoxide and methane oxidation under the stoichiometric conditions.

They have found that the catalytic activity depends on the pretreatment conditions (oxygen or hydrogen atmosphere) of the catalyst. They have investigated the detailed kinetics to determine the reaction rates and adsorption coefficients of Langmuir – type equations in the case of catalysts pretreatment under oxygen atmosphere and reaction calculated with oxygen excess.

All the catalysts have been prepared by the cooperating partners from France (Institute de Recherché Sur Catalyse, CNRS), Italy (Milan University), and Romania (Viga Refinery) to allow some variation and cooperation between the academic study and the practical applications. Samples of the catalysts were put in the quartz tube reactor and pretreated in the various conditions prior to the catalytic run.

The results of these catalysts in case of methane conversion to synthesis gas show that a total conversion between 0.5 and 12.5 % of methane can be achieved at 534 °C. Catalysts activity is influenced by pretreatment conditions and the specific activities are higher for the catalysts pretreated under hydrogen flow than reduced catalysts and the activity of Sn catalyst is the highest one. The highest rate of methane of methane combustion was achieved via Gallium oxide catalyst where the Vanadium oxide supported catalyst exhibited the lowest activity.

It has been shown that hydrogen pretreatment increases oxidation activity for tin and gallium catalysts and the high temperature hydrogen pretreatment (630°C) of tin and Gallium oxides catalysts significantly decrease the activation energy of methane combustion [31].

For specific feed mixture using Zink oxide catalysts, it has been found that the highest feed conversion (83 %) can be achieved using powder catalyst, where the lowest conversion (20 %) observed when the pellet catalyst was used, the paper shape catalyst gives a moderate conversion between the powder shape and pellet shape [32].

2.8.3 Palladium catalysts:

Methane combustion over palladium catalysts has been investigated by means of R. E. Hayes, and et al [33] in a monolith reactor. They have determined the rate equations and showed an approximately first order dependence on methane concentration and zero order dependence on oxygen concentration.

Significant inhibition by water was observed, but the inhibition by carbon dioxide was negligible. For the dry feed, catalyst activity and activation energy reduction was observed significantly above temperature above 820°C.

Different catalyst compositions were prepared and used to investigate methane conversion. For all these compositions, methane conversion increases with the increasing of the inlet gas temperature (the maximum inlet gas temperature was 900 K). The maximum conversion achieved was 25% for some of catalysts compositions, but in another cases, there were no or minimal conversion achieved (the conversion was zero or approximately zero) and the same trend was observed when the pre-burner was operating. Effect of channel inlet velocity was investigated; they have found that the conversion of methane decreases with increasing velocity.

The kinetic model was developed for palladium catalysts, and it has been shown that the rate constants increase with increasing temperature, and methane conversion was observed and presented when no water added or water was added to the feed. Also the axial wall temperature profiles were simulated at various inlet gas temperatures, it has been found that the wall temperature approximately increases linearly with the increasing of inlet gas temperature [33].

2.8.4 Platinum catalysts:

Beside Ni catalysts, platinum is one of the most important catalysts for synthesis gas production from natural gas, because of the low initial activity, the high stability, and the high performance of the reaction with steam at high temperatures. The higher resistance of coke formation of the catalyst supported on ceria is one of the features of platinum catalysts due to the metal – support interaction and the higher mobility of oxygen in the oxide lattice [34].

This catalyst has been studied by means of M. Souza, and et al using a fixed – bed flow – type quartz reactor loaded with 20 mg of catalyst under atmospheric pressure [34].

Using the same concept of autothermal reforming of methane to synthesis gas via Ni catalyst, which it combines partial oxidation and reforming of methane with CO₂ or

steam, this model was carried out with three different formulas of platinum catalysts, Pt/Al₂O₃, Pt / Zr₂O, and Pt / CeO₂, which were prepared by incipient wetness impregnation of the supports with an aqueous solution of chloroplatinic acid followed by drying at 120⁰C for 16 hours and calcinations in air at 550⁰C for 2 hours. All the samples contained about 1 wt % of platinum, which was determined X – ray fluorescence. This procedure formulated by Souza and Schmal [35].

The results of this study show that the oxygen conversion is 100 % starting from 450⁰C, all three catalysts presented similar activities, with Pt / Zr₂O was being slightly less active in a range of temperature between 450 – 600⁰C and the most active at temperature higher than 700⁰C.

At the end of the reactor, methane conversion of approximately 92 % was achieved via Pt / Zr₂O, which it reflects the higher methane conversion in case of a combination between partial oxidation and carbon dioxide reforming of methane.

In case of a combination between partial oxidation and carbon dioxide reforming using Pt / CeO₂ catalyst, the composition profiles show that a composition contains 33 % hydrogen and 38 % carbon monoxide can be achieved via this model [33].

This ratio between hydrogen and carbon monoxide is suitable for some chemicals production, but it is not suitable for production of methanol which is roughly around 2.5 (H₂ / CO), anyhow, it has been presented in this study that H₂ / CO product ratio can be manipulated according to the addition of carbon dioxide or steam to autothermal reformers and it is possible to achieve the optimum ratio for GTL (gas to liquid) processes (H₂ / CO = 2) by coupling steam reforming and partial oxidation of methane, but in some GTL processes such as hydrogen production or methanol production, a higher pressure downstream is intrinsically required to reduce the cost of compression [41].

This model has been derived under atmospheric pressure, so to use it for production of synthesis gas for methanol production, another case must be added. This case is the conversion of methane under higher pressure (25 – 30 bar) and another question must be answered about minimum and maximum H_2 / CO ratio can be achieved using high pressure models.

2.8.5 Effect of adding metals to catalysts:

Joelmir A. C. Diass and Jose M. Assaf [36] have investigated the effect of adding small amounts of Pt, Pd and Ir (<0.3 wt %) to nickel catalysts for the autothermal reforming of methane, it has been demonstrated that platinum, iridium, and palladium increase methane conversion during autothermal reforming process. Methane conversion during autothermal reforming was found to rise proportionally with the metal surface area. Therefore, it is proposed that the effect of these low contents of these noble metals in the catalyst is limited mainly to increase the area of the exposed metal surface to reaction, irrespective to the noble metal added [36].

2.8.6 Summary of literature review

From these literatures review, it can be seen that, most of the work in the area of synthesis gas production from natural gas is focused in three specific parts. The first part is the investigation of the kinetics of natural gas reactions which are taken as methane reactions. This part has been studied intensively by investigating the kinetics parameters using different operating conditions (mainly the operating temperature and pressure). The second part is the studies on the routes of synthesis gas production. These routes are partial oxidation, steam reforming and autothermal reforming using different types of feedstock such as natural gas and coal. The third part is the studies on the types of catalysts which can be used to produce synthesis gas. It is found that, most of the catalysts investigated are suitable for hydrogen production for fuel cells where less temperature and pressure are required.

CHAPTER III
MODELING OF SYNTHESIS
GAS LOOP

CHAPTER 3

3. MODELING OF SYNTHESIS GAS LOOP

3.0 Introduction

This chapter describes the development of the model that is used in this work. The model was derived to investigate the temperature profile of autothermal reformers as the main variable under study and the effect of the other reactor variables on it, thus, the rate of reactions and yield can be investigated according to temperature profile obtained.

This steady state model has taken the practical part which contains the operating conditions of the plants and combined it with the kinetics of methane reactions which describe the rate of reactions. This chapter consists of two main parts which are:

(a)- Research methodology:

This part describes the steps to develop the model of autothermal reformers by showing the information required to derive this model.

(b)- Model configuration:

This part comprises the equations of the model and the procedure of calculations of the parameters required in these equations depending on the plant data and kinetics parameters.

3.1 Research methodology

The objectives of this work can be achieved by dividing the work into steps according to the consequence of required information calculations to derive the final model of autothermal reformer. These steps can be divided as the following:

3.1.1 Data collection

As it is mentioned in the previous chapters, autothermal reformer is a part of a complex process to produce synthesis gas from natural gas.

To model this reformer, it is inevitable to get sufficient information and data about the whole process. These data can be achieved from two main sources which are:

a) Plants data

These are the data collected from PETRONAS Methanol Labuan Company which is taken as a case study.

This part contains:

- **Process Flow Diagram (PFD)**

This diagram is required to know the main steps of production of synthesis gas and to show the flow rate at each stream to finalize the total inputs and outputs of the autothermal reformer under study. This diagram is shown in appendix A.

- **Operating pressure**

The operating pressure and the partial pressures of compounds are required to calculate the rate of reactions. The pressure values are needed to choose the appropriate kinetics parameters which have been derived at different pressures according to the conditions of each experiment done.

- **Catalyst information**

This part contains:

- Catalyst name.
- Catalyst density.
- Catalyst pore size.
- Catalyst volume.

The catalyst density affects mainly the rate of reactions, conversion, and temperature profile, where the catalyst pore size is required to calculate the pressure drop inside the reactor according to Ergun equation [40].

- **Streams composition**

Streams compositions are required to calculate the fraction of each compound at each stream to finalize the compositions of the input and output of the reactor.

Composition of streams is shown in appendix A.

- **Autothermal reformer data**

The data required about the autothermal reformer are the design parameters which are required to build the reactor model and material balance, mainly it contains:

(I) Combustion temperature

Autothermal reformer contains combustion zone for methane combustion reaction. There are various types of burners for this combustion which can give different combustion temperatures, so, it is necessary to obtain the actual value of combustion temperature in this process because it affects intrinsically on the bed temperature and conversion of feed.

(II) Reactor cross-sectional area (A)

Reactor cross-sectional area is required for calculations of catalyst bed volume and conversion.

(III) Catalyst bed height

Catalyst bed height is required to calculate the catalyst bed density for conversion calculations and to calculate the void which is required for pressure drop calculations.

b) Data from literature:

The kinetics of methane reactions have been studied widely by means of many researchers either by investigating different catalysts or by different conditions.

The required data in this step are:

- Reactions enthalpy.
- Reactions rate equations:

This contains:

- a- Rate constants (k), reaction dependent.
- b- Adsorption constants (K).
- c- Equilibrium constants (K_i).

3.1.2 Kinetics model investigation:

There are different kinetics models derived using different catalysts and different operating conditions as it shown in the chapter 2.

In this step, a comparison between the conditions of kinetics models derivation and the plant operating conditions will be necessary to choose the appropriate model which matches the same operating conditions or approximately same conditions.

This comparison will be based on two main points which are:

3.1.2.1 The catalyst type:

It is crucial to develop a kinetics model involving Nickel catalyst which is used in this process.

3.1.2.2 Operating pressure and temperature:

Some of kinetics model derived at high pressure ($P > 25$ bar), such as Trimm and Lam [21], some of them derived at moderate pressure ($15 < P < 25$ bar) such as De Groote and Froment model [22], and some of them derived at approximately low pressure ($P < 15$ bar).

The priority will be for model achieved at the same pressure of the process. If there is no model achieved at this pressure, the kinetics model achieved at the nearest pressure will be used.

Same procedure will be followed to investigate the temperature of kinetics model to match the plant operating temperature.

3.1.3 Determination of reactions rates

Reactions rates will be calculated by combining the required data from plant operation and literature data with the chosen values for the kinetics model parameters in the reactions rate equations.

The data required for the rate equations are:

- Concentration of methane and oxygen.
These concentrations will be calculated from the over all material balance.
- Rate constants.
The rate constants will be calculated according to Arrhenius equation
- Adsorption constants
These constants will be calculated according to Trimm and Lam [21]
- Partial pressure of oxygen, methane, carbon monoxide, carbon dioxide, and hydrogen.
The partial pressure will be calculated according to Raoult's law which describes the partial pressure of component i as a function of the total pressure and the mole fraction of component i .

3.1.4 Reactor model and simulation:

3.1.4.1 Reactor model:

The reactor model will be built based on the final kinetic model achieved which shows the rate of reactions including all the kinetics parameters and mass balance which gives the flow rate and composition of the reactor feed.

The equation which shows the energy balance and temperature profile parameters will be included and discussed more on the model configuration part.

Assumptions of the model:

- One dimensional heterogeneous reactor model.
- Steady state operation.
- The reactor is adiabatic.
- Concentration and temperature gradients only occur in the axial direction.
- The catalyst is uniform.
- Momentum balance is ignored.

3.1.4.2 Reactor simulation:

The simulation of the reactor model will be built on MATLAB 7.1 software using loops configuration to include all the reactor parameters on the program of simulation to allow further study for them. The configuration of the algorithm followed to build the simulation model will be shown in the model solution procedure.

3.1.5 Reactor model validation:

The first validation of the model results will be achieved by comparing the temperature profile (the most important variable) achieved with the corresponding temperature measurements which include the temperature at top, middle, and bottom of autothermal reformer under study.

3.1.6 Effect of process variables study:

This step includes:

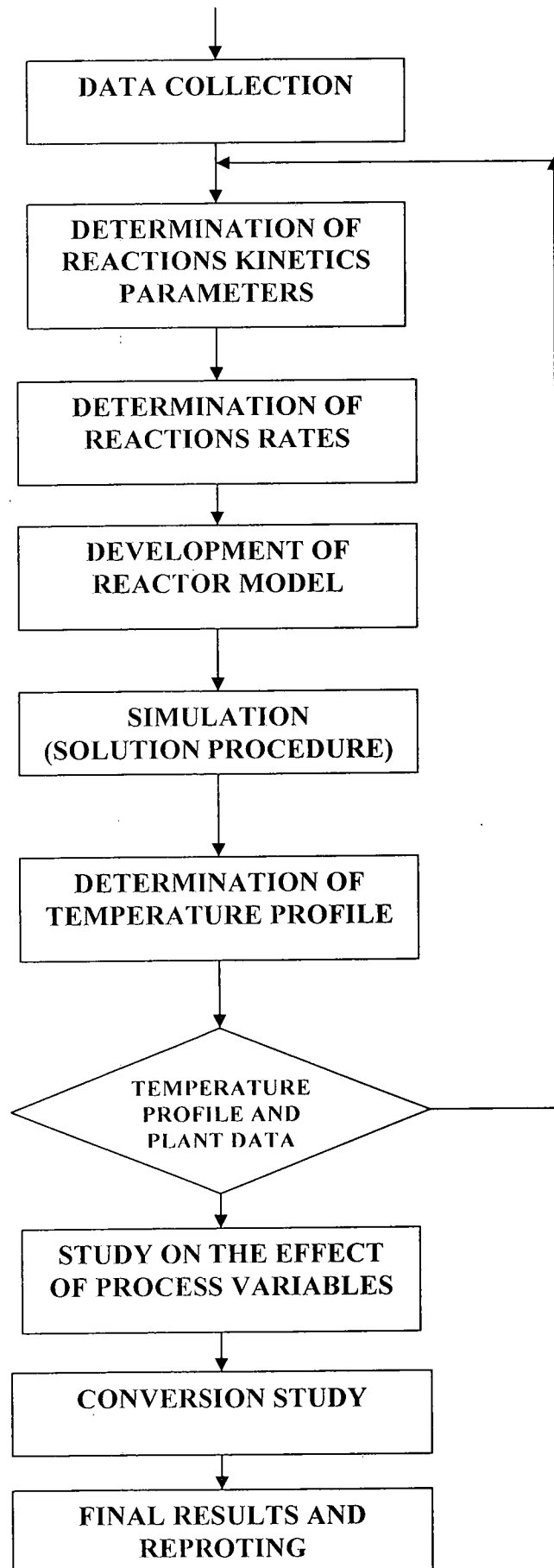
- Effect of catalyst volume on the temperature profile.
- Effect of gas superficial velocity on the temperature profile.
- Effect of burner temperature (combustion temperature) on the temperature profile.

The most important variable in this model is temperature, because it affects directly on the rate of reactions and conversion, so, the temperature profile will be studied first, and then, the corresponding rate of reactions and conversion can be achieved.

3.1.7 Calculations of conversion

This step will be taken to study the yield achieved using different values of reactor parameters used in the reactor model including:

- (I) Percentage of reacted and generated compounds at each unit along the catalyst bed height.
- (II) Molar flow rate of each compound at each unit of the catalyst bed.
- (III) The corresponding molar fractions of these compounds.



Methodology chart

3.2 Model Configuration

3.2.1 Process description

As it mentioned in the chapter 2 [1, 2], there are various industrial methods to produce synthesis gas from natural gas. A model of an autothermal reformer combined with steam reformers (appendix A) will be developed in this research by taking output of steam reformers and pure natural gas as the input of the autothermal reformer.

The feed of autothermal reformer under study consist of:

- 1- Steam.
- 2- Oxygen with a purity of 99.5 %.
- 3- Pure natural gas and steam reformer outlet.

Table 3.1 shows the composition of pure natural gas and steam reformer outlet which will be mixed to be fed to the autothermal reformer.

From the process flow diagram (PFD) and composition of each stream, over all material balance has been done to calculate the final input and output of the autothermal reformer including the flow rate and molar fraction of each compound (appendix B).

Table 0.1 Composition of natural gas and steam reformer outlet:

Stream	CH ₄ %	H ₂ %	CO ₂ %	CO %	O ₂ %
Pure natural gas	89	Trace	1.07	Trace	Trace
Steam reformer outlet	12.5	66.5	10.6	10	0.4

Tables 3.2 and 3.3 show the molar flow rates and molar fractions of compounds in the reactor input and output.

Table 0.2 Flow rates and Molar fractions of reactor input:

Compound	Flow rate kmol/hr	Molar fraction
CH ₄	2236	0.188
O ₂	1142	0.096
H ₂	5946	0.494
CO	880	0.074
CO ₂	940	0.079
Steam	630	0.053

Table 0.3 Flow rates and molar fractions of reactor output:

Compound	Flow rate kmol/hr	Molar fraction
CH ₄	297	0.025
O ₂	25	0.0021
H ₂	8087	0.68
CO	2438	0.205
CO ₂	1011	0.085
Steam	0	0

3.2.2 Reactor parameters

The average gas density (ρ) and heat capacity (C_p) were calculated using HYSIS software by applying the gas feed composition and operating conditions to be calculated. The most used catalyst pore size and density have been taken from Bischoff and Froment [37]. The other reactor parameters such as the reactor cross sectional area and reactor diameter were taken from the plant. table 3.4 shows these parameters.

Table 0.4 Reactor parameters:

Reactor diameter (d)	3.62 m
reactor cross sectional area (A)	10.287 m ²
Gas superficial velocity (u)	7.199 m/s
Catalyst density (ρ_c)	1970 kg/m ³
Catalyst pores diameter (Dp)	0.0018 m
Gas density (ρ)	3.894 kg/m ³
Heat capacity (C_p)	3.206 kJ/kg.K

3.2.3 Methane reactions

Experimentally, by controlling the inlet temperature higher than 450⁰C, carbon formation – which is not preferred- can be avoided [38]. Thus, reactions (5) to (8) can be ignored.

For the development of algorithm, only the main reactions as indicated by (1) to (4) are taken into consideration, the other side reactions (5) to (8) are assumed neglected.

These reactions are:

Exothermic combustion of natural gas:



Endothermic steam reforming reactions:



Water-gas shift reaction:



There are some side reactions can take place into the reactor as the following:

Carbon deposition according to Boudouard reaction:



Methane cracking:



Carbon gasification by steam or oxygen:



3.2.4 Calculations of kinetics model parameters

Autothermal reforming process model is basically a combination between three main parts. The first one is the constants which contain the rate constants (k), the adsorption constants and equilibrium constants (K). The second part is the rate equations, which contain the rate of each reaction and these equations are functions of the constants k and K . The third part is the energy equation which is a function of the rate equations.

3.2.4.1 Calculations of the reaction constants (k):

According to Arrhenius equation, the rate constant k is given by:

$$k = A * \exp\left(-\frac{E}{RT}\right) \quad 3.1$$

Where $A \equiv$ pre-exponential factor, reaction dependent.

$E \equiv$ activation energy (kJ/mol).

$R \equiv$ global gas constant (J/mol.deg).

$T \equiv$ temperature K.

For the parameters of this equation for each reaction, see table 3.5.

3.2.4.2 Calculations of the adsorption constants (K):

The adsorption constants K can be written according to Trimm and Lam (1980) [21] as:

$$K_i = A (K_i) \exp(-\Delta H_i / RT) \quad 3.2$$

The parameters of this equation (called Van't Hoff parameters) are given in table 3.6.

Table 0.5 Arrhenius parameter values for combustion, reforming, and water-gas shift reaction from Smet and et al (2001) [23].

Reaction	Kinetic model	A*	E (kJ/mol)
1a	Trimm and Lam (1996) [21,23]	8.11×10^5	86.0
1b	Trimm and Lam (1996) [21,23]	6.82×10^5	86.0
2	Xu and Froment [23,39]	1.17×10^{15}	240.1
3	Xu and Froment [23,39]	2.83×10^{14}	243.9
4	Xu and Froment [23,39]	5.43×10^5	67.1

*units: (1a), (1b): $\text{mol bar}^{-2} \text{kg}_{\text{cat}}^{-1} \text{s}^{-1}$; (2) $\text{mol bar}^{0.5} \text{kg}_{\text{cat}}^{-1} \text{s}^{-1}$; (3) $\text{mol bar}^{-1} \text{kg}_{\text{cat}}^{-1} \text{s}^{-1}$
(4) $\text{mol bar}^{0.5} \text{kg}_{\text{cat}}^{-1} \text{s}^{-1}$

Table 0.6 Van't Hoff parameters values for the adsorption reactions from Smet and et al (2001) [23].

Component	A (K_i)**	ΔH_i (kJ/mol)
CH ₄ (combustion)	1.26×10^{-1}	-27.3
O ₂ (combustion)	7.87×10^{-7}	-92.8
CH ₄	6.65×10^{-4}	-38.3
CO	8.23×10^{-5}	-70.7
H ₂	6.12×10^{-9}	-82.9
H ₂ O	1.77×10^5	88.7

**units: CH₄ (combustion), O₂ (combustion), CH₄, CO, H₂: bar^{-1} , H₂O: -

3.2.5 Energy balance

There are many parameters effecting the temperature variation inside the autothermal reformer. These parameters will either increase the temperature along the height of the bed or decrease it. The first parameter is the heat of each reaction ($-\Delta H$) which it reflects the type of a specific reaction whether it is endothermic or exothermic reaction; the second parameter is the rate of each reaction which effects directly the heat production or consumption inside the reactor according to the type of reactions.

Other parameters effect the consumption or generation of reactions materials and the reaction kinetics include the gas superficial velocity (u_s), gas density (ρ_g), heat capacity (C_p), and The catalyst bulk density (ρ_b).

De Groote and Froment [22] have connected all these parameters experimentally in the equation bellow (3.3) which can be used to predict the temperature profile along the reactor.

3.2.5.1 Energy equation:

$$\frac{dT}{dz} = \frac{\rho_b}{u_s \rho_g C_p} \sum_{i=1}^4 \eta_i r_i (-\Delta H)_i \quad 3.3$$

Catalyst bulk density (ρ_b), is given by the following equation:

$$\rho_b = \frac{M_c}{V_T} \quad 3.4$$

where:

M_c is the mass of catalyst

V_T is the volume of reactor bed

Mass of catalyst can be calculated as the following:

$$M_c = \rho_c \cdot V_c \quad 3.5$$

where:

ρ_c is the catalyst density.

V_c is the volume of catalyst.

The volume of reactor bed (V_T) can be calculated as the following

$$V_T = A \cdot h \quad 3.6$$

Since the reactor is adiabatic, the concentration and temperature gradients only occur in the axial direction. Intraparticle diffusion limitations are expressed here in terms of effectiveness factors (η) [22].

The values of the effectiveness factors which taken from De Groot and Froment [22] are:

$\eta_1 = 0.05$ for the total combustion of CH_4 to CO_2 and H_2O

$\eta_2 = 0.07$ for CO production by steam reforming

$\eta_3 = 0.06$ for CO_2 production by steam reforming

$\eta_4 = 0.7$ for water-gas shift reaction

3.2.6 Kinetic equations

The rate of complete combustion of methane to CO₂ and H₂O has been published by means of Trimm and Lam (1980) [21] as the following equation:

$$r_1 = \frac{k_1[CH_4][O_2]}{(1 + K_1[CH_4] + K_2[O_2])^2} + \frac{k_2[CH_4][O_2]^{\frac{1}{2}}}{1 + K_1[CH_4] + K_2[O_2]} \quad 3.7$$

Smet et al. (2001) [23] have shown that, this proposed equation is valid at temperature above 830 K, and O₂ / CH₄ ratios between 0.3 and 5. These conditions are matching the conditions of this model where the lowest temperature used is 1100^o C and O₂ / CH₄ ratio is 0.5.

The first term of the rate equation of methane combustion accounts for the reaction between molecularly adsorbed methane and oxygen, while the second term describes the reaction between molecularly adsorbed methane and gaseous oxygen.

The rates of steam reforming reactions (reactions (2) and (3)), and water gas shift reaction (reaction (4)) have been described by Xu and Froment [24, 25] on nickel catalysts according to the following reactions:

$$r_2 = \frac{k_1 / P_{H_2}^{2.5} (P_{CH_4} P_{H_2O} - P_{H_2}^3 P_{CO} / K_3)}{(1 + K_{CO} P_{CO} + K_{H_2} P_{H_2} + K_{CH_4} P_{CH_4} + K_{H_2O} P_{H_2O} / P_{H_2})^2} \quad 3.8$$

$$r_3 = \frac{k_5 / P_{H_2}^{3.5} (P_{CH_4} P_{H_2O}^2 - P_{H_2}^4 P_{CO_2} / K_5)}{(1 + K_{CO} P_{CO} + K_{H_2} P_{H_2} + K_{CH_4} P_{CH_4} + K_{H_2O} P_{H_2O} / P_{H_2})^2} \quad 3.9$$

$$r_4 = \frac{k_4 / P_{H_2} (P_{CO} P_{H_2O} - P_{H_2} P_{CO_2} / K_4)}{(1 + K_{CO} P_{CO} + K_{H_2} P_{H_2} + K_{CH_4} P_{CH_4} + K_{H_2O} P_{H_2O} / P_{H_2})^2} \quad 3.10$$

In previous work, the coke formation zones were based upon thermodynamic calculations. Wagner and Froment [25] predicted the zones in which coke formation is possible through methane cracking and through the Boudouard reaction by means of experimentally determined (threshold constants). To go beyond this and to predict the amounts of coke that can be formed on the catalyst, kinetics equations of coke formation are required. These were also derived by Wagner and Froment [24] from experiments in a differentially operated electrobalance reactor. These coke formation rates are as the following:

$$r_5 = \frac{k_6 P_{CO} - k_7 P_{CO_2} / P_{CO}}{(1 + K_{CO_2} P_{CO_2} / P_{CO})} \quad 3.11$$

$$r_6 = \frac{k_8 P_{CH_4} / P_{H_2}^{\frac{3}{2}} - k_9 P_{H_2}^{\frac{1}{2}}}{(1 + K_{H_2} P_{H_2})} \quad 3.12$$

$$r_7 = \frac{k_{10} P_{H_2O} / P_{H_2}}{(1 + K_{H_2} P_{H_2} + K_{H_2O} P_{H_2O} / P_{H_2})^2} \quad 3.13$$

$$r_8 = f(P_{O_2}) \quad 3.14$$

It has been found that, the carbon formation using nickel catalysts only occurs when the temperature is lower than 450⁰C [28], the plant data supports this finding, where no coke formation observed at temperatures higher than 450⁰C. In case if the temperature is lower than 450⁰C, the above rate equations of coke formation can be applicable.

3.2.7 Calculation of the pressure drop

The equation used most to calculate pressure drop in a packed bed is Ergun equation [40]:

$$\frac{dP}{dz} = -\frac{G}{\rho \cdot g_c \cdot D_p} \left(\frac{1-\Phi}{\Phi^3} \right) \left[\frac{150(1-\Phi)\mu}{D_p} + 1.75G \right] \quad 3.15$$

In calculating the pressure drop using the Ergun equation, the only one parameter that varies with the pressure in the right – hand side of Ergun equation is the gas density, so, another formula from this equation has been derived [40]:

At the end of the reactor where $z = L$:

$$\frac{P}{P_o} = \left(1 - \frac{2B_o L}{P_o} \right)^{0.5} \quad 3.16$$

Where P = final pressure at the reactor outlet

P_o = initial pressure at the reactor inlet

$$B_o = \frac{G(1-\phi)}{g_c \cdot \rho_o \cdot D_p \cdot \phi^3} \left[\frac{150(1-\Phi)\mu}{D_p} + 1.75G \right] \quad 3.17$$

G = superficial mass velocity

$$G = \frac{Q}{A} \quad 3.18$$

Where:

Q is the mass flow rate.

$$G = 3870 \text{ kg/h.m}^2$$

Φ is the porosity it is given by:

$$\Phi = \frac{V_v}{V_T} \quad 3.19$$

V_v is the volume of void

Total bed volume = 76.1238 m³

$$V_v = V_T - V_c \quad 3.20$$

$$= 76.1238 - 31 = 45.1238 \text{ m}^3$$

$$\Phi = 0.593$$

g_c = conversion factor = 10⁻⁸ (for SI units)

D_p = diameter of the particle in the bed = 0.0018 m

μ = viscosity of the gas passing through the bed
= 0.0667 kg/m.h

Applying these parameters:

$$B = 0.6$$

This leads to:

$$P = 27.5 \text{ bar}$$

$$\Delta P = 2.5 \text{ bar}$$

This value of pressure drop is neglected compare to the total operating pressure. In other cases (different operating conditions and reactor parameters), if the value of the pressure drop is not neglected, the height of the bed, z , will be taken as variable, so, the pressure drop at each position inside the reactor can be calculated as well as the corresponding partial pressure of each compound, the rate constants, the rate of each reaction, and then the temperature and conversion at this position.

3.2.8 Solution procedure

Equation (3.3) contains some crucial parameters affect intrinsically on the temperature profile, such as the catalyst mass –or volume- which affects the bulk density, also the flow rate of the feed which affects the gas superficial velocity.

In this model, there are three main parts; the first part is the kinetics constants (rate constants, adsorption constants, and equilibrium constants) which are functions of temperature, the second part is the rate of reactions which are functions of kinetics constants, and the third part is the bed temperature which is a function of rate of reactions.

This model appears like a loop which can not be solved individually, in other words, all these variables must be solved simultaneously. So, to achieve the relations between all these parameters, this model must be built as one unit.

The key of this loop is the inlet temperature (because it is the first variable to start the calculations of constants and rate of reactions), so, it will be taken as the starting point to solve the model. This algorithm used is as the following:

- 1- The reactor was divided into small reactors by dividing the catalyst bed height (7 m) into 7000 units (the height of each unit is 1 mm) represent these batch reactors.
- 2- The kinetics constants were calculated at the inlet temperature according to equations (3.1) and (3.2).
- 3- The rate of reactions (r_1 to r_4) will be calculated from the values of kinetics constants and the other reactor parameters (partial pressures, oxygen concentration) according to equations (3.7), (3.8), (3.9), and (3.10).
- 4- From the values of reactions rates (r_1 to r_4), the outlet temperature can be calculated according to equation (3.3).

- 5- From the inlet temperature and outlet temperature, the average temperature at the first unit can be calculated.
- 6- The outlet temperature of the first unit will be the inlet temperature of the second unit.
- 7- Same procedure will be followed to calculate the kinetics constants, rate of reactions, and the temperature at each unit until the last unit which represents the outlet of the reactor, so each variable can be plotted along the reactor (e.g. rate of reactions or temperature with the catalyst bed height).
- 8- Different values for the reactor parameters such as different catalyst volumes, different superficial velocities, and different inlet temperatures can be varied to study the effect of each parameter on the temperature profile and rate of reactions.

3.2.9 Calculations of conversion

The conversion of each compound can be calculated using the following set of differential equations (equations 3.7 to 3.10) which proposed by Bischoff and Froment [37] and describe the conversion of the feed as functions of reactor parameters.

After fixing the catalyst bulk density, cross sectional area, flow rate of methane and oxygen, and effectiveness factors, the conversion varies with two variables; the catalyst bed height and the rate of reaction which are vary again with the catalyst bed height z .

To solve these equations, the catalyst bed height was discrete into units of distance, so, the rates of reactions at each unit remain constant. According to the values of rate of reactions, the conversion of each compound was calculated at each position and by integrating all the units, the total conversion of each compound can be achieved.

To calculate the conversion of compounds if any variable changed (e.g. conversion at different combustion temperatures), first, the specific value of the variable under study was applied, then, the corresponding rates of reactions were calculated at these new conditions, these new values of reactions rates were applied in the conversion equations to calculate the new conversion following the same procedure.

$$\frac{dX_{CH_4}}{dz} = \frac{\rho_b A}{F_{CH_4}^0} (\eta_1 r_1 + \eta_2 r_2 + \eta_3 r_3) \quad 3.21$$

$$\frac{dX_{O_2}}{dz} = \frac{\rho_b A}{F_{O_2}^0} (2\eta_1 r_1) \quad 3.22$$

$$\frac{dX_{CO}}{dz} = \frac{\rho_b A}{F_{CH_4}^0} (\eta_2 r_2 - \eta_4 r_4) \quad 3.23$$

$$\frac{dX_{CO_2}}{dz} = \frac{\rho_b A}{F_{CH_4}^0} (\eta_1 r_1 + \eta_3 r_3 + \eta_4 r_4) \quad 3.24$$

The overall selectivity can be calculated by taking the carbon monoxide as the desired product where the carbon dioxide is the undesired product according to equation 3.25 [40].

$$S_{overall} = \frac{\text{Flow rate of the desire product}}{\text{Flow rate of the undesired product}} \quad 3.25$$

CHAPTER IV
RESULTS AND
DISCUSSION

CHAPTER 4

4. RESULTS AND DISCUSSION

4.0 Introduction

This chapter shows and discusses the results of the autothermal reformer model. The results show the temperature profile as a function of the catalyst bed height and its variation with the catalyst volume, and the corresponding rate of reactions.

In order to validate the model, the variation of the predicted temperature profile against the actual plant data and the other researchers was done. Based on this variation, the effect of the catalyst volume, gas superficial velocity and combustion temperature are studied and shown in this chapter as well as the corresponding rate of reactions and conversion of methane and oxygen to carbon monoxide and carbon dioxide. The conversion and yield are compared with the other researcher's results which are based on the partial oxidation process[22,23].

4.1 Variation of autothermal reformer temperature profile

In this process, there is no or minimal carbon formation in both steam reformer and autothermal reformer due to high temperature (higher than 450°C) and suitable steam to carbon ratio (1.7)- i.e. carbon in form of carbon monoxide and carbon dioxide.

Solving Equation 3.3 gives Figure4.1a.

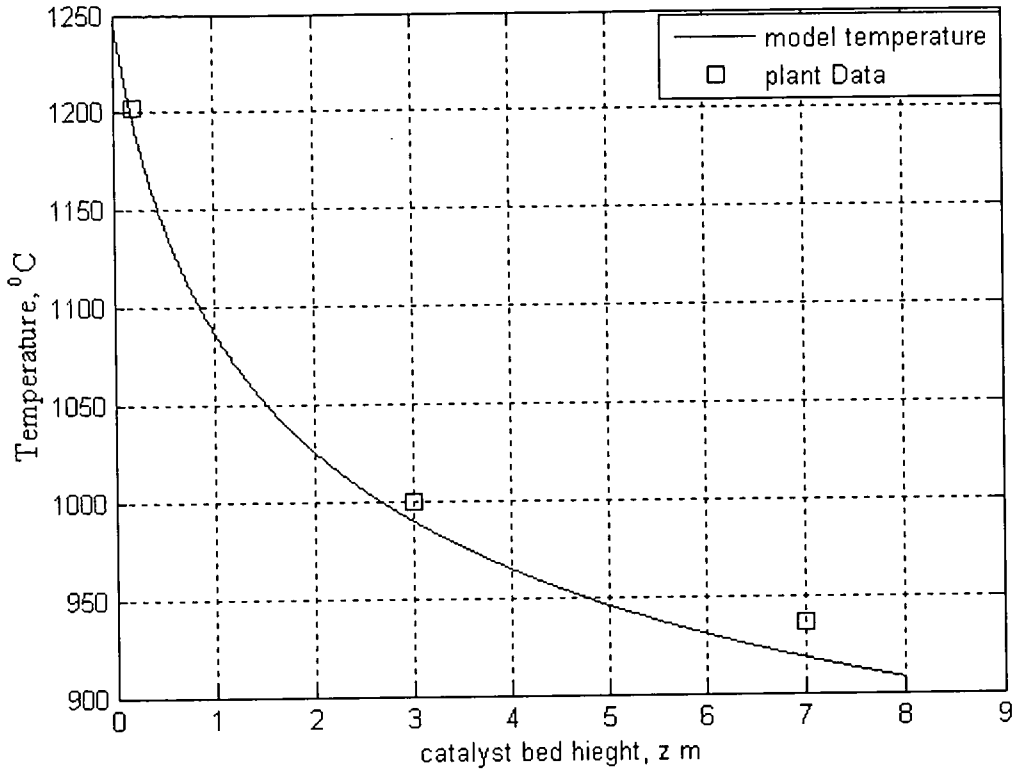


Figure 4.1a: Temperature profile along the catalyst bed height of the autothermal reformer.

Figure 4.1a reflects the value of temperature at each position inside the reactor which is achieved by the rate of each reaction at that position.

In this Figure, the temperature decreases with the increasing of the distance inside the reactor due to the majority of endothermic reactions which they use the heat energy to complete the reactions.

The reactors cross sectional area can be taken into account to express the temperature profile in Figure 4.1a in term of catalyst volume instead of distance. So, for specific catalyst volume, the same behavior as in Figure 4.1a can be observed as shown in Figure 4.1b.

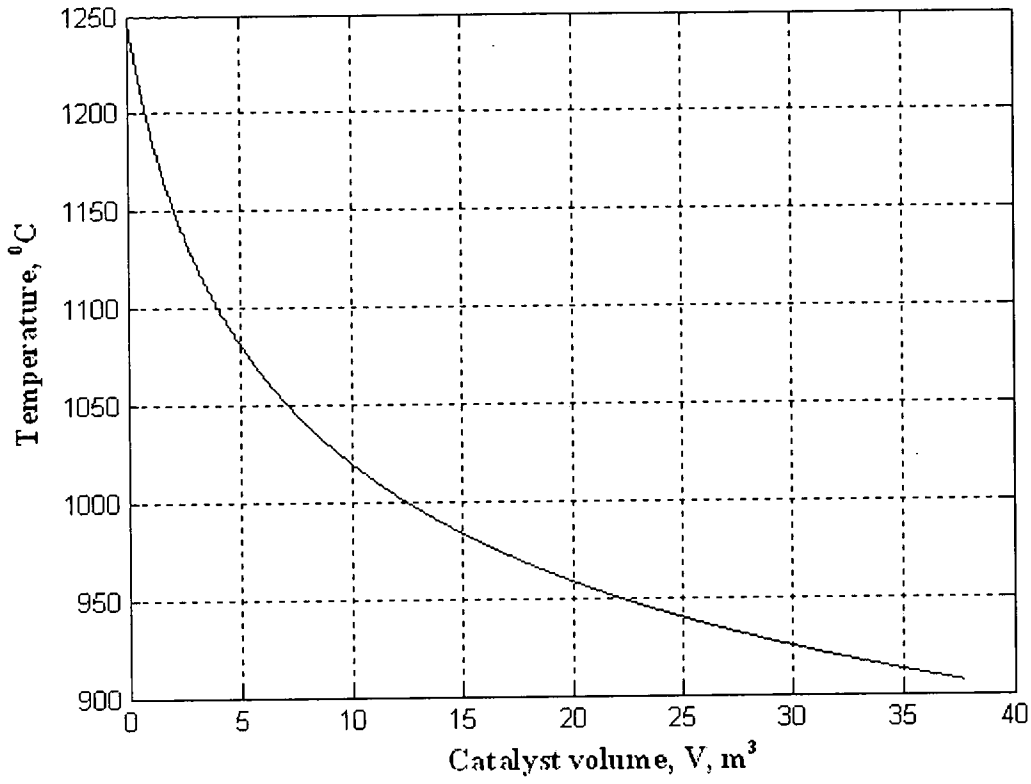


Figure 4.1b Temperature profile with the catalyst volume.

4.1.1 Comparison between the predicted temperature profile and actual plant data

It can be seen from Table 4.1 that, a lower temperature at each position can be achieved compared to the temperature measured at three positions inside the catalyst bed.

Table 4.1 Comparison between the temperatures at different positions with PML data.

Position	Model temperature	PML temperature	Partial Oxidation on rhodium [14] (2006)
Top (after the reactor inlet)	1200 ⁰ C	1202 ⁰ C	1000 ⁰ C
Middle (after 3 meters from the inlet)	980 ⁰ C	1000 ⁰ C	800 ⁰ C
Bottom (at the end of the catalyst bed)	920 ⁰ C	936 ⁰ C	730 ⁰ C

According to Table 4.1, lower temperature at each position along the catalyst bed of the autothermal reformer can be achieved in this model, especially in the middle part of the catalyst which is lower by 20⁰C, and the bottom of the catalyst bed which is lower by 16⁰C. This leads for longer catalyst life and safer operating conditions.

The difference between the predicted model temperature and the actual plant data is about 2 %. This difference is due to the total operating pressure in the model which is 30 bar and the operating pressure used to derive the kinetics model parameters which is 25 bar. The same trends of temperature profiles have been achieved by R. Horn [14] (2006) in the production of synthesis gas from natural gas via partial oxidation on rhodium catalyst as it shown in Table 4.1.

4.2 Rate of reactions

Figures 4.2 to 4.5 show the predicted rate of reactions as a function of temperature by solving the rate equations of reaction 1, 2, 3, and 4. The rate of these reactions are functions of the rate constants, equilibrium constants and adsorption constants which are functions of temperature.

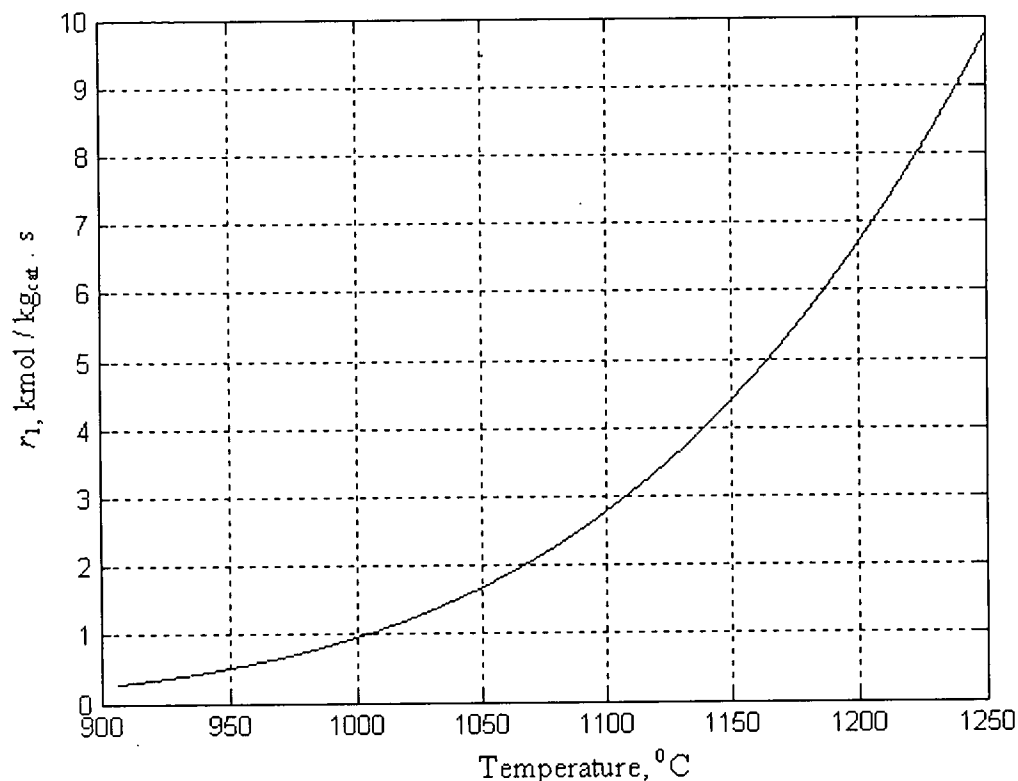


Figure 4.2 Rate of reaction 1 as a function of temperature.

Due to the exothermicity of reaction 1 (ΔH is negative), the value of the adsorption constants K_1 and K_2 decrease with the increasing of temperature according to Equation 3.2, so, it can be seen in Figure 4.2 that, the rate of this reaction increases with the increasing of temperature according to Equation 3.7.

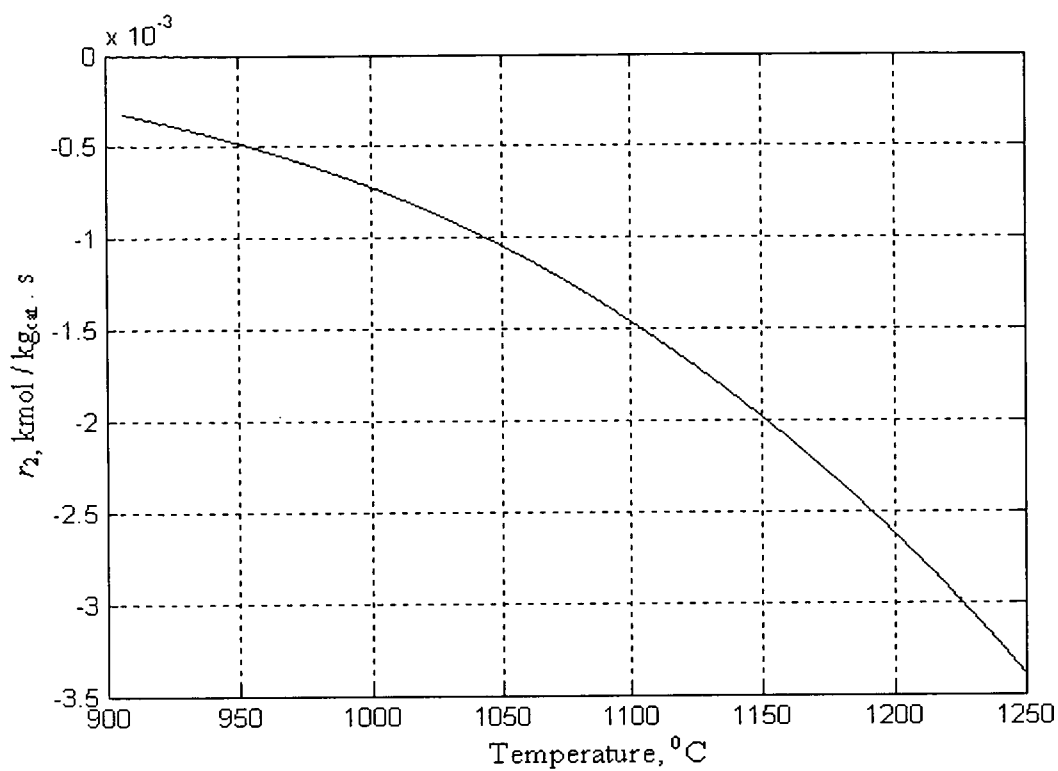


Figure 4.3 Rate of reaction 2 as a function of temperature.

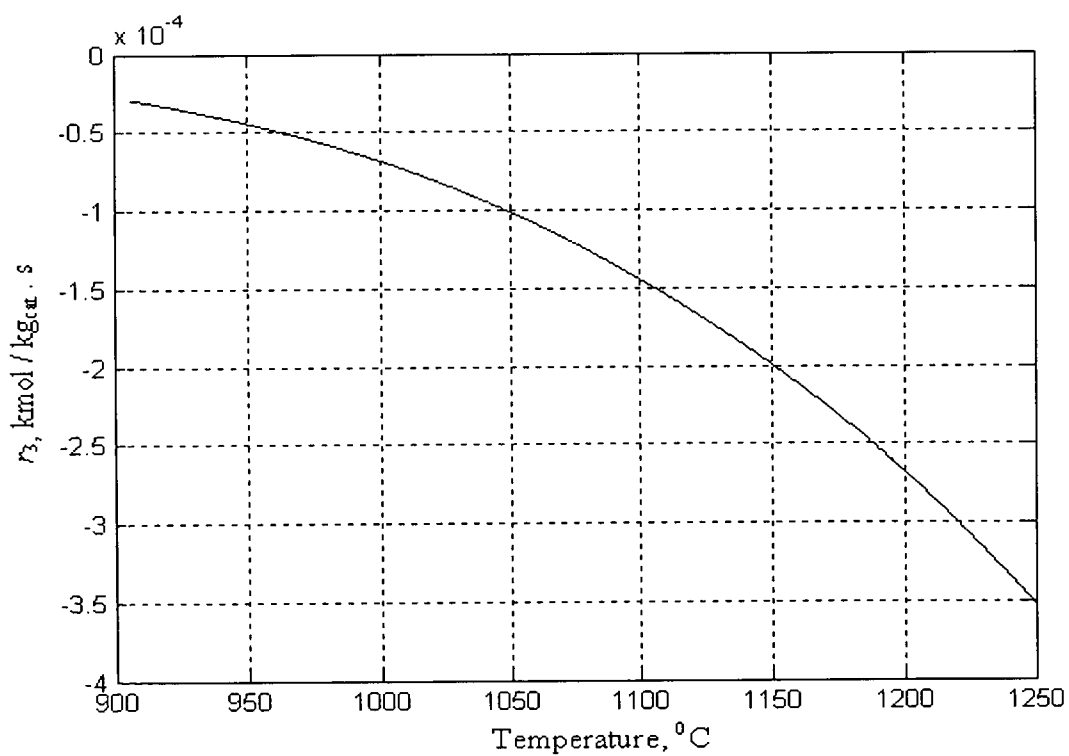


Figure 4.4 Rate of reaction 3 as a function of temperature.

For the steam reforming reactions (reactions 2 and 3), the value of (ΔH) is positive, so, the value of the equilibrium constants K_3 and K_5 increase with the increasing of temperature (Equation 3.2). According to Equations 3.8 and 3.9, higher temperature leads for lower rate of reactions as shown in Figures 4.3 and 4.5.

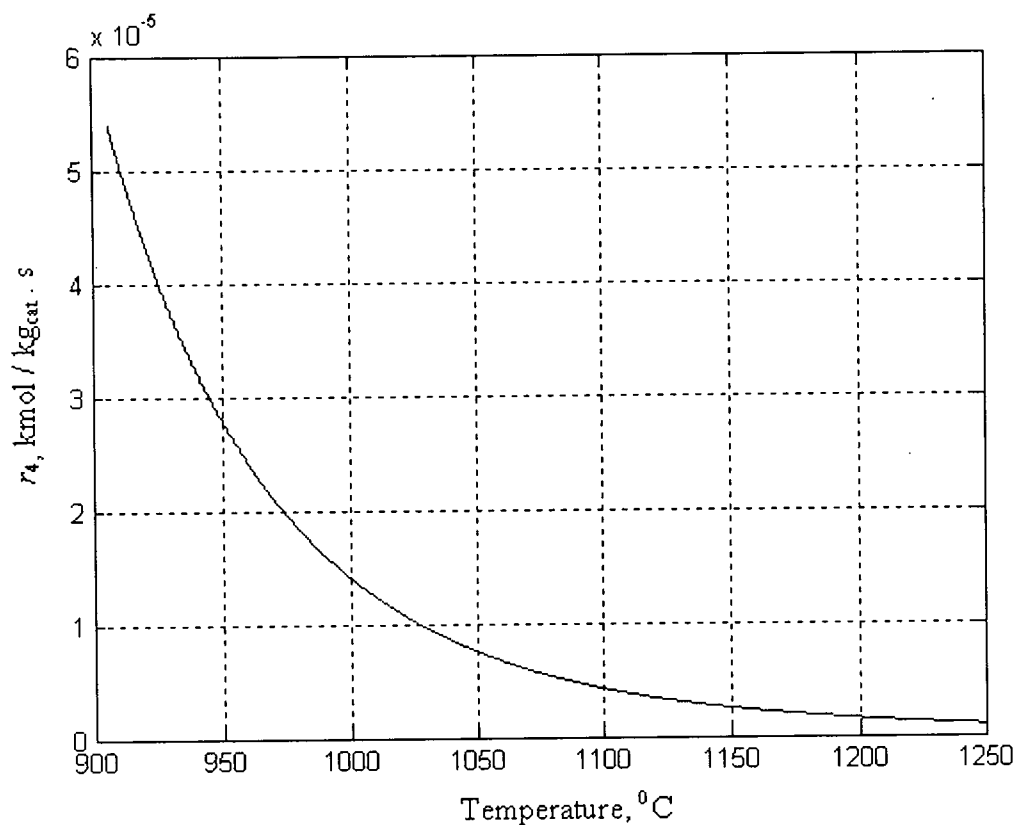


Figure 4.5 Rate of reaction 4 as a function of temperature.

For the rate of reaction (4), (ΔH) is negative, according to Equation 3.2, K_4 decreases with the increasing of temperature, this leads for lower rate in the reversible direction as it shown in Figure 4.5.

The general, there are too many parameters effecting the rate of each reaction, such as the rate constants (k) which increases with the increment of temperature as long as the activation energy is positive (see Eq. 3.1), also the equilibrium constants (K) affect on the rate of reactions in two ways:

4.2.1 Rate of reactions as functions of distance:

As long as the temperature decreases with the increment of distance (height) inside the reactor, the rate of reaction 1 will decrease with the increment of distance. But the rate of reactions 2, 3, and 4 will increase with the increasing of the catalyst bed height, because the temperature decreases along the catalyst bed as shown in Figures 4.6, 4.7, 4.8, and 4.9.

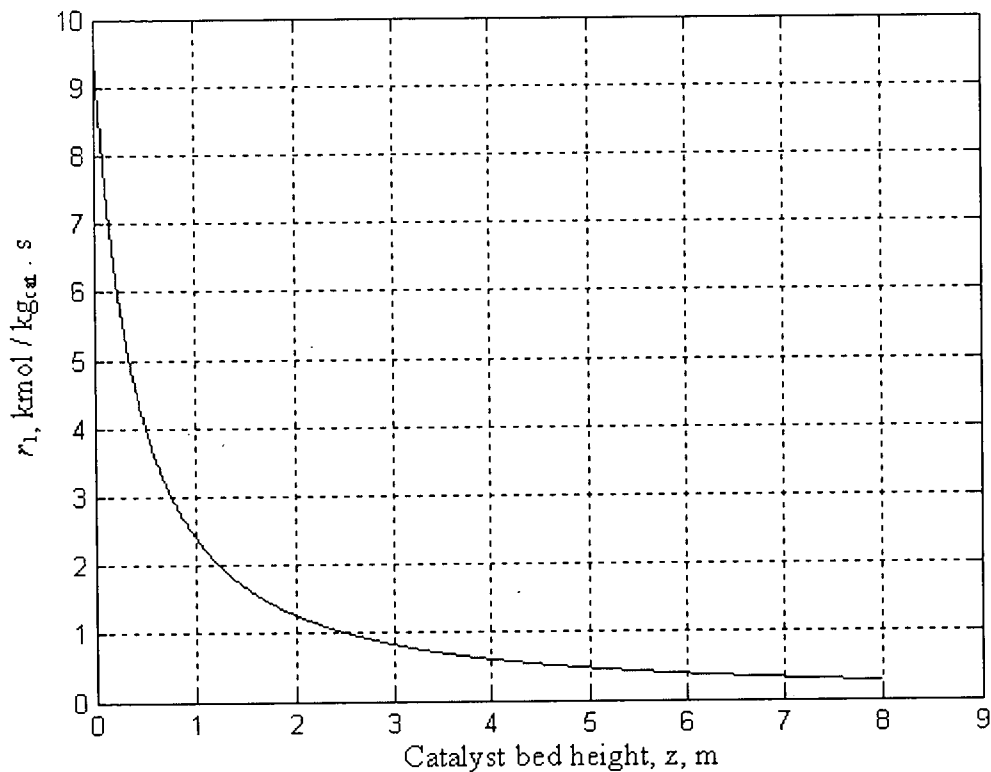


Figure 4.6 Rate of reaction 1 as a function of distance inside the reactor, z m.

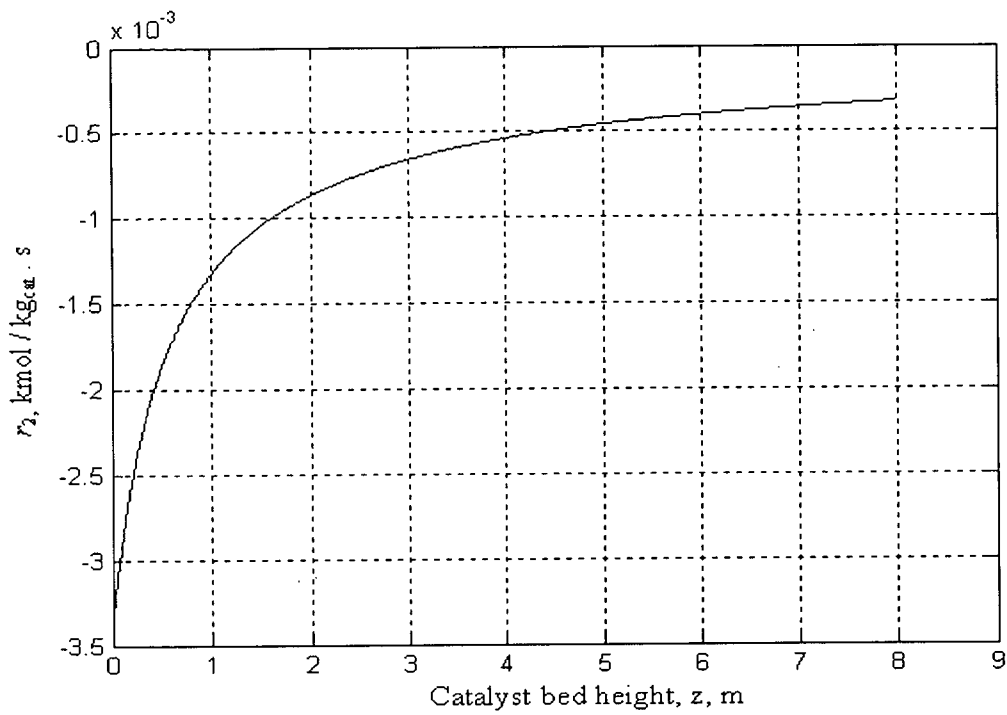


Figure 4.7 Rate of reaction 2 as a function of distance inside the reactor, z m.

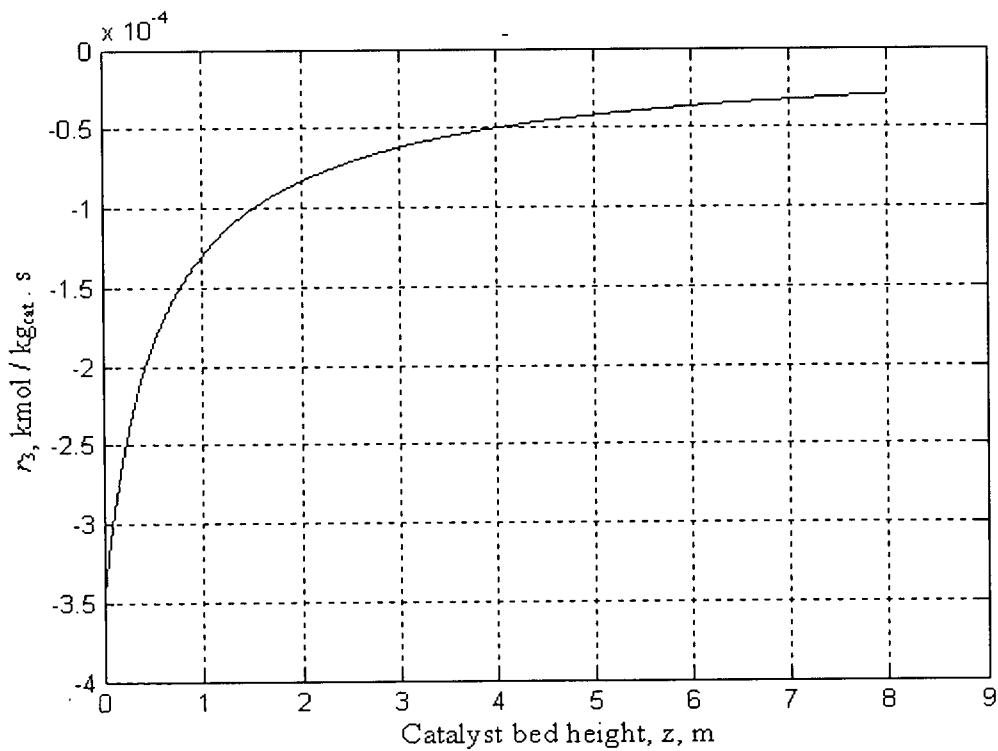


Figure 4.8 Rate of reaction 3 as a function of distance inside the reactor, z m.

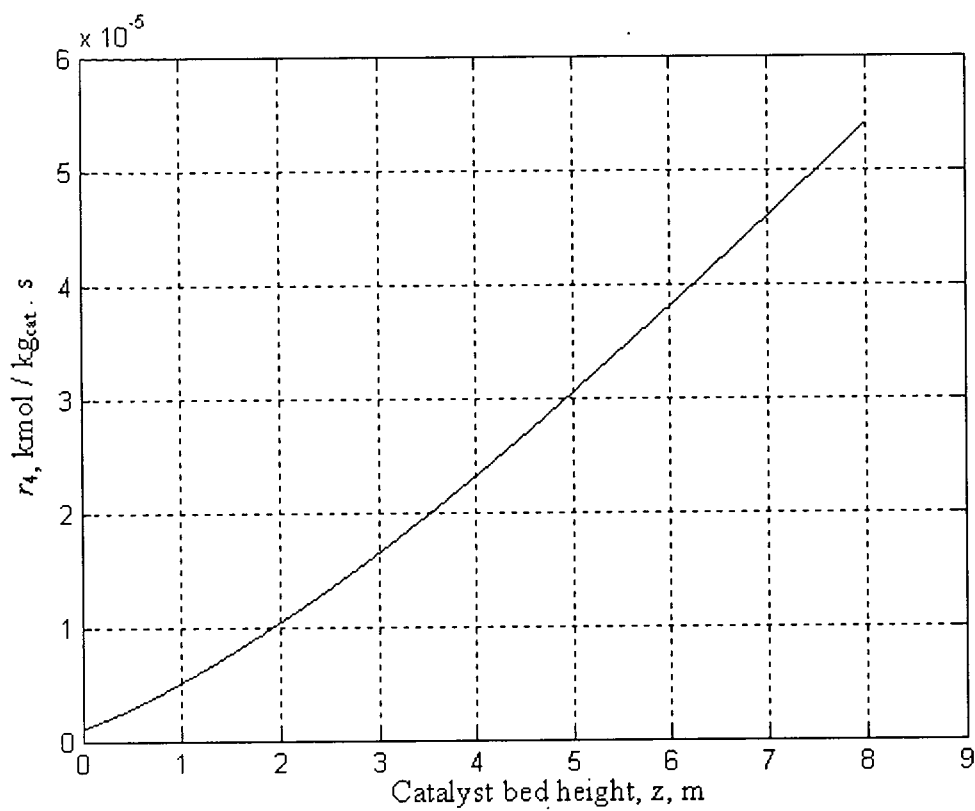


Figure 4.9 Rate of reaction 4 as a function of distance inside the reactor, z m.

4.3 Effect of catalyst volume:

The catalyst volume effects on the total bulk density (ρ_b) which increases with the increment of the catalyst volume (Equation 3.4). In order to investigate the effect of the catalyst volume on the autothermal reformer temperature profile, different values of the catalyst volume were applied into the model; these values were selected based on the actual catalyst volume in PML plant which is 31 m^3 .

Figure 4.10 shows the temperature profile using different catalyst volumes.

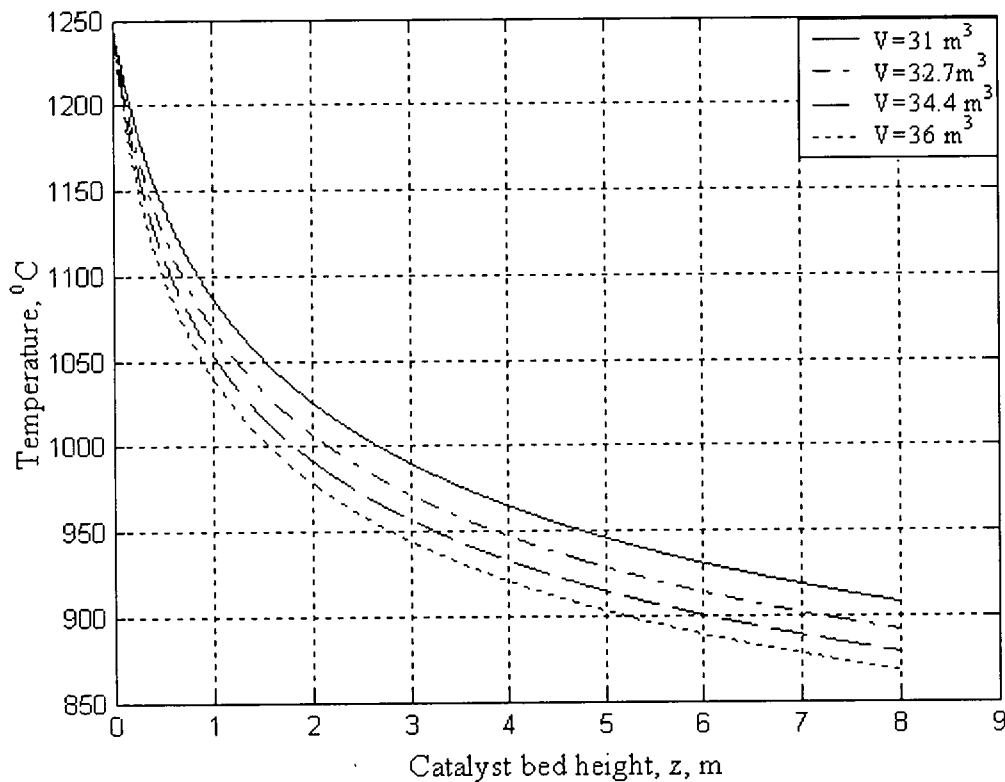


Figure 4.10 Temperature profile using different catalyst volumes.

In Figure 4.10, it can be seen that a higher catalyst volume gives higher bulk density, hence better reaction, hence more heat will be consumed as long as the endothermic reactions are more predominant (after methane combustion the majority will be for the endothermic reactions). This means the temperature will be lower at any specific position

when a higher catalyst volume (the highest catalyst volume gives the lowest temperature at any position) is used. It can be concluded that, lower catalyst volume gives higher temperature profile, and higher catalyst volume gives lower temperature profile as shown in Figure 4.10.

4.4 Effect of gas superficial velocity:

In order to investigate the effect of gas superficial velocity on the temperature profile of the autothermal reformer, four values of this velocity were selected and applied into the model. To achieve the best variation some of the values are selected lower than the actual plant velocity and some of the values are higher than it (the actual plant superficial velocity is 7.2 m/s). Figure 4.11 shows the variation of temperature profile using different gas superficial velocities.

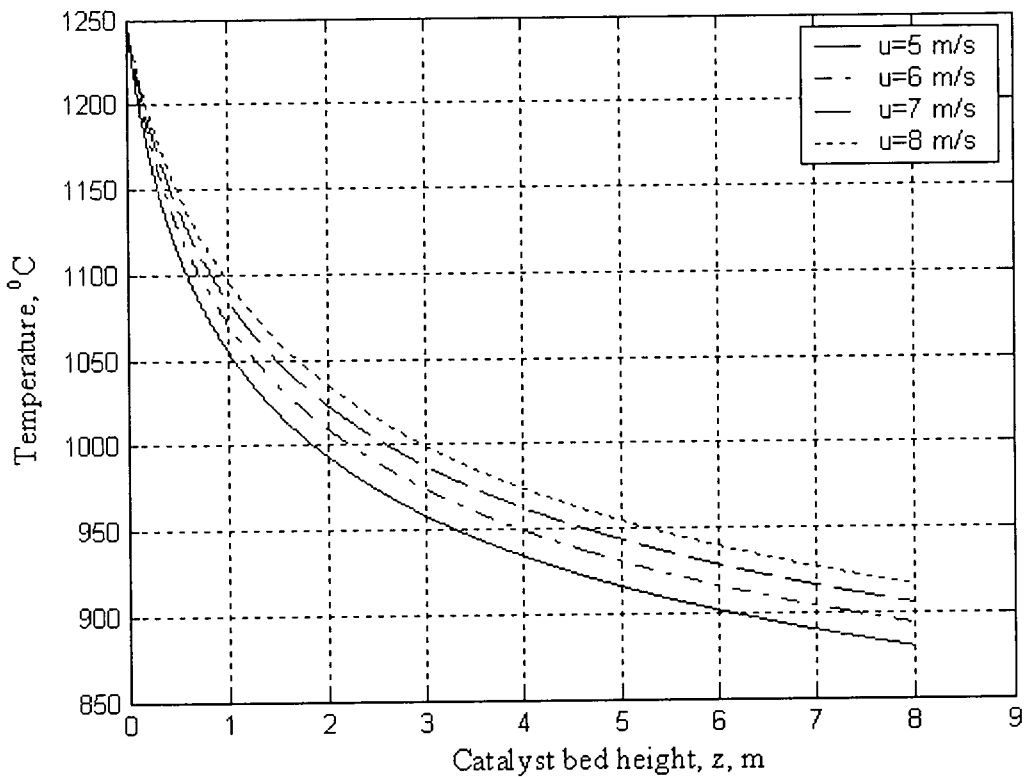


Figure 4.11 Temperature profile with different superficial velocities (u_s)

For a given catalyst volume (31m^3), it can be observed that in Figure 4.11, higher gas superficial velocity gives a higher temperature at any position z .

There are two main factors affecting the net value of heat consumption:

- a- Higher superficial velocity means lower residence time, hence less reaction, hence for endothermic reactions means less heat will be consumed. That means higher superficial velocity gives higher temperature at any position z .

- b- Higher superficial velocity allows more reaction materials per unit time which it means more heat will be consumed. That means higher superficial velocity gives lower temperature at any position z .

According to Figure 4.11, the first factor is more predominant.

4.5 Effect of burner temperature (combustion temperature):

There are various types of industrial headers of methane combustion, and each type of these headers gives specific combustion temperature. In order to study the effect of these combustion temperatures, different values are selected and applied into the model, these values are higher and lower than the actual plant combustion temperature which is 1250°C as it shown in Figure 4.12.

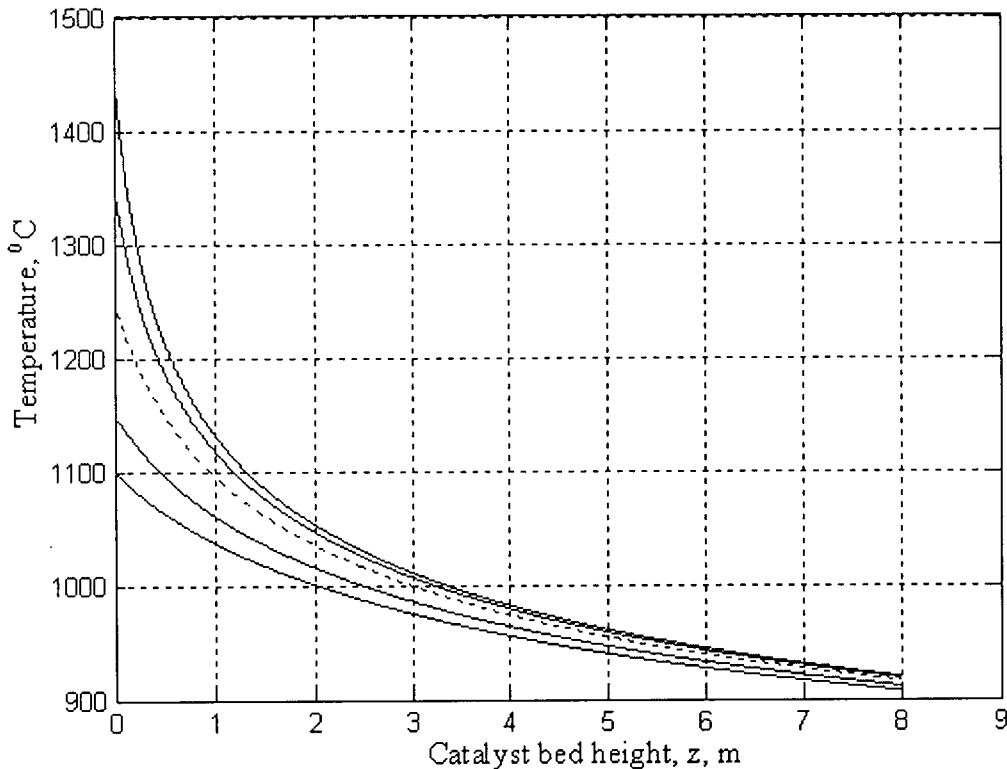


Figure 4.12 Temperature profile using different burner temperatures.

It is expected that, lower combustion temperature gives lower bed temperature at each position inside the reactor as indicated by Figure 4.12.

In spite of the wide range of combustion temperature used to study the effect of burner temperature on the temperature profile (1100°C up to 1400°C), approximately, same outlet temperature can be achieved, because any additional heat will be utilized to increase the rate of endothermic reactions. This that means the excess heat will be absorbed by the reactants to produce carbon monoxide and carbon dioxide.

The ability to keep the outlet temperature in the same range using different combustion temperatures will be suitable and more practical, because it gives permission to keep the heat recovery system (heat exchangers) as it is. It will effect only on the composition of the outlet, so, it is necessary to study the yield achieved via each combustion temperature used.

4.6 Rate of reactions using different combustion temperatures:

To study the yield achieved using different inlet temperatures, it is inevitable to calculate the corresponding rate of reactions via each inlet temperature:

The Figures bellow (4.13, 4.14, 4.15, and 4.16) show the rate of reactions using different inlet temperatures.

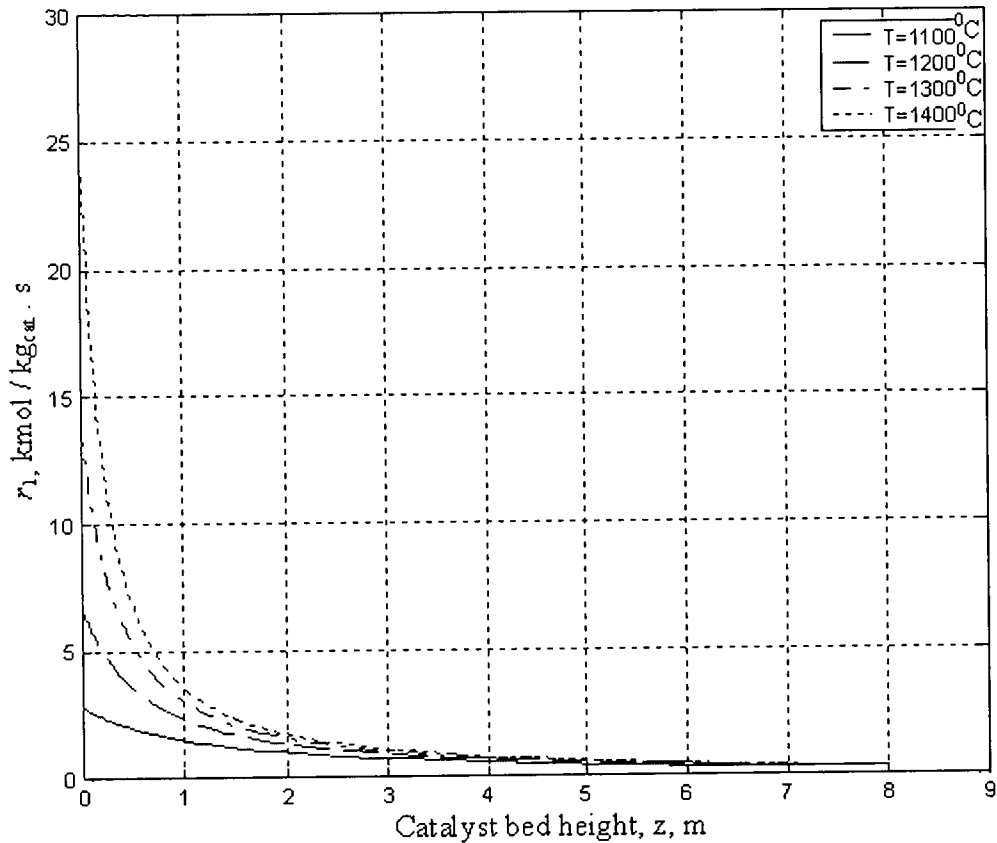


Figure 4.13 Rate of reaction (1) using different inlet temperatures.

It can be observed in Figure 4.13 that, higher combustion temperature gives higher rate of combustion reaction.

After the third meter of catalyst bed height, the rates of reaction (1) are approximately constant due to the high consumption of oxygen in the first part of the catalyst bed.

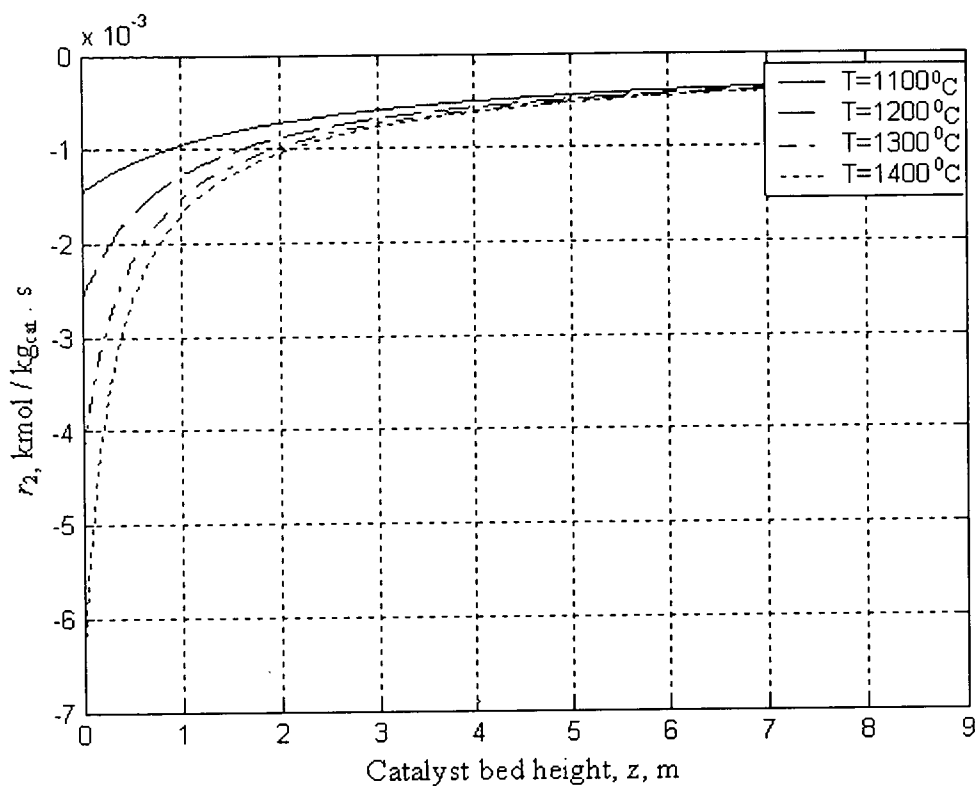


Figure 4.14 Rate of reaction (2) using different inlet temperatures.

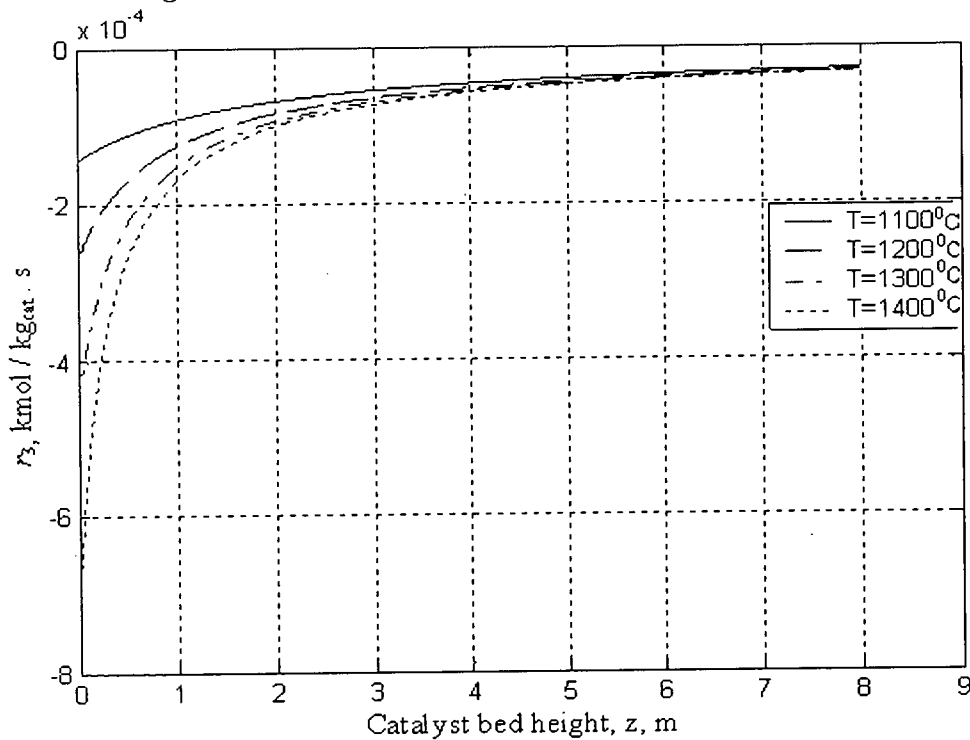


Figure 4.15 Rate of reaction (3) using different inlet temperatures.

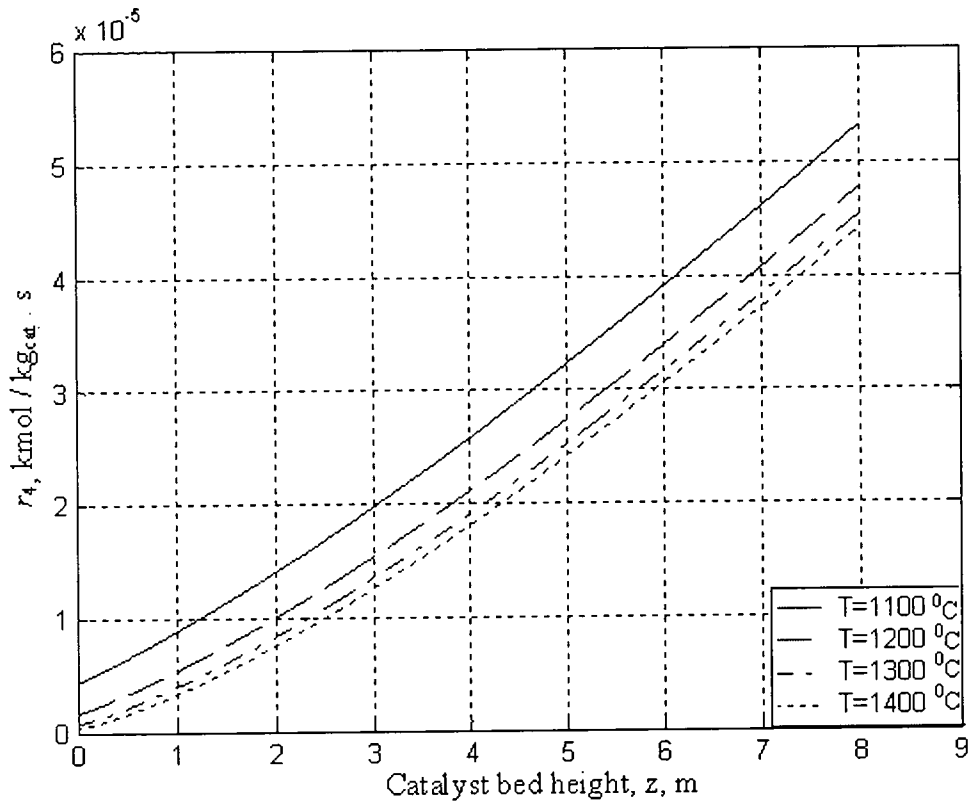


Figure 4.16 Rate of reaction (4) using different inlet temperatures.

4.7 Conversion study

The percentages of consumed methane and oxygen and generated carbon monoxide and carbon dioxide have been calculated after each unit of catalyst bed height by taking the value of the rate of each reaction and apply it into Equations 3.21 to 3.24.

Figures 4.17 to 4.21 show these percentages at different combustion temperatures.

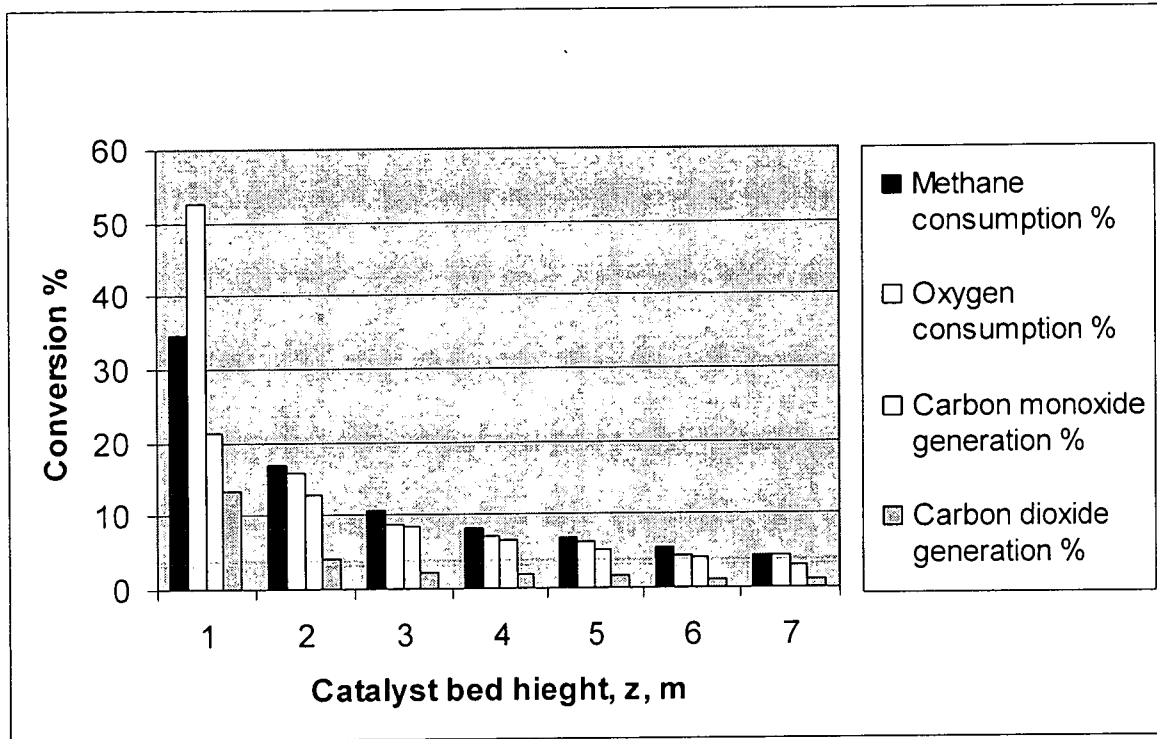


Figure 4.17 Percentage of consumption and generation at combustion temperature of 1250°C):

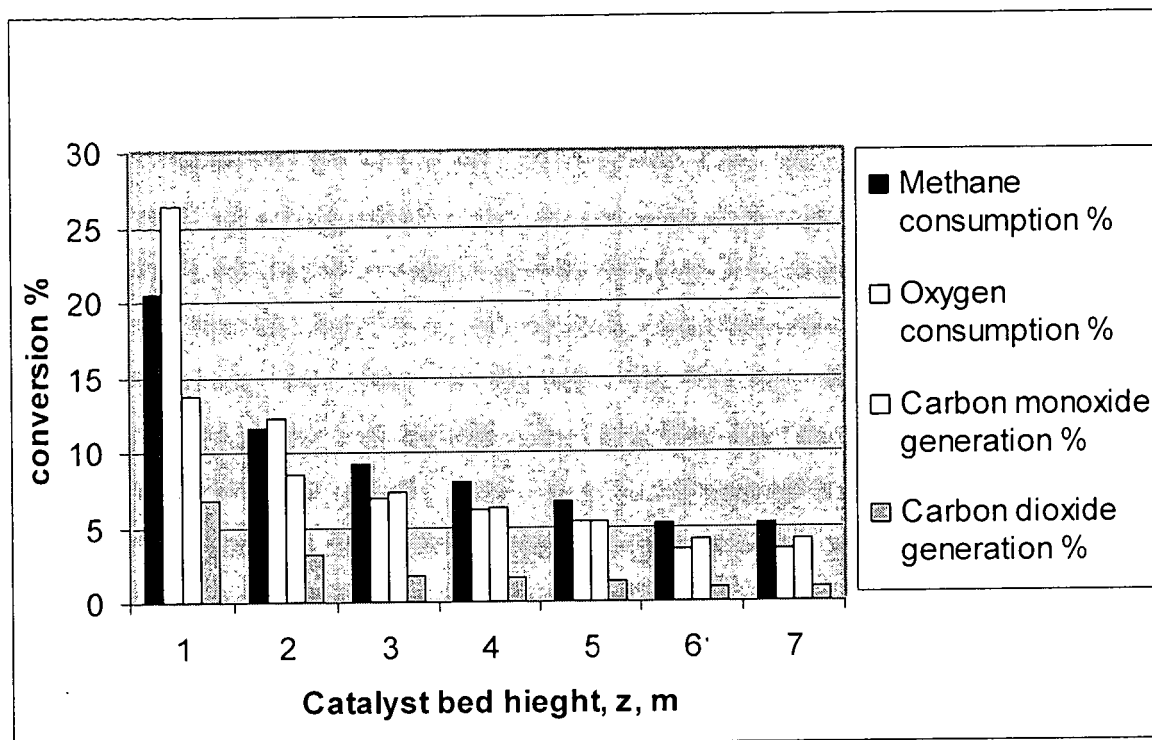


Figure 4.18 Percentage of consumption and generation at combustion temperature of 1100°C:

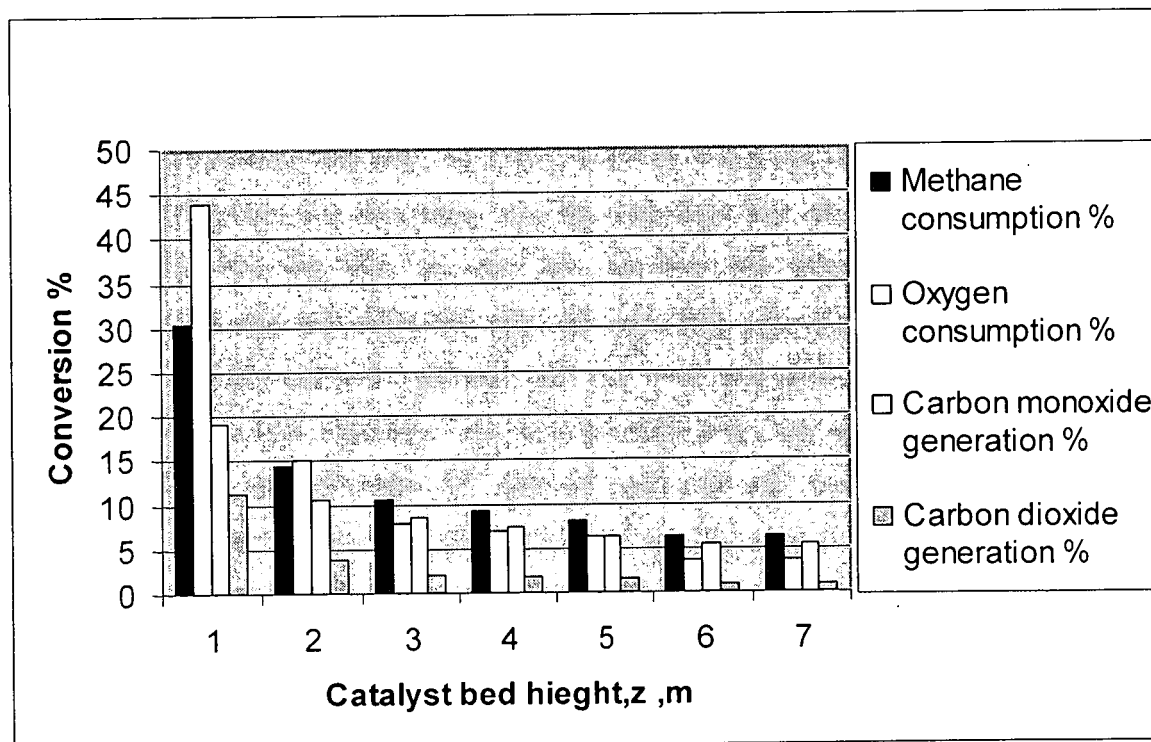


Figure 4.19 Percentage of consumption and generation at combustion temperature of 1200°C:

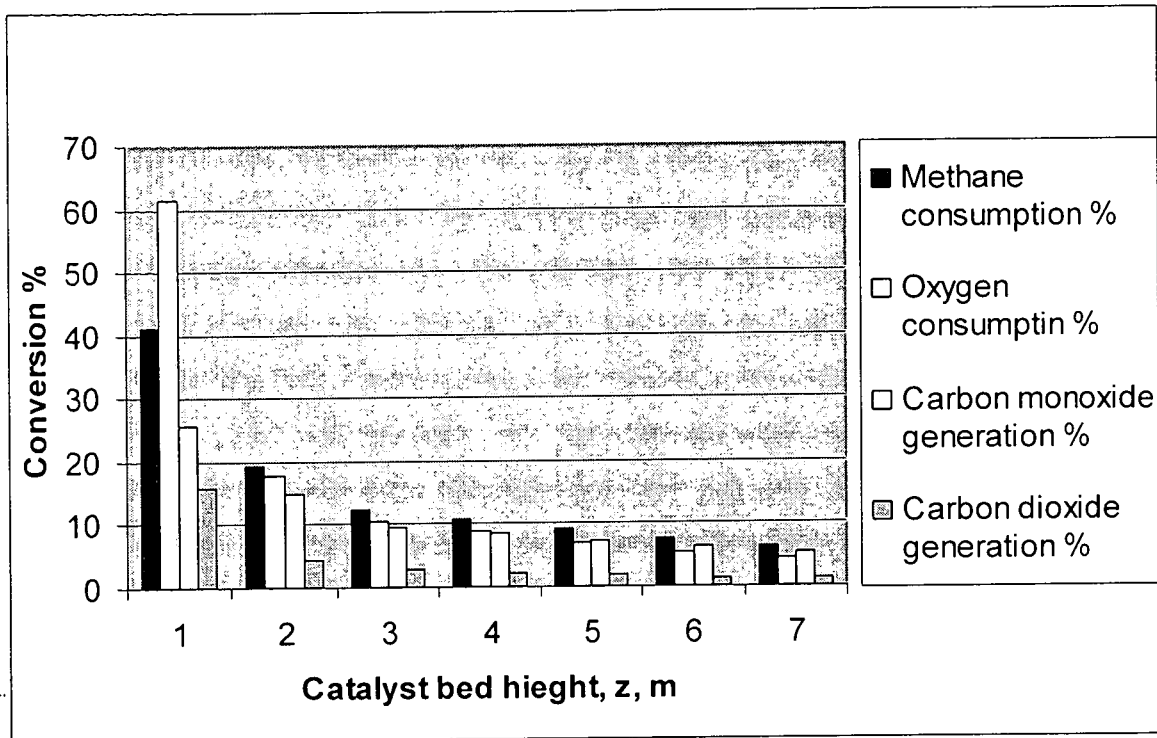


Figure 4.20 Percentage of consumption and generation at combustion temperature of 1300°C:

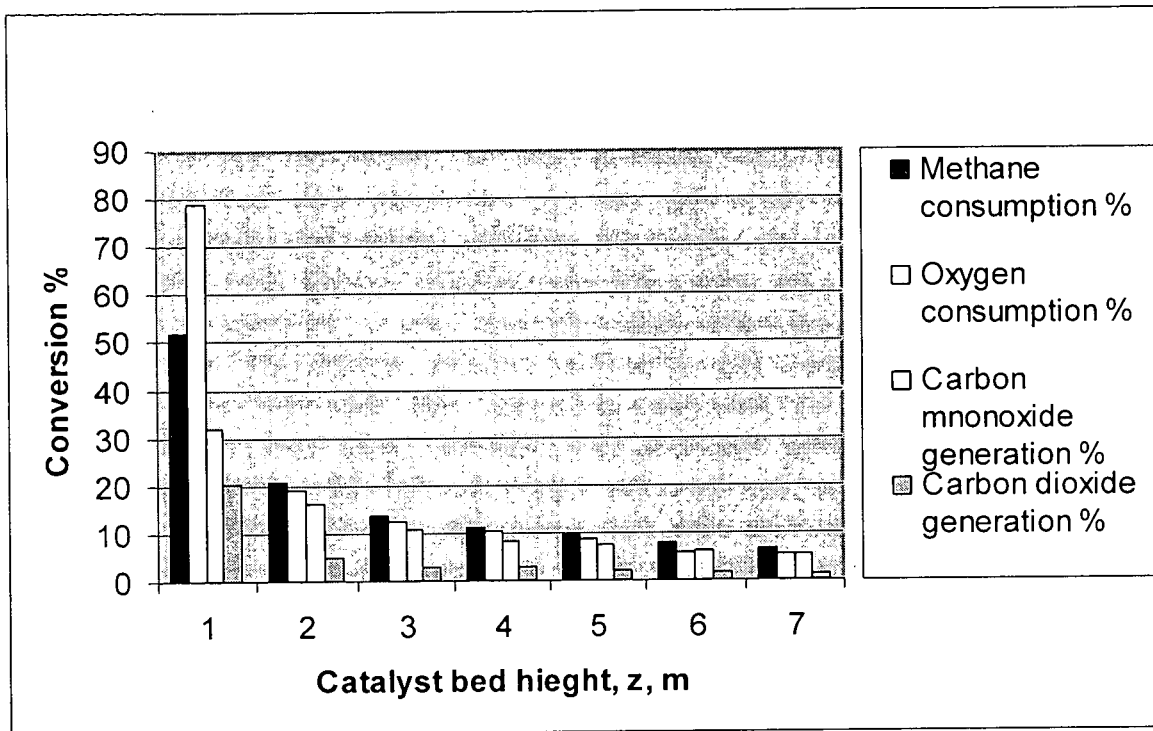


Figure 4.21 Percentage of consumption and generation at combustion temperature of 1400°C :

Obviously it can be seen from Figures 4.17 to 4.21 that the percentage of consumed and generated materials increase with the increasing of combustion temperature, this will be reflected in the molar flow rates and molar fractions.

Figures 4.22 to 4.26 bellows show the molar flow rates of compounds along the catalyst bed height from the inlet to the outlet of the reactor. The output from the last catalyst bed height unit (where $z = 7$ m) is the total output of the reactor.

4.7.1 Molar flow rates and molar fractions

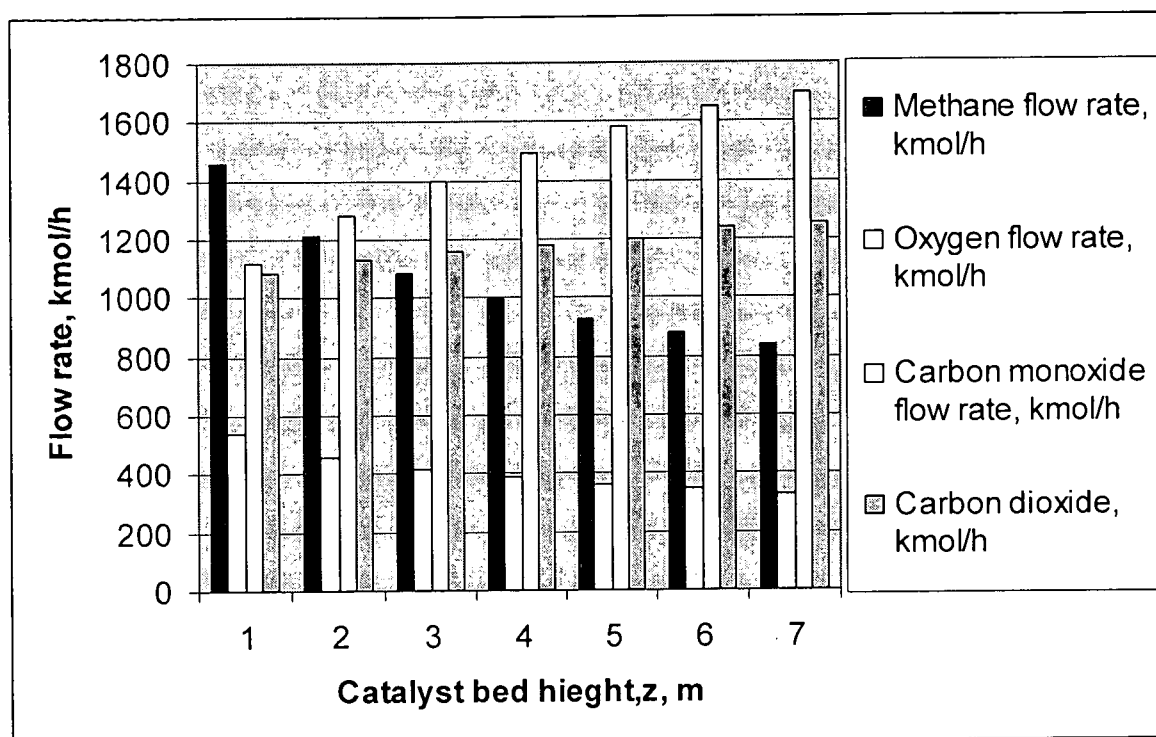


Figure 4.22 Output flow rates after each meter of catalyst bed height where the combustion temperature of 1250°C was used:

Table 4.2 Molar fractions of compounds after each meter of catalyst bed height ($T=1250^{\circ}\text{C}$):

Distance z m	1	2	3	4	5	6	7
x_{CH_4}	0.347	0.298	0.267	0.245	0.228	0.215	0.203
x_{O_2}	0.128	0.111	0.102	0.095	0.089	0.085	0.08
x_{CO}	0.226	0.314	0.345	0.369	0.388	0.404	0.412
x_{CO_2}	0.295	0.277	0.286	0.291	0.295	0.297	0.304

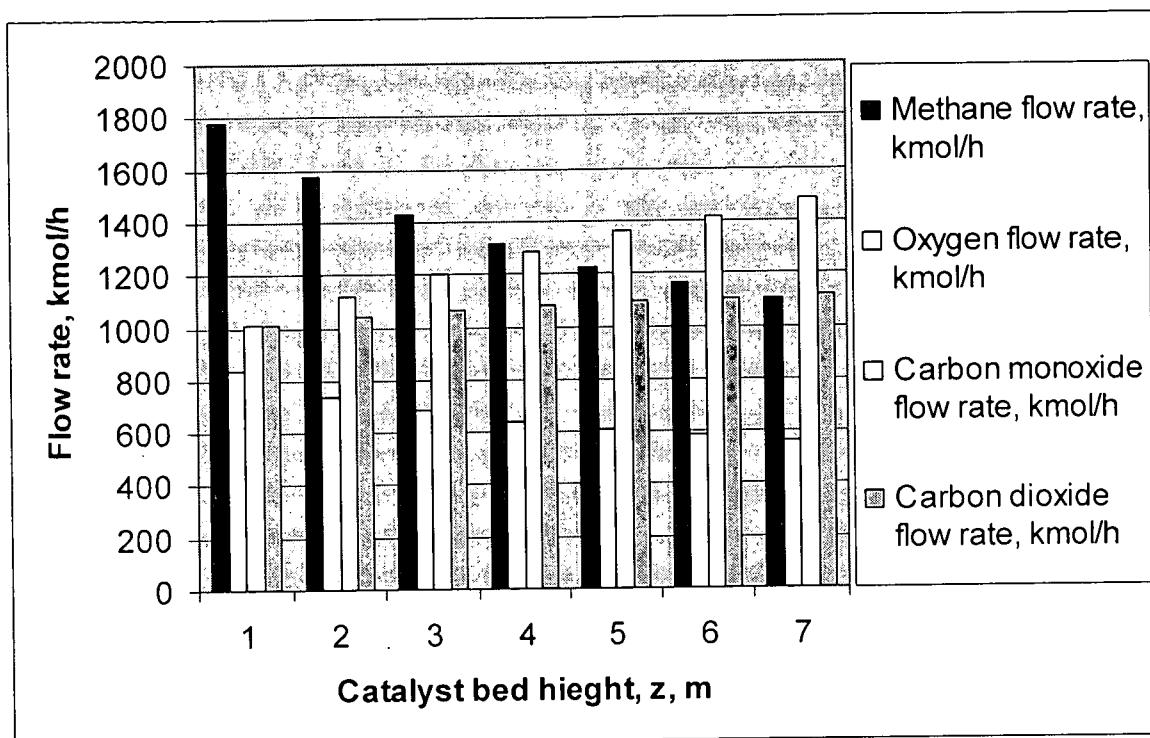


Figure 4.23 Output flow rates after each meter of catalyst bed height where the combustion temperature of 1100°C was used:

Table 4.3 Molar fractions of compounds after each meter of catalyst bed height ($T = 1100^{\circ}\text{C}$):

Distance z m	1	2	3	4	5	6	7
x_{CH_4}	0.382	0.352	0.326	0.304	0.286	0.272	0.258
x_{O_2}	0.181	0.165	0.157	0.149	0.142	0.137	0.133
x_{CO}	0.22	0.25	0.275	0.298	0.317	0.332	0.347
x_{CO_2}	0.217	0.233	0.242	0.25	0.255	0.259	0.262

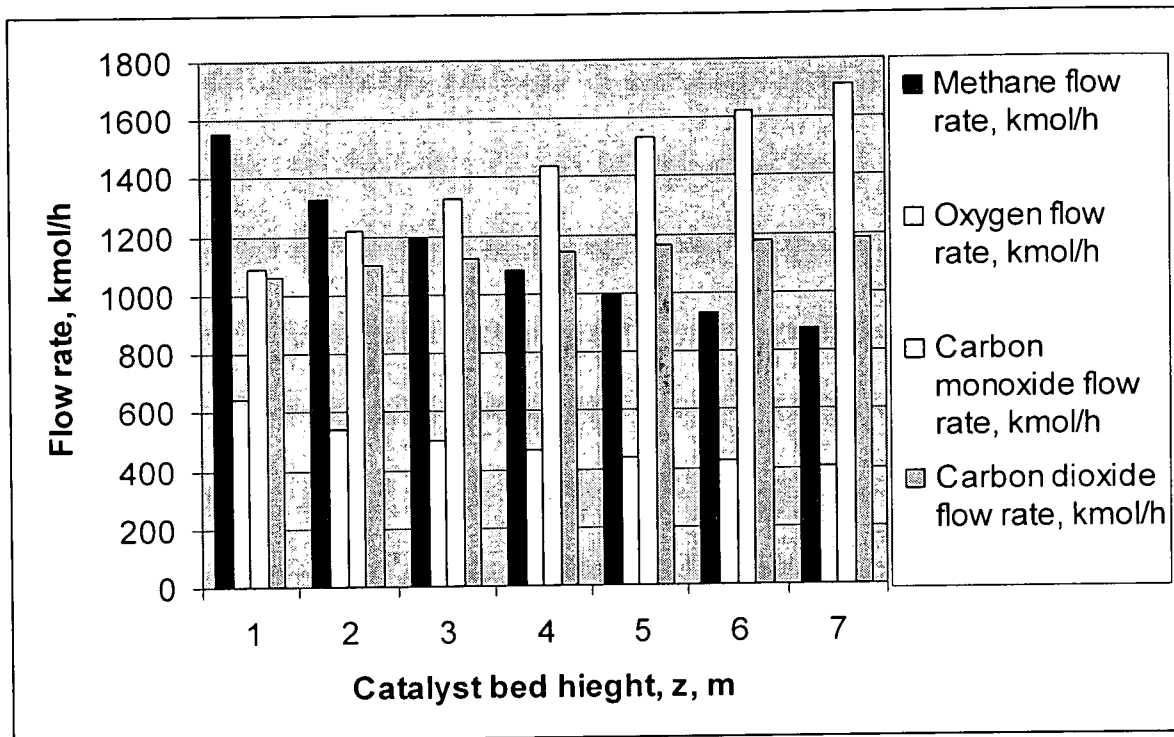


Figure 4.24 Output flow rates after each meter of catalyst bed height where the combustion temperature of 1200°C was used:

Table 4.4 Molar fractions of compounds after each meter of catalyst bed height ($T = 1200^{\circ}\text{C}$):

Distance z m	1	2	3	4	5	6	7
x_{CH_4}	0.358	0.317	0.287	0.262	0.241	0.225	0.209
x_{O_2}	0.147	0.13	0.121	0.113	0.106	0.102	0.097
x_{CO}	0.251	0.29	0.321	0.348	0.371	0.390	0.41
x_{CO_2}	0.244	0.263	0.271	0.277	0.282	0.283	0.284

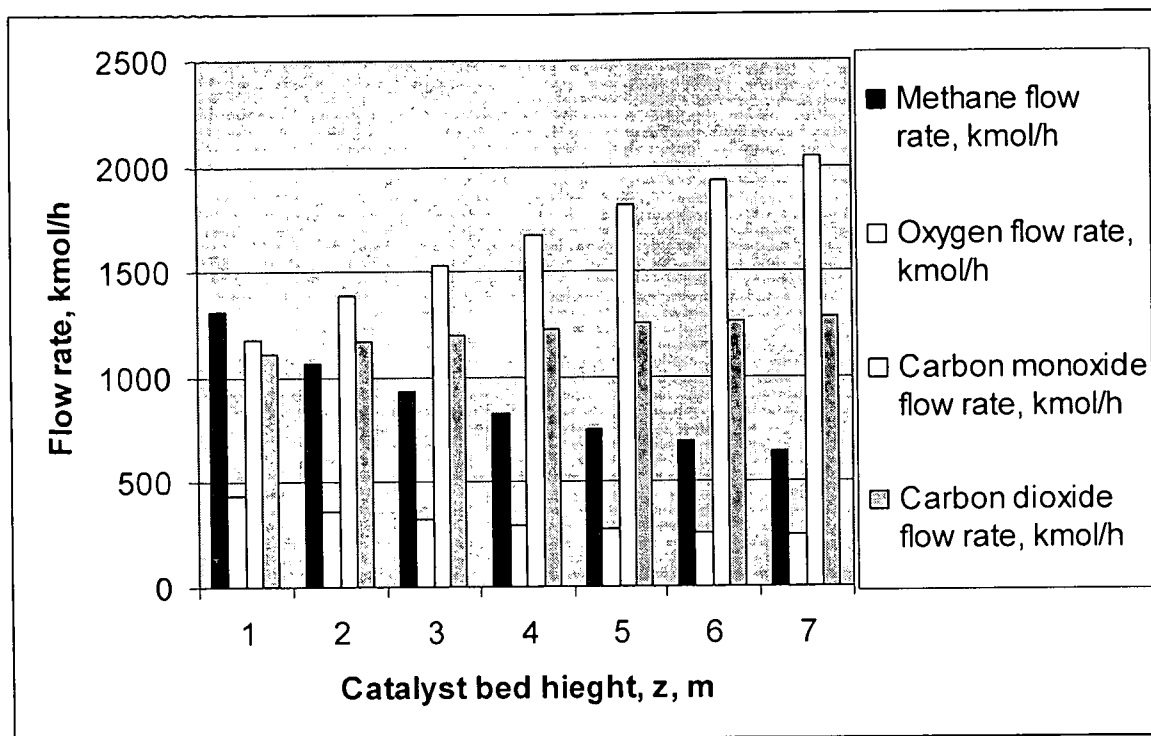


Figure 4.25 Output flow rates after each meter of catalyst bed height where the combustion temperature of 1300°C was used:

Table 4.5 Molar fractions of compounds after each meter of catalyst bed height ($T = 1300^{\circ}\text{C}$):

Distance z m	1	2	3	4	5	6	7
x_{CH_4}	0.325	0.266	0.233	0.206	0.184	0.167	0.154
x_{O_2}	0.109	0.091	0.081	0.073	0.067	0.062	0.059
x_{CO}	0.292	0.349	0.385	0.416	0.443	0.465	0.483
x_{CO_2}	0.275	0.294	0.301	0.305	0.306	0.306	0.306

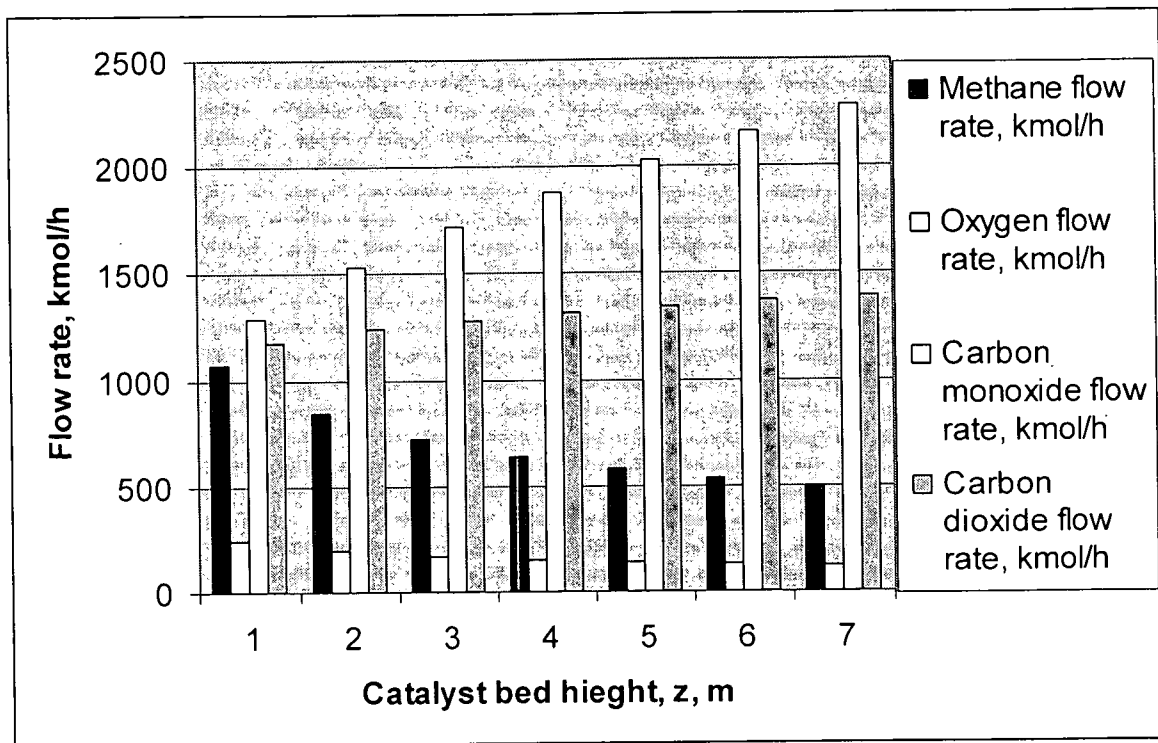


Figure 4.26 Output flow rates after each meter of catalyst bed height where the combustion temperature of 1400°C was used:

Table 4.6 Molar fractions of compounds after each meter of catalyst bed height ($T = 1400^{\circ}\text{C}$):

Distance z m	1	2	3	4	5	6	7
x_{CH_4}	0.284	0.222	0.186	0.161	0.142	0.128	0.116
x_{O_2}	0.063	0.051	0.044	0.038	0.034	0.031	0.029
x_{CO}	0.341	0.402	0.441	0.471	0.495	0.516	0.532
x_{CO_2}	0.312	0.325	0.329	0.33	0.329	0.329	0.329

It can be seen from Figures 4.22 to 4.26 above that, the highest consumption of methane and oxygen which gives the highest generation of carbon monoxide and carbon dioxide can be achieved when the maximum combustion temperature (1400°C) was used (Figure 4.26). This higher combustion temperature means a higher combustion rate (exothermic

reaction), thus more heat will be generated, and this leads to higher rate of endothermic reactions (production of carbon monoxide and carbon dioxide).

In spite of this fact, it is not preferable to operate the reactor at the highest combustion temperature, because a higher temperature profile will be generated and this will effect on the catalyst life, thus the main task is to achieve a suitable yield using a suitable temperature.

This task can be achieved by comparing the yield achieved in Figure 4.22 (actual plant temperature) and Figures 4.24 and 4.25 (different combustion temperatures).

If lower combustion temperature used (Figure 4.24), lower temperature profile can be achieved as shown in Figure 4.12. Thus longer catalyst life and safer operating conditions can be achieved. But at the same time lower conversion of feed input is observed and if this trend is acceptable, it is recommended to operate at lower combustion temperature.

On the contrary, if higher combustion temperature used as shown in Figure 4.25, higher conversion of feed input and higher yield can be achieved. But at the same time the temperature profile will be higher and this may leads to lower catalyst life.

Using the typical plant combustion temperature (1250°C), the molar fractions of compounds have been plotted as in Figure 4.27.

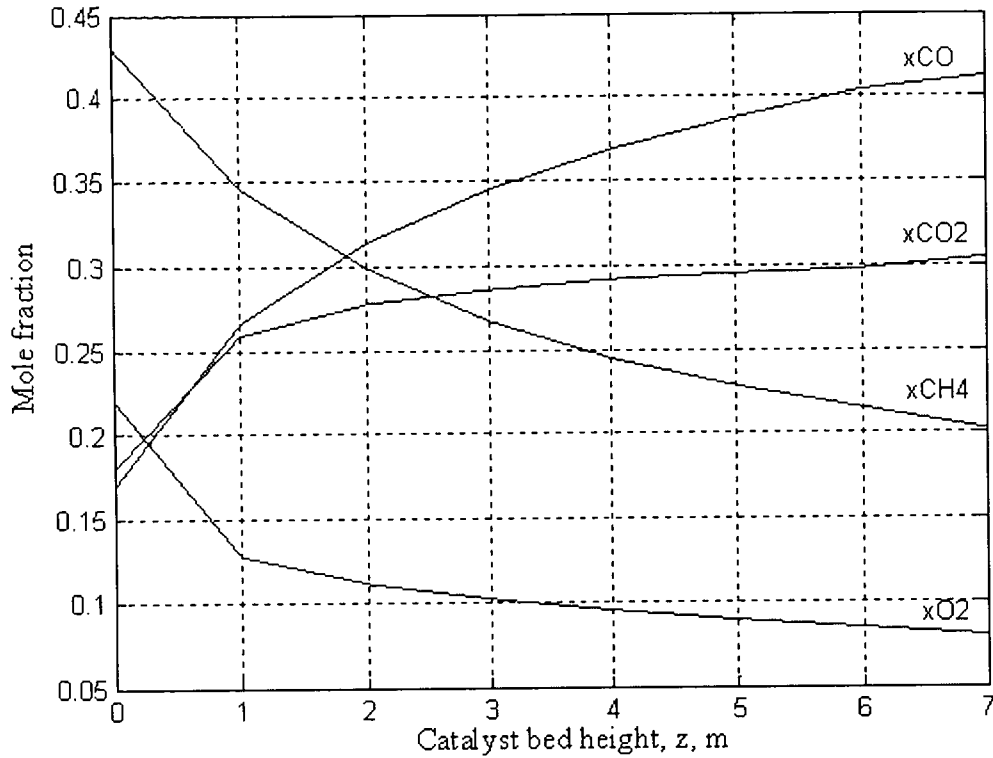


Figure 4.27 Molar fractions of compounds as function of catalyst bed height, z .

Figure 4.27 shows consumption of methane and oxygen at each unit of catalyst bed height as well as production of carbon monoxide and carbon dioxide.

4.7.2 Molar fractions at different temperatures

The molar fractions of individual compounds have been plotted at different temperatures as it shown in Figures 4.28, 4.29, 4.30, and 4.31.

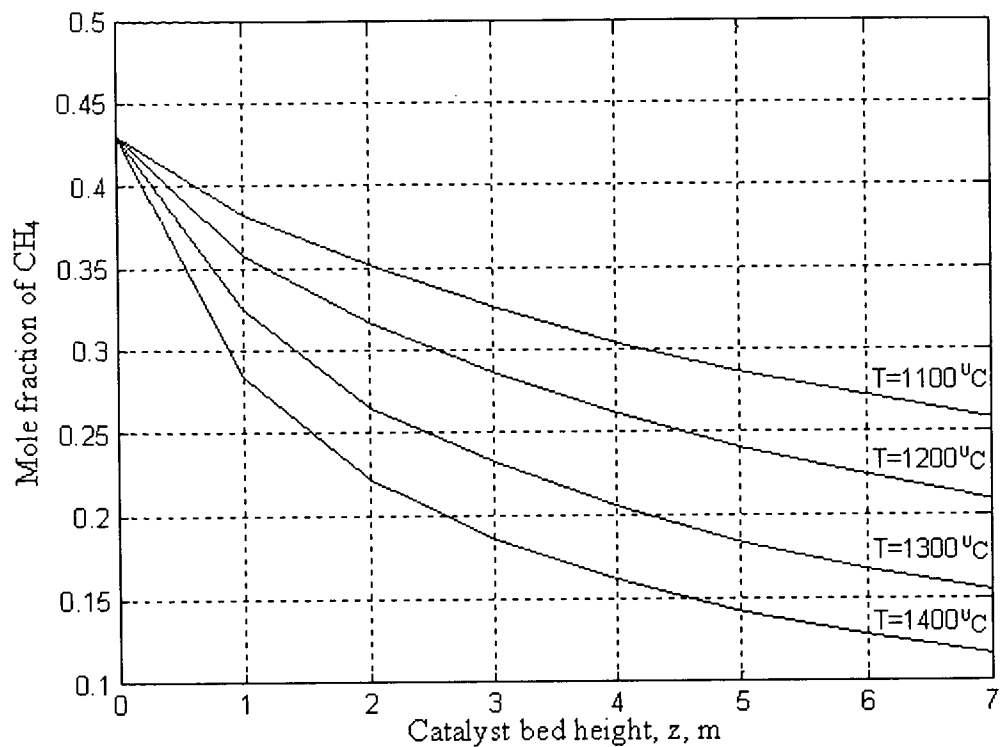


Figure 4.28 Molar fraction of methane at different combustion temperatures.

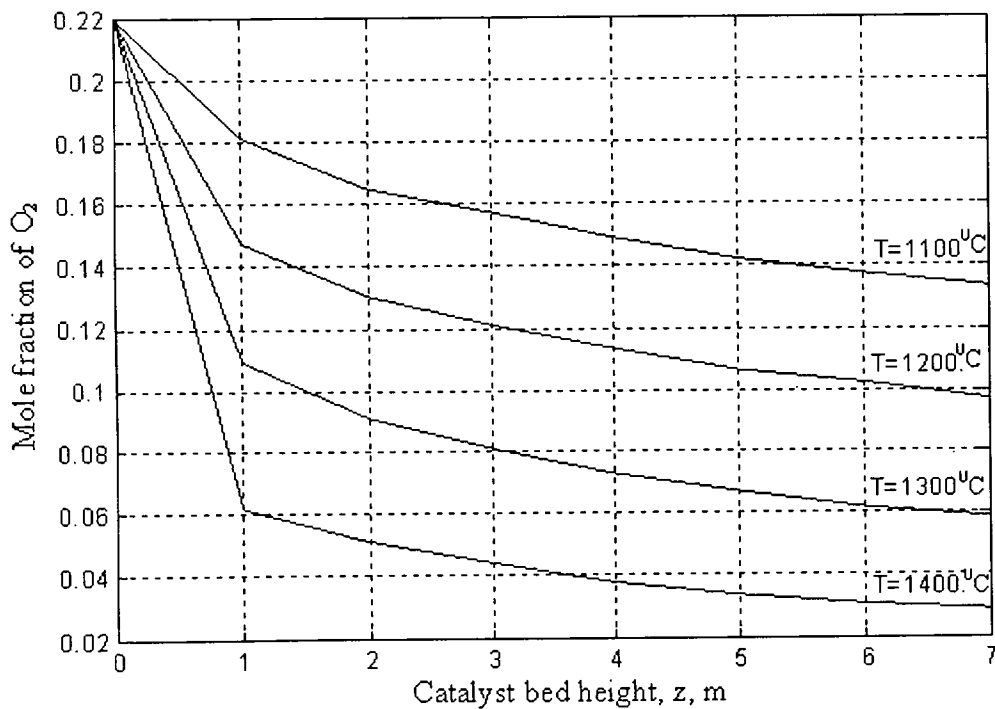


Figure 4.29 Molar fraction of oxygen at different combustion temperatures.

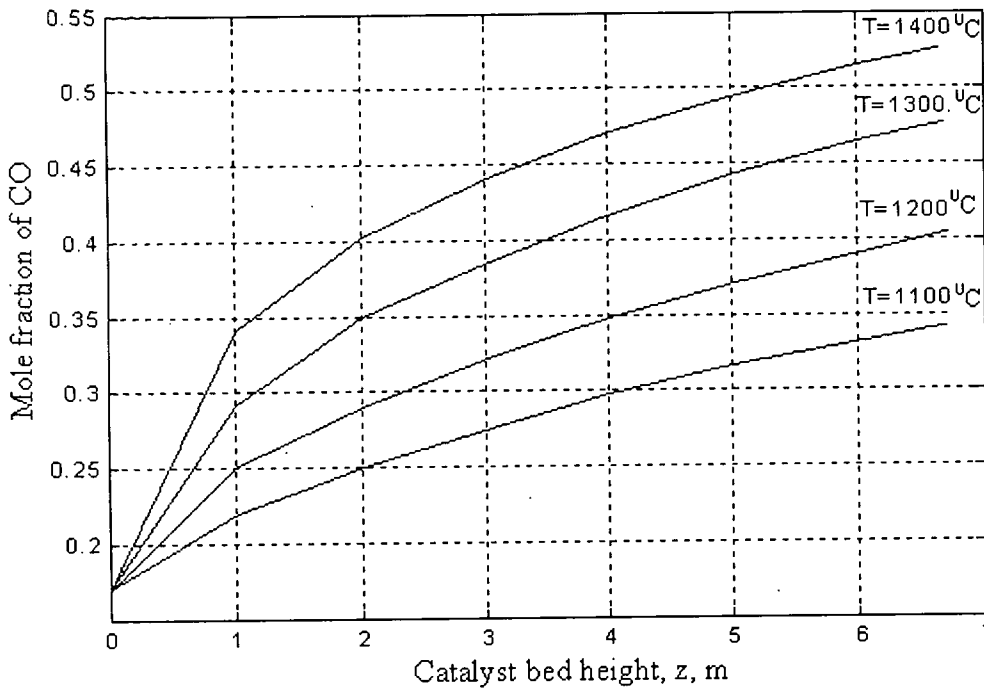


Figure 4.30 Molar fraction of carbon monoxide at different combustion temperatures.

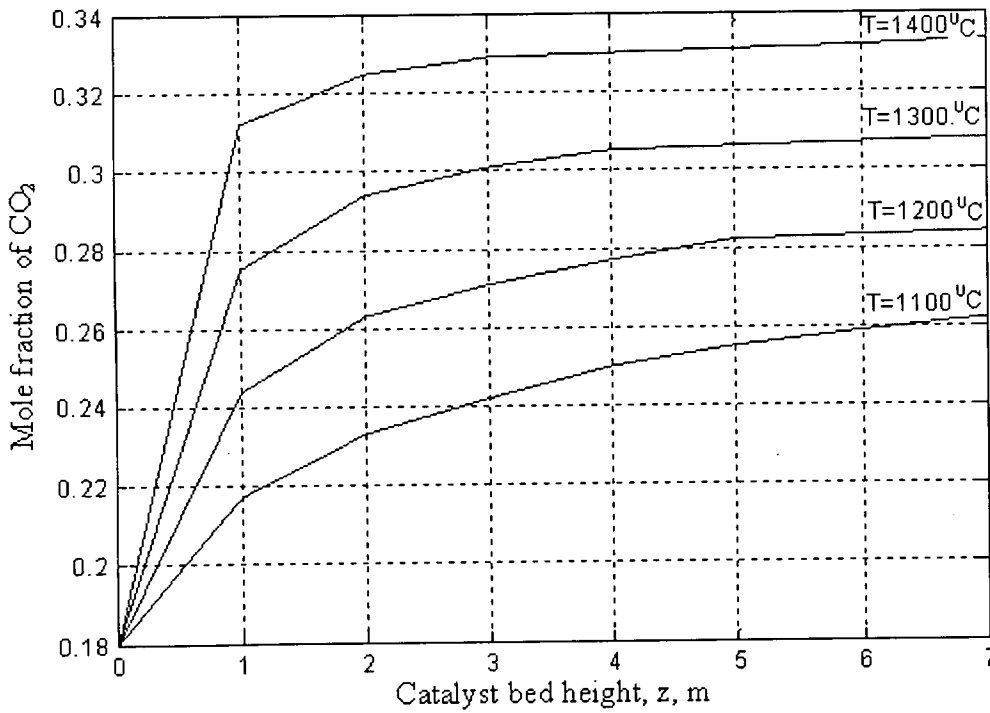


Figure 4.31 Molar fraction of carbon dioxide at different combustion temperatures.

4.7.3 Calculations of the overall selectivity

The corresponding overall selectivity at different temperatures are calculated by taking the carbon monoxide as the desired product and the carbon dioxide as the undesired product. The results are shown in Table 4.1.

Table 4.7 selectivity at different combustion temperatures.

Combustion temperature, T (°C)	Amount of produced CO, (kmol/h)	Amount of produced CO ₂ (kmol/h)	Overall selectivity $S_{\text{overall}} = F_{\text{CO}}/F_{\text{CO}_2}$
1100	600	175	3.43
1200	831	246	3.38
1300	1161	344	3.37
1400	1403	447	3.14

4.7.4 Comparison between autothermal reforming and partial oxidation

Partial oxidation of methane to synthesis gas process has been studied by means of De Groot and Froment (1996) [22].

Table 4.8 shows the conversion achieved from this model (at combustion temperature of 1400°C) and partial oxidation process where a temperature of 1444°C was recorded as the maximum bed temperature.

Table 4.8 Conversion of compounds via autothermal reforming and partial oxidation.

compound	Autothermal reformer	Partial oxidation [22]
CH ₄	78 %	97 %
O ₂	90 %	99 %
CO	61.5 %	67.3 %
CO ₂	32 %	27.4 %

In autothermal reforming process, steam reforming reactions are highly endothermic, so, more heat will be absorbed to complete the reactions, and this leads for less conversion of methane and oxygen than partial oxidation where no endothermic reactions are included (or just minimal side reactions).

In spite of the higher conversion of methane and oxygen in partial oxidation process, autothermal reforming still preferred for production of synthesis gas, because the additional amount of CO_2 can be recycled for further processing (CO_2 reforming) to produce more synthesis gas (according to economical point of view). In addition, partial oxidation leads to coke formation which may cause catalyst deactivation where as in autothermal reforming there is no coke formation included.

CHAPTER V
CONCLUDING REMARKS

CHAPTER 5

5. CONCLUDING REMARKS

5.1 Conclusions

One dimensional heterogeneous adiabatic fixed-bed reactor with supported nickel catalyst is used to model the autothermal reformer for synthesis gas production. The model has been derived using the kinetics parameters of methane reactions and the process data where the rate of coke formation is neglected since suitable CH_4/O_2 ratio of 1.7 in the feed and natural gas stream temperature of higher than 850°C are used.

A procedure to combine the kinetics model with material and energy balance was proposed and applied in this work to develop a reactor model that enable temperature predictions in the unit. This combination between the kinetics of methane reactions and the plant operation data has given this model a practical base which makes it applicable in the plants operation.

The model has been validated against the process data by comparing the temperature profile achieved in this model and the temperature recorded from the plant which it measured at different positions inside the catalyst bed. It is found that the difference between the temperature achieved in this model and the temperature measured in the plant is between 16°C - 20°C , which is about 2% less than the measured temperature. Depending on this verification, the model can be used for further studies and investigations of the other process variables on the temperature profile and the rate of reactions.

Three process variables were varied to predict the temperature profile of the autothermal reformer and the rate of reactions as well as conversion, these parameters are catalyst

volume, gas superficial velocity, and combustion temperature (burner temperature). It is found that each 1.5 m³ reduced of catalyst volume increases the bed temperature by about 16^o C. While each 1 m/s increase of gas superficial velocity decreases the bed temperature by about 15^o C. As for the effect of combustion temperature and it has been found that, the outlet temperature of the reactor remains approximately constant in spite of the wide range of combustion temperature used (1100^o - C 1400^o C). This is due to the utilization of excess heat by endothermic reactions to accelerate the rate of these reactions. These results of the effect of combustion temperature give the ability to change the combustion temperature without changing the outlet temperature, so, the heat recovery system will not be changed in spite of the burner used, the effect of this combustion temperature will be only on the conversion of feed which is studied and provided in this thesis. The combustion temperature can be changed either by changing the type of the burner or by changing the combustion fuel.

Due to some commercial regulations such as the production design and the products price, it is not easy and favorable to change the feed flow rate (gas superficial velocity), so to optimize this process, it is better to change the catalyst volume or the combustion temperature.

Most of the previous works in synthesis gas production were focused either in the kinetics of methane reaction or studying different types of catalysts, and all the temperature profiles produced were based on recording the temperature at different positions lab-scales reactors. The contribution of this thesis is the procedure to combine the kinetics of the reactions with the mass and energy balance to develop the autothermal reformer model and this model has been derived and validated. Two effective parameters which are not studied before were investigated in this work; these parameters are the combustion temperature and the catalyst volume.

5.2 Future work

Methanol production process consists of three main steps; the first step is steam reforming units, second is autothermal reforming reactors, and the third step is methanol synthesis reactors. This thesis is focused on the middle step (autothermal reforming). The future work in this process will be oriented for further studies on the other parts of methanol production process which are the steam reforming and methanol synthesis reactors. The work will focus on two main routes which are optimization and process control

The optimization study will be developed by studying the effect of process variables and how to achieve the optimum operating conditions without changing the conceptual design of the process units.

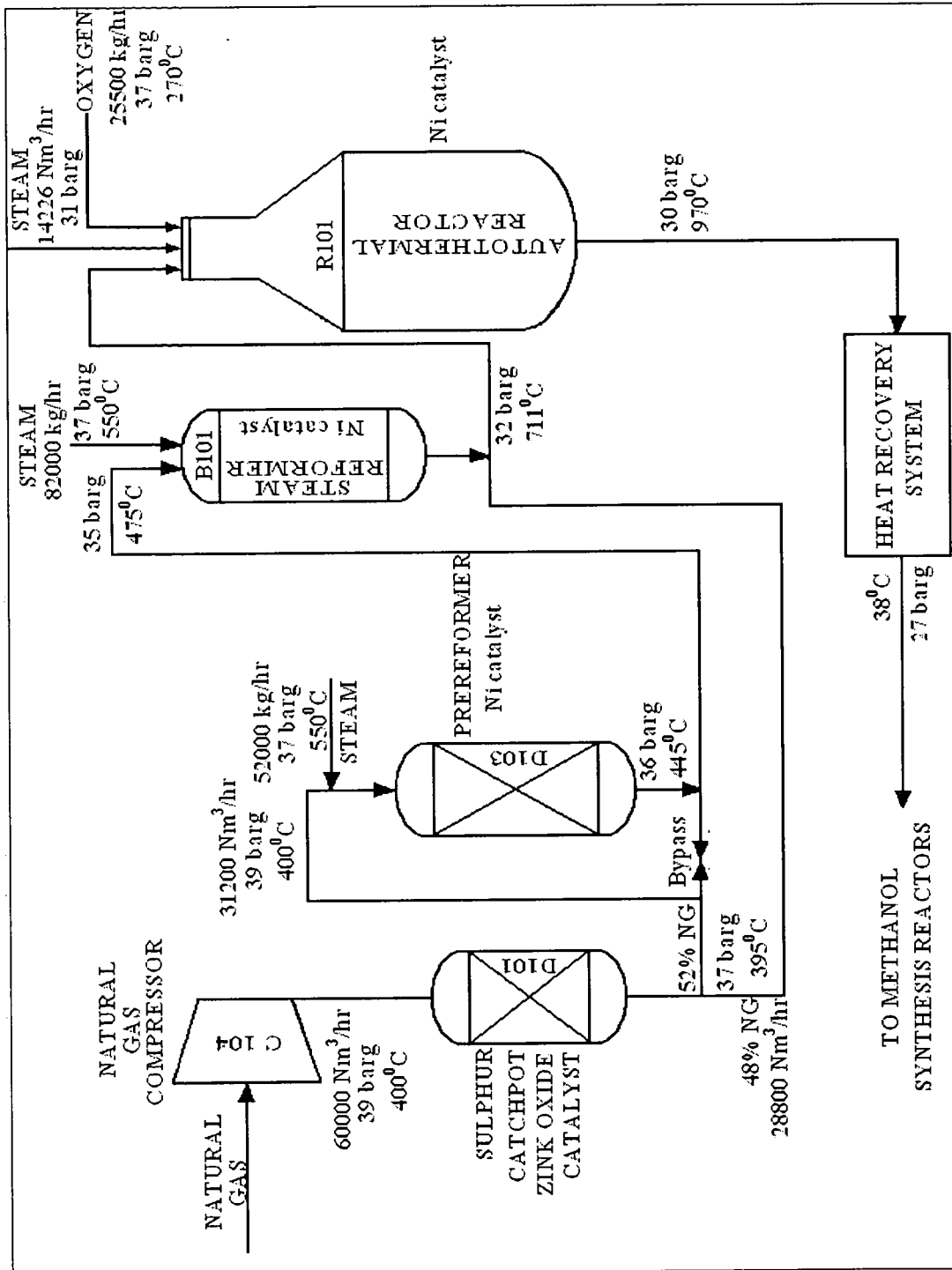
As for the process control, the study will focus on the ability to apply the new concepts of process control such as the Modeling Predictive Control (MPC) and Real Time Optimization (RTO).

APPENDICES

APPENDIX

Appendix A

Process flow diagram (PFD)



Appendix B

Table B1: Composition of desulphurized natural gas.

	Propane %	CO2 %	Ethane %	Methane %
1-Dec	2.71	1.07	4.82	89.13
2-Dec	2.58	1.12	4.57	89.4
3-Dec	2.81	1.10	3.79	89.93
4-Dec	2.85	1.1	4.34	89.13
5-Dec	3.14	1.05	5.18	88.05
6-Dec	3.27	1.03	4.84	88.12
7-Dec	3.23	1.07	4.82	88.1
8-Dec	3.23	1.03	4.54	88.53
9-Dec	3.03	0.99	4.74	88.46
10-Dec	2.66	1.05	4.52	89.36
11-Dec	3.03	1.05	4.46	88.94
12-Dec	3.1	1.04	4.45	88.83
13-Dec	3.07	1.04	4.75	88.58
14-Dec	3.02	1.04	4.67	88.67
15-Dec	2.9	1.03	5.12	88.46
16-Dec	2.85	1.08	4.17	89.48
17-Dec	3.07	1.06	4.49	88.86
18-Dec	2.9	1.03	5.09	88.48
19-Dec	3.3	1.08	4.59	88.27
20-Dec	2.99	1.05	4.34	89.13
21-Dec	3.13	1.05	4.25	88.94
22-Dec	3.23	1.05	4.15	88.8
23-Dec	3.27	1.07	4.32	88.66
24-Dec	3.25	1.08	4.26	88.7
25-Dec	3.25	1.07	4.23	88.83
26-Dec	3.16	1.07	4.19	88.94
27-Dec	3.32	1.09	4.23	88.73
28-Dec	2.72	1.02	4.86	89.18
29-Dec	3.22	1.06	4.67	88.46
30-Dec	3.13	1.05	4.2	89.12

Table B2: Composition of steam reformer outlet (B 101)

H2 %	O2 %	N2 %	CO2 %	CH4 %	CO %	CO+CO2
66.48	0.05	0.14	10.76	12.78	9.79	20.55
66.09	0.06	0.18	10.85	12.88	9.94	20.79
66.62	0.03	0.08	10.59	12.73	9.95	20.54
66.18	0.04	0.11	10.69	13.1	9.88	20.57
65.88	0.03	0.07	10.82	13.45	9.75	20.57
66.31	0.02	0.06	11.11	13.02	9.48	20.59
66.24	0.03	0.08	11.33	12.96	9.36	20.69
66.5	0.03	0.07	10.91	12.65	9.84	20.75
66.24	0.14	0.43	11.13	12.34	9.72	20.85
67.13	0.03	0.06	11.14	12.16	9.48	20.62
66.66	0.04	0.11	11.26	12.45	9.48	20.74
66.36	0.03	0.06	11.48	12.57	9.5	20.98
66.27	0.03	0.06	10.79	13.15	9.7	20.49
66.58	0.05	0.11	10.79	12.67	9.8	20.59
66.73	0.04	0.09	10.73	12.51	9.9	20.63
66.92	0.04	0.09	10.54	12.27	10.14	20.68
66.87	0.04	0.09	10.54	12.36	10.1	20.64
66.8	0.05	0.12	10.59	12.37	10.07	20.66
66.57	0.04	0.09	10.63	12.55	10.12	20.75
66.89	0.04	0.1	10.6	12.25	10.12	20.72
66.19	0.06	0.15	10.81	12.72	10.07	20.88
66.15	0.12	0.36	10.73	12.53	10.11	20.84
66.67	0.03	0.06	10.43	12.58	10.22	20.65
66.18	0.04	0.08	10.77	12.66	10.27	21.04
66.72	0.03	0.04	10.66	12.43	10.12	20.78
66.74	0.04	0.08	10.64	12.32	10.18	20.82
66.97	0.03	0.04	10.46	12.28	10.22	20.68
67.35	0.04	0.07	10.55	12.14	9.85	20.4
66.53	0.05	0.1	10.63	12.64	10.05	20.68
66.43	0.04	0.09	10.67	12.9	9.87	20.54
66.84	0.04	0.08	10.61	12.18	10.25	20.86

Table B3: Composition of autothermal reformer outlet (R 101).

H2 %	O2 %	N2 %	CO2 %	CH4 %	CO %	SN
67.95	0.21	0.16	8.44	2.48	20.76	2.04
68	0.2	0.12	8.5	2.68	20.5	2.05
68.05	0.21	0.11	8.41	2.59	20.63	2.05
67.82	0.21	0.11	8.42	2.77	20.67	2.04
67.61	0.2	0.09	8.52	3.05	20.53	2.03
67.75	0.21	0.05	8.77	2.92	20.3	2.03
67.68	0.2	0.07	9.14	3.03	19.88	2.02
67.62	0.2	0.11	8.78	2.92	20.37	2.02
67.83	0.21	0.14	8.85	2.62	20.35	2.02
68.15	0.24	0.18	8.9	2.48	20.04	2.05
68.02	0.21	0.11	9.07	2.64	19.95	2.03
68.04	0.22	0.12	9.13	2.45	20.04	2.02
68.35	0.19	0.06	8.35	2.78	20.27	2.10
67.83	0.24	0.23	8.45	2.67	20.58	2.05
68.15	0.21	0.08	8.54	2.64	20.38	2.06
68.34	0.22	0.11	8.32	2.46	20.55	2.08
68.67	0.21	0.06	8.2	2.54	20.32	2.12
68.14	0.22	0.09	8.37	2.58	20.6	2.06
67.92	0.23	0.08	8.38	2.71	20.68	2.05
67.94	0.23	0.06	8.48	2.58	20.71	2.04
67.75	0.22	0.07	8.45	2.79	20.72	2.03
67.87	0.23	0.11	8.45	2.51	20.83	2.03
67.78	0.22	0.12	8.39	2.74	20.75	2.04
67.6	0.24	0.15	8.44	2.68	20.89	2.02
67.97	0.21	0.06	8.43	2.68	20.65	2.05
68.1	0.21	0.08	8.4	2.53	20.68	2.05
68.04	0.22	0.07	8.33	2.67	20.67	2.06
67.97	0.25	0.09	8.43	2.72	20.54	2.06
67.77	0.24	0.11	8.51	2.7	20.67	2.03
67.96	0.24	0.1	8.42	2.71	20.57	2.05
67.81	0.26	0.12	8.42	2.65	20.74	2.04

Appendix C

Over all material balance around D103 and B101:

Table.1: composition of natural gas and steam reformer outlet:

stream	CH ₄ %	H ₂ %	CO ₂ %	CO %	O ₂ %
Pure natural gas	89	Trace	1.07	Trace	Trace
Steam reformer outlet	12.5	66.5	10.6	10	0.4

Using the correction factor to convert to volumetric flow rate:

$$\text{Mass flow rate} = \text{normal volumetric flow rate} * \text{molecular weight} / 22.414$$

$$F_1 = \text{natural gas flow rate to D103} = 31200 \text{ Nm}^3/\text{h}$$

$$S_1 = \text{steam flow rate to D103} = 52000 \text{ kg/h} = 64751.5 \text{ Nm}^3/\text{h}$$

$$S_2 = \text{steam flow rate to B101} = 82000 \text{ kg/h} = 102108.5 \text{ Nm}^3/\text{h}$$

$$P = \text{out put flow rate of B101} = F_1 + S_1 + S_2 = 198060 \text{ Nm}^3/\text{h}$$

From table 1 above, the flow rate of each component in the output stream of B101 is as the following:

$$B_{H_2} = 0.665 * 198060 = 131710 \text{ Nm}^3/\text{h}$$

$$B_{O_2} = 0.0005 * 198060 = 100 \text{ Nm}^3/\text{h}$$

$$B_{CO_2} = 0.106 * 198060 = 20995 \text{ Nm}^3/\text{h}$$

$$B_{CO} = 0.1 * 198060 = 19806 \text{ Nm}^3/\text{h}$$

$$B_{CH_4} = 0.125 * 198060 = 24757 \text{ Nm}^3/\text{h}$$

Pure natural gas flow rate to R101 = 28800 Nm³/h

F'_{CH_4} = methane flow rate in the natural gas stream = 0.885*28800 = 25488 Nm³/h

Oxygen flow rate to R101 = 25500 Nm³/h

Steam flow rate to R101 = 8044 + 3381 kg/h
= 14226 Nm³/h

The total flow rate of CH₄ = 24757 + 25488 = 50245 Nm³/h

The total flow rate of O₂ to R101 = 25500 + 100 = 25600 Nm³/h

[O₂/ CH₄ = 0.51]

Total flow rate to R101 = steam reformer outlet + NG + oxygen + steam
= 198060 + 28800 + 25500 + 14226
= 266586 Nm³/h

ence, the flow rate of each component to the autothermal reformer is as the following:

F_{CH_4} = 50249 Nm³/h

F_{O_2} = 25600 Nm³/h

F_{H_2} = 131710 Nm³/h

F_{CO_2} = 20995 Nm³/h

F_{CO} = 19806 Nm³/h

Total flow rate to R101 (kg/h) = 266586 * 13.81/22.414
= 164252 kg/h

Total flow rate to R101 (kmol/h) = mass flow rate / average molecular weight
= 164252 / 13.81
= 11893 kmol / h

Mole fraction of the components:

$$x_{\text{CH}_4} = 50245 / 266586 = 0.188$$

$$x_{\text{O}_2} = 25600 / 266586 = 0.096$$

$$x_{\text{H}_2} = 131710 / 266586 = 0.494$$

$$x_{\text{CO}_2} = 20995 / 266586 = 0.079$$

$$x_{\text{CO}} = 19806 / 266586 = 0.074$$

$$x_{\text{steam}} = 14226 / 266586 = 0.053$$

Then:

$$F_{\text{CH}_4} = 0.188 * 11893 = 2236 \text{ kmol / h}$$

$$F_{\text{O}_2} = 0.096 * 11893 = 1142 \text{ kmol / h}$$

$$F_{\text{H}_2} = 0.5 * 11893 = 5946 \text{ kmol / h}$$

$$F_{\text{CO}_2} = 0.079 * 11893 = 940 \text{ kmol / h}$$

$$F_{\text{CO}} = 0.074 * 11893 = 880 \text{ kmol / h}$$

$$F_{\text{steam}} = 0.053 * 11893 = 630 \text{ kmol / h}$$

The pressure of the feed = 30 bar

From Rault's law

$$P_i = P * x_i$$

Where P_i is the partial pressure of component i, P is the total pressure, and x_i is the mole fraction of component i.

$$P_{\text{CH}_4} = 30 * 0.188 = 5.64 \text{ bar}$$

$$P_{\text{O}_2} = 30 * 0.096 = 2.88 \text{ bar}$$

$$P_{\text{H}_2} = 30 * 0.494 = 14.82 \text{ bar}$$

$$P_{\text{CO}_2} = 30 * 0.079 = 2.37 \text{ bar}$$

$$P_{\text{CO}} = 30 * 0.074 = 2.22 \text{ bar}$$

$$P_{\text{H}_2\text{O}} = 30 * 0.053 = 1.6 \text{ bar}$$

Output composition:

$$y_{\text{CH}_4} = 0.025$$

$$y_{\text{H}_2} = 0.68$$

$$y_{\text{CO}_2} = 0.085$$

$$y_{\text{CO}} = 0.205$$

$$y_{\text{O}_2} = 0.0021$$

$$y_{\text{steam}} = 0$$

$$\begin{aligned} \text{R101 output flow rate} &= 198060 + 28800 + 25500 + 14226 \\ &= 266586 \text{ Nm}^3/\text{h} \\ &= 11893 \text{ kmol / h} \end{aligned}$$

Output flow rate of the components:

$$F'_{\text{CH}_4} = 0.025 * 266586 = 6665 \text{ Nm}^3/\text{h}$$

$$F'_{\text{O}_2} = 0.0021 * 266586 = 560 \text{ Nm}^3/\text{h}$$

$$F'_{\text{CO}} = 0.205 * 266586 = 54650 \text{ Nm}^3/\text{h}$$

$$F'_{\text{CO}_2} = 0.085 * 266586 = 22665 \text{ Nm}^3/\text{h}$$

$$F'_{\text{H}_2} = 0.68 * 266586 = 181278 \text{ Nm}^3/\text{h}$$

In term of molar flow rate:

$$F'_{\text{CH}_4} = 0.025 * 11893 = 297 \text{ kmol / h}$$

$$F'_{\text{O}_2} = 0.0021 * 11893 = 25 \text{ kmol / h}$$

$$F'_{\text{CO}} = 0.205 * 11893 = 2438 \text{ kmol / h}$$

$$F'_{\text{CO}_2} = 0.085 * 11893 = 1011 \text{ kmol / h}$$

$$F'_{\text{H}_2} = 0.68 * 11893 = 8087 \text{ kmol / h}$$

Reactor parameters:

Reactor diameter (d) = 3.62 m

Cross sectional area (A) = $\pi/4 * d^2 = 10.287 \text{ m}^2$

Gas velocity (u) = volumetric flow rate / A
= 7.199 m/s

Catalyst density = 1970 kg/m^3

Average Gas density = 3.894 kg/m^3

Average Heat capacity (Cp) = 3.206 kJ / kg.K

Appendix D

Input - Output programme

```
function main(T)

T= 1250;
Az=0.001;
z=0;
i=1;

while (z<8)
    z=z+Az;
    a(i)=z;
    CCH4 = 0.188;
CO2 = 0.096;
K3 = 0.18;
K4 = 2.7;
K5 = 1.06;
% Kinetics parameters

%values of A

A1=8.11*10^5;
A2=6.82*10^5;
A3=1.17*10^15;
A4=5.43*10^5;
A5=2.83*10^14;
% values of Activation energies E for the rate constants
E1=-86000;
E2=-86000;
E3=-240100;
E4=-67100;
E5=-243900;

% delta H for adsorption constants

dH1=-27300;
dH2=-92800;
dH3=-38300;
dH4=-70700;
dH5=-82900;
dH6=88000;
```

% values of the partial pressures

PCH4 = 4;
PH2 = 6;
PCO2 = 1.6;
PCO = 0.27;
PH2O = 15.7;

%global gas constant

R = 8.314;

% gas superficial velocity

u = 7.2;

% reactor parameters

% catalyst density

Dc = 1970;

%total bed volume

VT=76.1238;

%gas density

Dg = 3.894;

% gas heat capacity

Cp = 3.206;

% reactions enthalpy

AH1 = -803;
AH2 = 207;
AH3 = 198;
AH4 = -41;

%total bed density

Db=77.6367;

% model equations

% rate constants

```
k1=A1*exp(E1/(R*T));
k2=A2*exp(E2/(R*T));
k3=A3*exp(E3/(R*T));
k4=A4*exp(E4/(R*T));
k5=A5*exp(E5/(R*T));
```

%equilibrium constants for combustion reactions (rate of reaction 1)

```
K1=1.26*10^-1*exp(-dH1/(R*T));
K2=7.87*10^-7*exp(-dH2/(R*T));
```

%adsorption constants

```
KCH4=6.65*10^-4*exp(-dH3/(R*T));
KCO=8.23*10^-5*exp(-dH4/(R*T));
KH2=6.12*10^-9*exp(-dH5/(R*T));
KH2O=177*10^5*exp(-dH6/(R*T));
```

% Rate of reactions

```
r1=k1*CCH4*CO2/(1+K1*CCH4+K2*CO2)^2+k2*CCH4*CO2^0.5/(1+K1*C
CH4+K2*CO2);
c(i)=r1;
r2=k3/PH2^2.5*(PCH4*PH2O-
PH2^3*PCO/K3)/(1+KCO*PCO+KH2*PH2+KCH4*PCH4+KH2O*PH2O/PH2)^2
;
d(i)=r2;
r3=k5/PH2^3.5*(PCH4*PH2O^2-
PH2^4*PCO2/K5)/(1+KCO*PCO+KH2*PH2+KCH4*PCH4+KH2O*PH2O/PH2)^
2;
e(i)=r3;
r4=k4/PH2*(PCO*PH2O-
PH2*PCO2/K4)/(1+KCO*PCO+KH2*PH2+KCH4*PCH4+KH2O*PH2O/PH2)^2;
f(i)=r4;
```

% Energy equation (At expresses the temperature deviation)

```
At=(Db / (u*Dg*Cp) * (.05 * r1 * AH1 + .07 * r2 * AH2 + .06
* r3 * AH3 + .7 * r4 * AH4))*Az;
```

%average temperature in the specific unit

```
Tav=T+At/2;
```

```
%outlet temperature of each unit

T=T+At;

b(i)=Tav;
i=i+1;
end
plot(a,b)
grid;
title ('');
xlabel('catalyst bed height, z m');
ylabel ('temperature');
```

REFERENCES

- [1] Jacob A. Moulijn and et al., Chemical process technology.2001, WILEY.
- [2] Joan M. Ogden. Review of small stationary reformers for hydrogen production. Princeton, NJ 08544 (2001).
- [3] S.S. Bharadwaj, L.D. Schmidt. Catalytic partial oxidation of natural gas to signals. Fuel Processing Technology 42 (1995) 109-127.
- [4] Inyong Kang, Joongmyeon Bae, and Gyujong Bae. Performance comparison of autothermal reforming for liquid hydrocarbons, gasoline and diesel for fuel cell applications. Journal of Power Sources 163 (2006) 538–546.
- [5] Lurgi Mega Methanol. Lurgi Oel Chemie GmbH- Lurgiallee 5- D-60295 Frankfurt am Main.
- [6] D.L. Hoang, S.H. Chan, and O.L. Ding. Hydrogen production for fuel cells by autothermal reforming of methane over sulfide nickel catalyst on a gamma alumina support. Journal of Power Sources 159 (2006) 1248–1257.
- [7] D.L. Hoang and S.H. Chan. Modeling of a catalytic autothermal methane reformer for fuel cell applications. Applied Catalysis A: General 268 (2004) 207–216.
- [8] Cunping Huang, Ali T-Raissi. Thermodynamic analyses of hydrogen production from sub-quality natural gas Part II: Steam reforming and autothermal steam reforming. Journal of Power Sources 163 (2007) 637–644.

- [9] P.J. Dauenhauer, J.R. Salge, and L.D. Schmidt. Renewable hydrogen by autothermal steam reforming of volatile carbohydrates. *Journal of Catalysis* 244 (2006) 238–247.
- [10] Kazuhisa Murata , Masahiro Saito, Megumu Inaba, and Isao Takahara. Hydrogen production by autothermal reforming of sulfur-containing hydrocarbons over re-modified Ni/Sr/ZrO₂ catalysts. *Applied Catalysis B: Environmental* 70 (2007) 509–514.
- [11] James R. Lattner and Michael P. Harold. Autothermal reforming of methanol: Experiments and modeling. *Catalysis Today* 120 (2007) 78–89.
- [12] Sauri Gudlavalleti, Tijmen Ros , and Dick Liefink. Thermal sintering studies of an autothermal reforming catalyst. *Applied Catalysis B: Environmental* 74 (2007) 252–261.
- [13] Baitao Li, Kenji Maruyama, Mohammad Nurunnabi, and Kimio Kunimori, Keiichi Tomishige. Temperature profiles of alumina-supported noble metal catalysts in autothermal reforming of methane. *Applied Catalysis A: General* 275 (2004) 157–172.
- [14] R. Horn, K.A. Williams, N.J. Degenstein, L.D. Schmidt. Syngas by catalytic partial oxidation of methane on rhodium: Mechanistic conclusions from spatially resolved measurements and numerical simulations. *Journal of Catalysis* 242 (2006) 92–102.
- [15] Vasant R. Choudhary, Kartick C. Mondal, Ajit S. Mamman. High-temperature stable and highly active/selective supported NiCoMgCeO_x catalyst suitable for autothermal reforming of methane to syngas. *Journal of Catalysis* 233 (2005) 36–40.

- [16] C. Palm, P. Cremer, R. Peters, D. Stolten. Small-scale testing of a precious metal catalyst in the autothermal reforming of various hydrocarbon feeds. *Journal of Power Sources* 106 (2002) 231–237.
- [17] F. Basile, G. Fornasari, F. Trifirò, A. Vaccari. Partial oxidation of methane, effect of reaction parameters and catalyst composition on the thermal profile and heat distribution. *Catalysis Today* 64 (2001) 21–30.
- [18] Grigorios Kolios, Jörg Frauhammer, and Gerhart Eigenberger. A simplified procedure for the optimal design of autothermal reactors for endothermic high-temperature reactions. *Chemical Engineering Science* 56 (2001) 351–357.
- [19] Ib Dybkjær. Tubular reforming and autothermal reforming of natural gas - an overview of available processes. *Fuel Processing Technology* 42 (1995) 85–107.
- [20] D.A. Hickman and L.D. Schmidt, *AIChE J.*, 39(7)(1993) 1164-1177.
- [21] D. L. Trimm and C. W. Lam. (1980). The combustion of methane on Platinum-alumina fibre catalysts. Kinetics and mechanism. *Chemical engineering science*, 35, 1405-1413.
- [22] A. M. De Groote and G. F. Froment. (1996). Simulation of the catalytic partial oxidation of methane to synthesis gas. *Applied catalysis A*, 138, 245-264.
- [23] C.R.H. De Smet, M. H. J. M. de Croon, R. J. Berger, G. B. Marlin, J. C. Schouten. (2001). Design of adiabatic fixed-bed reactors for the partial oxidation of methane to synthesis gas. Application to production of methanol and hydrogen for fuel-cells. *Chemical engineering science* 56 4849-486.

- [24] E.S. Wagner and G.F. Froment, *Hydrocarbon Process.*, 7 (1992) 69.
- [25] E.S. Wagner and G.F. Froment, Unpublished results, 1992.
- [26] Ostrowski, T., Giroir-Fendler, A., Mirodatos, C., & Mleckzo, L. (1998). Comparative study of the catalytic partial oxidation of methane to synthesis gas in fixed-bed and fluidized-bed membrane reactors. *Catalysis Today*, 40, 181–190.
- [27] Chunshan Song, Wei Pan. Tri-reforming of methane: a novel concept for catalytic production of industrially useful synthesis gas with desired H₂/CO ratios. *Catalysis Today* 98 (2004) 463–484.
- [28] Joelmir A.C. Dias, José M. Assaf. The advantages of air addition on the methane steam reforming over Ni/Al₂O₃. *Journal of Power Sources* 137 (2004) 264–268.
- [29] S.C. Tsang, J.B. Claridge, M.L.H. Green. Recent advances in the conversion of methane to synthesis gas. *Catalysis Today* 23 (1995) 3–15.
- [30] C. T Goralski Jr. R. P. O'Connor, L. D. Schmidt. Modeling homogeneous and heterogeneous chemistry in the production of syngas from methane. *Chemical Engineering Science* 55 (2000) 1357 – 1370.
- [31] P.T. Wierzchowski, L.W. Zatorski. Kinetics of catalytic oxidation of carbon monoxide and methane combustion over alumina supported Ga₂O₃, SnO₂ or V₂O₅. *Applied Catalysis B: Environmental* 44 (2003) 53–65.

- [32] Hirotaka Koga a, Shuji Fukahori a, Takuya Kitaoka a,* , Akihiko Tomoda b, Ryo Suzuki b, Hiroyuki Wariishi. Autothermal reforming of methanol using paper-like Cu/ZnO catalyst composites prepared by a papermaking technique. *Applied Catalysis A: General* 309 (2006) 263–269.
- [33] Robert E. Hayes, Stan T. Kolaczkowski, Paul K. C. Li, Serpil Awdry. The palladium catalysed oxidation of methane: reaction kinetics and the effect of diffusion barriers. *Chemical Engineering Science* 56 (2001) 4815–4835.
- [34] Mariana M. V. M. Souza, Octavio R. Macedo Neto, Martin Schmal. Synthesis Gas Production from Natural Gas on Supported Pt Catalysts. *Journal of Natural Gas Chemistry* 15(2006)21-27.
- [35] Souza M M V M, Schmal M. *Catal Lett*, 2003, 91: 11.
- [36] Joelmir A.C. Dias□, José M. Assaf. Autothermal reforming of methane over Ni/_-Al₂O₃ catalysts: the enhancement effect of small quantities of noble metals. *Journal of Power Sources* 130 (2004) 106–110.
- [37] Gilbert F. Froment, Kenneth B. Bidchoff. *Chemical reactors analysis and design (second edition)*. 0-471-51044-0, 1990. WILEY.
- [38] Ann M. De Groote*, Gilbert F. Froment. The role of coke formation in catalytic partial oxidation for synthesis gas production. *Catalysis Today* 37 (1997) 309-329.
- [39] J. Xu and G. F. Froment (1989). Methane steam reforming, methanation and water-gas shift reaction: intrinsic kinetics. *A.I.Ch.E Journal*, 35, 88-96.
- [40] H. Scott Fogler. *Elements of chemical reaction engineering (third edition)*. 0-13-973785-5, 1999. Prentice Hall International Series.

-
- [41] G.F. Froment. Production of synthesis gas by steam- and CO₂-reforming of natural gas. *Journal of Molecular Catalysis A: Chemical* 163 (2000) 147–156.
- [42] Numaguchi, and K. Kikuchi. (1988). Intrinsic kinetics and design simulation in a complex reaction network: steam-methane reforming. *Chemical engineering science*, 43, 2295-2301.
- [43] Donald R. Coughanowr (1991). *Process systems analysis and control*. McGRAW-HILL.